

*Synthesis and Characterization of Novel
Ionomers based on
Styrene Butadiene Copolymers*

Thesis submitted to the
Cochin University of Science and Technology
in partial fulfillment of the requirements for
the award of the degree of

Doctor of philosophy

Under the
FACULTY OF TECHNOLOGY
By

Mr. Jacob Samuel

DEPARTMENT OF POLYMER SCIENCE AND RUBBER TECHNOLOGY
COCHIN UNIVERSITY OF SCIENCE AND TECHNOLOGY
KOCHI- 682022, KERALA, INDIA.

December 2002

Department of Polymer Science and Rubber Technology
COCHIN UNIVERSITY OF SCIENCE AND TECHNOLOGY
Kochi - 682 022, India

Date: 28-12-2002

Certificate

This is to certify that the thesis entitled "*Synthesis and Characterization of Novel Ionomers based on Styrene Butadiene Copolymers*", which is being submitted by **Mr. Jacob Samuel**, in partial fulfillment of the requirements of the degree of Doctor of Philosophy, to the Cochin University of Science and Technology (CUSAT), Kochi, India is a record of the bonafide research work carried out by him under our joint guidance and supervision.

Mr. Samuel has worked on this research problem for about three years and four months (1999 - 2002) in the Department of Polymer Science and Rubber Technology of CUSAT. In our opinion the thesis has fulfilled all the requirements according to the regulations. The results embodied in this thesis have not been submitted for any other degree or diploma.

Thomas Kurian

Thomas Kurian

(Supervising Teacher)



K. E. George

(Co- supervising Teacher)

Declaration

I here by declare that the thesis entitled "Synthesis and Characterization of Novel Ionomers based on Styrene Butadiene Copolymers" is the original work carried out by me under the joint supervision of **Dr. Thomas Kurlan**, Reader, and **Dr. K. E. George**, Professor Department of Polymer Science and Rubber Technology, Cochin University of Science and Technology, Kochi, India. No part of this thesis has been presented for any other degree from any other institution.

Kochi

28-12-2002



Jacob Samuel

For I am grateful to...

I take this opportunity to express my hearty thanks and profound respect to my supervisors Dr. Thomas Kurian, and Prof. K. E. George, Department of Polymer Science and Rubber Technology, Cochin University of Science and Technology, for their valuable guidance, and unfailing inspiration, throughout the tenure of my research.

I express my sincere gratitude to Prof. Rani Joseph, Dr. Philip Kurian, Dr. Eby Thomas Thachil, Dr. Sunil K Narayanan Kuttu, Prof. (Retd.) A. P. Kuriakose for their personal interest and valuable advice.

I am grateful to Prof. K. T Mathew, Department of Electronics, Cochin University of Science and Technology for providing the opportunity to work in his research group. I am also thankful Dr. Joe Jacob, Research Associate, Department of Electronics, Cochin University of Science and Technology for his immense help during my stint there to carryout the dielectric measurements.

Thommachan Xavier, who has been with me for more than two years, gave solace and encouragement during hours of research is gratefully acknowledged. I am greatly indebted to Mr. Rajan George, Mr. Bobby Johnson George (R&D officer CEAT LTD), Mr. Soney Varghese, Dr. Rohith John, Mr. Bejoy, and Mr. Sunil for their valuable help during my research.

I appreciate the friendship of my co-researchers, Ushamani, Honey, Shiney, Merina, Bipin, Jaya, Lily, Lovely, Thomas, Rinku, Nisha and non-teaching staff, the Department of Polymer Science and Rubber Technology, Cochin University of Science and Technology for their whole-hearted support during the period.

The good wishes, support and encouragement of my family members, especially my parents, brothers, and sister-in law throughout the course of this work are gratefully acknowledged.

I owe greatly to CSIR for the award of Senior Research Fellowship.

Above all my praises are due to The Almighty, without the grace of whom the whole episode would have reduced to nothing.

Jacob Samuel

Contents

Abbreviations

Abstract

Glossary of symbols

Chapter 1: General Introduction	1
Chapter 2: Experimental	33
Chapter 3: Ionomers based on Styrene Butadiene Copolymers	48
Chapter 4: Effect of Fillers on the Properties of ZnS-SBR Ionomers	75
Chapter 5: Dielectric properties of ZnS-SBR Ionomers.....	87
Chapter 6: Technological Compatibilisation of the SBR/NBR Blends.....	114
Chapter 7: Conclusion and Future outlook	140

List of publications

* Detailed contents are given at the beginning of each chapter

Abbreviations

ASTM	-	American Society for Testing and Materials
CBS	-	N-cyclohexyl-2-benzothiazole sulfenamide
DCE	-	Dichloroethane
DSC	-	Differential Scanning Calorimetry
DMTA	-	Dynamic Mechanical Thermal Analysis
FTIR	-	Fourier Transform Infra Red
FTNMR	-	Fourier Transform Nuclear Magnetic Resonance
GHz	-	Giga Hertz
HAF	-	High Abrasion Furnace Black
HSR	-	High Styrene Rubber
ISM	-	Industrial, Scientific and Medical
Meq	-	Milliequivalents of sulphonic acid/100 g of rubber
NBR	-	Acrylonitrile-Co- Butadiene Rubber
Phr	-	Parts per hundred rubber
SBR	-	Styrene Butadiene Rubber
SEM	-	Scanning Electron Microscopy
TGA	-	Thermo gravimetric Analysis
TMTD	-	Tetra Methyl Thiuram Disulfide
TPE	-	Thermoplastic elastomer
UTM	-	Universal Testing Machine
XRFS	-	X-ray Fluorescence Spectroscopy
ZnS-SBR	-	Zinc Sulphonated Styrene Butadiene Rubber
ZnS-HSR	-	Zinc Sulphonated High Styrene Rubber

Abstract

Novel thermo-reversible zinc sulphonated ionomers based on styrene butadiene rubber (SBR), and high styrene rubber (HSR) were synthesized by sulphonation followed by neutralization with zinc. The sulphonate content of the ionomer was estimated by using x-ray fluorescence spectroscopy. Presence of sulphonate groups has been confirmed by FTIR and FTNMR spectra. The TGA results show improvement in the thermo-oxidative stability of the modified rubber. Both DSC and DMTA studies show that the incorporation of the ionic groups affect the glass rubber transition of the base polymer. Introduction of ionic functionality in to the base material improved the physical properties. Retention of the improved physical properties of the novel ionomers even after three repeated cycles of mixing and molding may be considered as the evidence for the reprocessability of the ionomer. Effect of particulate fillers (HAF black, silica and zinc stearate) on the properties of the zinc sulphonated styrene butadiene rubber ionomer has been evaluated. Incorporation of fillers results in improvement in mechanical properties. Zinc stearate plays the dual role of reinforcement and plasticization. The evaluation of dielectric properties of zinc sulphonated styrene butadiene rubber ionomers at microwave frequencies reveal that the materials show conductivity at semiconductor level. The real and imaginary parts of the complex permittivity increases with increase in ionic functionality. Use of the 38.5 ZnS-SBR ionomer as a compatibiliser for obtaining the technologically compatible blends from the immiscible SBR/NBR system has been discussed.

Glossary of symbols

E'	-	Storage Modulus
J	-	Heating Coefficient
$\tan \delta$	-	Loss tangent or dissipation factor
T_g	-	Glass rubber Transition Temperature
ϵ'	-	Dielectric Constant (Real Part)
ϵ''	-	Dielectric Constant (Imaginary Part)
σ'	-	Complex Conductivity (Real Part)
σ''	-	Complex Conductivity (Imaginary Part)
α_f	-	Absorption coefficient
δ_f	-	Skin depth

Chapter 1

General Introduction

- 1.1 *Introduction*
 - 1.2 *Reasons for interest in ionomers*
 - 1.3 *Historical background*
 - 1.4 *Definition of ionomers*
 - 1.5 *Composition of an ionomer*
 - 1.6 *Synthesis of ionomers*
 - 1.7 *Structure of ionomers*
 - 1.8 *Classification of ionomers*
 - 1.9 *Properties of ionomer*
 - 1.10 *Application of ionomers*
 - 1.11 *Recent studies on ionomers*
 - 1.12 *Scope and objective of the work*
 - 1.13 *Conclusion*
 - 1.14 *References*
-

1.1. Introduction

Appreciable enhancement in mechanical properties of relatively non-polar polymers, and copolymers can be achieved by the introduction of ionic groups¹⁻⁴. Ion-containing polymers are referred to as ionomers when the concentration of ionic groups is low (10 – 15 mol%). By controlling the many variables that are involved such as the ion content, degree of neutralization, nature of counter ion, and additives it is possible to prepare ionomers that have wide range of properties suitable for industrial applications⁵⁻¹⁶.

Ionic thermoplastic elastomers have the unique ability to behave as cross-linked elastomers at ambient temperatures, and to melt and flow at elevated temperatures like thermoplastics. These materials are emerging as important industrial polymers as they could be processed by thermoplastics processing techniques avoiding a vulcanization step, and recycled.

Over the past several years there has been considerable interest in sulphonate containing ionomers, and systems based on several thermoplastics and elastomers have been described¹⁷⁻³⁷. It has been reported that the sulphonate-ionic interactions are stronger than the corresponding carboxylate – ionic interactions in a low polarity polymer matrix, because of the higher degree of polarity inherent in the sulphonate system²⁷.

1. 2. Reasons for interest in ionomers

The unique properties of ionomers are sources of growing and continuing industrial and academic interest. The study of ionic interactions in polymer systems represents one of the liveliest areas of research activity in modern polymer science. The industrial interest is due to the fact that ionic interactions permit control of the physical properties

of polymers, even at low ionic concentrations. The modulus, glass transition temperature, viscosity, melt strength, transport and many other properties are influenced dramatically by ion incorporation. A very important reason for industrial interest is the strength of columbic interactions, which may permit the use of ionomers as additives in composites, as tie coats between two dissimilar polymer layers, in miscibility enhancement, and in the modification of mechanical and rheological properties. The presence of ions enhances conductivity of these materials above their glass transition temperatures. This feature is of interest in the design of solid-state electrolytes. Another unique feature of ionomers is their super perm selectivity. The relationship between chemical structure, morphology, and physical properties of the materials are of great academic interest. Thus exploration of ionomers is a very vital tool for the modification and control of the properties of polymers.

1.3. Historical background

Since 1965, when the term ionomers was coined³⁸ the field has grown exponentially. One example of an early synthesis of a material of this type is the work by Littman and Marvel³⁹ on polymers that were later named ionenes⁴⁰. Shortly thereafter, a carboxylated elastomer based on butadiene and acrylic acid copolymers was vulcanised with sulphur using ZnO as accelerator⁴¹. Ionic crosslinks were apparently not recognized at that time. However, not long after that, it was noted that the incorporation of carboxylate groups in to elastomers exerts a major influence on their properties⁴². The polymeric behaviour of halatotelechelecs was explored as early as 1944⁴³. Work on styrene ionomers were started in the mid 1960s⁴⁴. In the 1960s and early 1970s, a number of investigators explored the structure and properties of these ionomers. Another important event was the appearance of a patent on ionic polyurethanes⁴⁵.

A crucial event in 1966 was the appearance of a patent on ethylene ionomers under the trade name surlyn⁴⁶ by Du Pont. The existence of hard ionic clusters in carboxylated elastomers was proposed in 1968 by Tobolsky et al.⁴⁷. The new decade saw the appearance of the first theoretical paper on ionomers of Eisenberg¹⁸. The same year that saw the announcement of perfluorosulphonated materials (Nafion, Du Pont).

Dasgupta reported ionomers based on polyvinyl butyral⁴⁸ in 1992. Reports of other ionomers based on random ethylacrylate zwitter ionic copolymer⁴⁹, polyurethane anionomers⁵⁰, styrene-coumarin copolymer ionomers⁵¹, poly(1,4-butylene isophthalate)⁵² polyester ionomers⁵³ etc include the valid contributions of the period extending from 1991 to 1996.

1.4 Definition of Ionomers

In 1965, Rees and Vaughan defined ionomers as olefin-based polymers containing a relatively small percentage of ionic groups in which "strong ionic interchain forces play the dominant role in controlling properties"⁵⁴. Due to the introduction of new polymer backbones and more ionic character being incorporated into ionomers, it was recognized that there were problems with this definition. These new ionomers behaved very similarly to polyelectrolytes, especially in solvents with high dielectric constants. This confusion between polyelectrolytes and ionomers lead to a new definition by Eisenberg and Rinaudo⁵⁵ in 1990. The new definition stated that ionomers are "polymers in which the bulk properties are governed by ionic interactions in discrete regions of the material (ionic aggregates)", specifically in materials where the ion content is less than about 15 mol %. This new definition attributes the behavior of ionomers to their properties, thereby differentiating an ionomer from a polyelectrolyte.

1.5 Composition of an Ionomer

Typically, ionomers are low dielectric copolymers comprised of nonionic repeat units and ionic groups. Alkali metals, alkaline earth metals and transition metals, for example, act as counter ions for these acid (anionic) polymers. Distribution of these ionic groups along the backbone chain is an important variable. The ionic groups can be synthetically placed randomly or systematically within the primary polymer chain as end groups on polymer chains or as pendant groups in a copolymer^{1,56}. Regardless of the ionic group placement, the groups facilitate the formation of ionic aggregates. The ionic aggregates act as effectively physical crosslinks, which give rise to ionomers with thermoplastic characteristics.

1.6 Synthesis of Ionomers

There are two main techniques for the preparation of ionomers of practical interest: (i) copolymerization of a low levels of functionalised monomer with an olefinically unsaturated comonomer, and (ii) direct functionalisation of a preformed polymer⁵⁷. Ionomers of commercial interest have either carboxylate or sulphonate groups as the ionic species. Other salts such as phosphonates, sulphates, thioglycolates, ammonium or pyridinium salts have been reported⁴.

Typically, carboxylate ionomers are prepared by direct copolymerisation of acrylic or methacrylic acid with ethylene, styrene or similar comonomers by free radical copolymerisation⁴⁶. Weiss et al.⁵⁸⁻⁶¹ prepared ionomers by a free radical emulsion copolymerisation of sodium-sulphonated styrene with butadiene. Allen et al.⁶² prepared copolymer of n-butylacrylate with salts of sulphonated styrene. Salamone et al.⁶³⁻⁶⁸ copolymerised styrene, methylmethacrylate, or n-butyl acrylate with a cationic-anionic monomer pair, 3-methacrylamidopropyltrimethylammonium 2-acrylamide-2-methylpropane sulphonate.

The direct functionalisation of preformed polymers has been the common method for the preparation of sulphonate ionomers. Makowski et al.,⁶⁹ prepared lightly sulphonated polystyrene and ethylene-propylene diene terpolymers by reaction with acetylsulphate in homogeneous solution. Bishop et al.⁷⁰ described the sulphonation of polyetheretherketone with chlorosulphonic acid or sulphuric acid. Zhou and Eisenberg⁷¹ prepared sulphonated polycis1,4-polyisoprene using acetylsulphate. Rahrig et al.⁷² sulphonated polypentenamer using a 1:1 complex of SO₃ with triethylphosphate. Peiffer et al.⁷³ sulphonated a copolymer of styrene and 4-vinyl pyridine polyampholytes with acetyl sulphate. Huang et al.⁷⁴ made zwitterionomers by reacting a polyurethane segmented copolymer with γ -propane sultone. This was converted to an anionomer⁷⁵ by reaction with metal acetate. Kennedy and coworkers⁷⁶⁻⁷⁸ prepared linear and triarm star telechelic sulphonated polyisobutylene by heterogeneous sulphonation of an olefin-terminated polyisobutylene with acetyl sulphate. Omeis et al.⁷⁹ synthesised telechelic sulphonated polystyrene and polybutadiene by terminating an anionic polymerization with 1,3-propane sultone. Sulphonation of EPDM has been conducted in the molten state, in an extruder using the same sulphonation agents, which are typically employed in solution⁸⁰. The continuous melt sulphonation was conducted in oil extended EPDM at temperatures in the range 90°C to 100°C. The rapid reaction involving the unsaturation in EPDM leads to conversions of 80 to 100%, with residence times of about 6 to 12 minutes. Neutralization with metal stearate was conducted in the extruder. The extruder reaction technique offers the advantages of shorter reaction times, elimination of solvent handling problems, and simplification of the polymer finishing steps.

1.7 Structure of Ionomers

The first successful theoretical attempt to deduce the spatial arrangement of salt groups in ionomers was that of Eisenberg¹⁶. The past few years have witnessed an

almost explosive growth of research in to the structure of ionomers. A wide range of ionomers have been investigated by techniques such as small angle X-ray⁷³⁻⁷⁵⁸¹⁻⁸³, and neutron scattering⁸⁴, mechanical and dielectric measurements⁸⁵⁻⁸⁶ Mossbauer⁸⁷ ESR⁸⁸, IR⁸⁹ Raman⁹⁰, and NMR⁹¹ spectroscopy; solution properties and electron microscopy⁹²⁻⁹³. A number of morphological models have been proposed in order to account for the observations from a wide variety of experimental techniques⁹⁴⁻⁹⁵. These techniques have provided evidence for strong molecular associations of the ionic groups that lead to microphase separated ion-rich domains.

1.7.1 Multiplet-cluster concept

Multiplets are group of few ion pairs that are tightly aggregated and exclude all non-ionic material. Geometric constraints limit their size to 0.6 nm diameter. The strength of electrostatic interaction between ion pairs, and the ion content, which determines the proximity of ion pairs to one another, are the important parameters that affect multiplet formation. The characteristics of the host polymer such as low dielectric constant and low Tg favour ionic aggregation, whereas high dielectric constant and high Tg inhibit multiplet formation. Each ion pair in a multiplet effectively anchors the polymer chain at the point to which it is attached. Hence, the mobility of the polymer chain in the immediate vicinity of the multiplet is expected to be greatly reduced relative to that of a chain in the bulk polymer, with the mobility increasing gradually with increasing distance from the multiplet.

Clusters are collections of several multiplets that form a domain locally rich in ionic material but containing a significant fraction of non-ionic material as well. Clusters are envisioned to be of the order of 5 to 10 nm in diameter. The number of ionic groups existing in clusters is strongly dependent on polarity of the polymer matrix, ionic functionality and the temperature. At low ion content with a low polarity matrix, only

multiplets are favoured, whereas with increasing ion content, cluster formation is favoured.

1.7.1.1 Shapes of multiplets

As was expected, the shape of the multiplets in a material such as sulphonated polystyrene neutralized with Zn^{2+} was found to be spherical in a study by Li et al.⁹⁸, who used high-voltage electron microscopy to observe the ionic domains. The existence of non-spherical multiplets has been postulated⁹⁹, they have been shown to exist in random ionomers in bulk in only one system¹⁰⁰. The structures of multiplets in some telechelics¹⁰¹, ionenes^{102,103} and perfluorosulphonate ionomers in solution^{104,105} were reported to be non-spherical. At higher ion content restricted mobility regions of independent multiples overlap and exceed the threshold size for independent phase behaviour ($50-100 \text{ \AA}^0$) at which they exhibit their own Tg. This region of restricted mobility is the cluster¹⁰⁶.

1.7.1.2 Cluster models

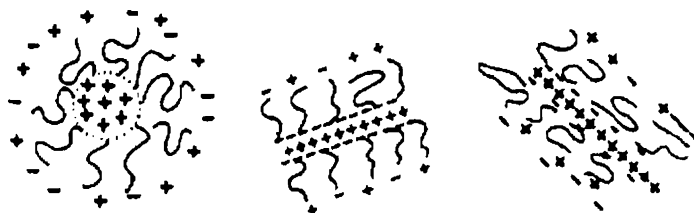
(i) Hard-sphere model

In an early study, Delf and MacKnight¹⁰⁷ assigned the SAXS peak to scattering from the ionic aggregates. Subsequently, Marx et al¹⁰⁸. suggested that the peak arises from the ionic aggregates, which were taken to be small particles located on a paracrystalline lattice. This treatment provided a quantitative fit to the experimental small-angle x-ray data. A similar model was proposed by Binsbergen and Kroon¹⁰⁹. In their model, the scattering moieties are points at the centers of randomly packed spheres. Yarusso and Cooper¹¹⁰ proposed a modified hard-sphere model in which the multiplets have a liquid like order at a distance of closest approach, determined by the hydrocarbon layer attached to and surrounding each multiplet. This model was in good agreement with the SAXS profiles and assumed the existence of multiplets of high

electron density surrounded by a layer of hydrocarbon material of much lower electron density immersed in a medium of intermediate ion content, which was equivalent to a hard sphere diameter somewhat larger than that of the multiplet itself.

(ii) Core-Shell model

Macknight et al.¹¹¹ developed a model based on the radial distribution function of scattered x-rays for the partially neutralized cesium salt of polyethylene-co-methacrylic acid. This model assumes that the ionomer pairs form a core that is surrounded by a shell of material of low electron density, which is, in turn, is surrounded by another shell of somewhat higher electron density. The central core is taken to have a radius of 8-10 Å and to contain ~50 ion pairs. The hydrocarbon shell surrounding this multiplet is in the order of 20 Å . A modification was suggested by Roche et al.⁹⁹, who suggested a lamellar sandwiched geometry (Scheme 1.1).



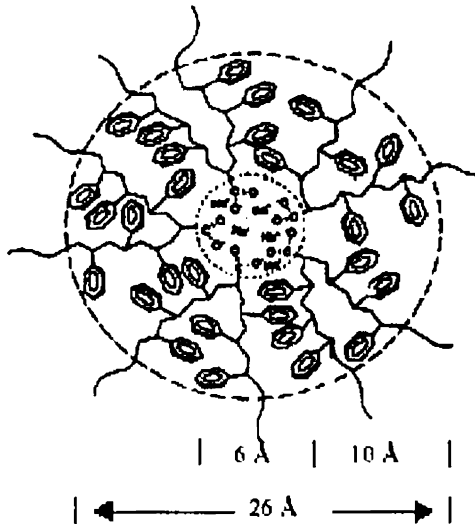
Scheme 1.1 Intracluster Lamellar Shell core models

The central lamella of high electron density material (high ionomers content) is sandwiched between lamellae of low electron density hydrocarbon material, which is in turn sandwiched between layers of intermediate electron density. Interlamellar distances are taken to be responsible for the ionic peak.

(III) Eisenberg-Hird-Moore model

The models described above serve as the starting point for the new model, called Eisenberg-Hird-Moore (EHM) model¹¹². The EHM model is shown in the scheme 1.2. One of the novel features of the model is that the mobility of the material immediately surrounding the multiplet is reduced relative to that of the bulk material. There are several reasons for this behavior. One is the simple immobilization effect owing to the anchoring of chain to the multiplet.

The mobility of a species is a function of its molecular weight. Anchoring a chain to multiplet increases the effective molecular weight of the segment adjacent to the multiplet, which reduces the mobility. Another factor is crowding of chains. Because the electrostatic energy released in the process of multiplet formation is considerable and the surface energies are important, a certain amount of



Scheme 1.2. A multiplet in poly(S-co-MANa) ionomer

crowding in the immediate vicinity of the multiplet is to be expected due to the driving forces, which tend to enlarge the multiplet¹¹³. Finally it is not unreasonable to expect a certain amount chain extension in the immediate vicinity of the multiplet¹¹⁴, which helps the multiplet to accommodate a larger number of chains. All these factors contribute to a reduction in the mobility.

1.8 Classification of Ionomers

1.8.1 Thermoplastic Ionomers

(I) Ionomers based on poly (ethylene)

These are copolymers with pendant carboxylate groups in which the poly(ethylene) backbone is the major component. The most widely used ionomers of this class have been based on poly (ethylene-co-methacrylic acid) (EMAA). Recently the popularity of poly (ethylene-co-acrylic acid) (EAA) series ionomers too is on the rise. The methacrylic or acrylic acid content of these ionomers is generally in the range 3-10 weight % .The metal cation used for neutralization may be monovalent (e.g. Na⁺ or Li⁺), divalent (e.g. Ba²⁺, Mg²⁺ or Zn²⁺), or trivalent (e.g. Al³⁺). The characteristic properties of these materials include excellent tensile properties, good clarity, and high melt viscosities¹¹⁵. Another property of practical interest is the marked reduction in haze after neutralization. In the case of conventional low-density polyethylene, the polymer is translucent owing to spherulitic crystallinity. In the case of ionomers; degree of crystallinity is comparable to that of conventional polyethylene. However, ionic interactions are invoked to effect two changes: nucleation of crystallites, and increase in viscosity that slows down the growth of crystallites into spherulites¹¹⁶.

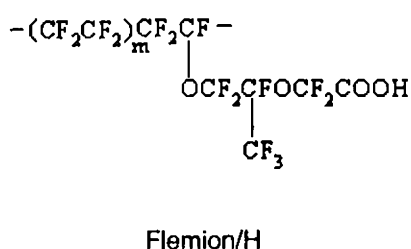
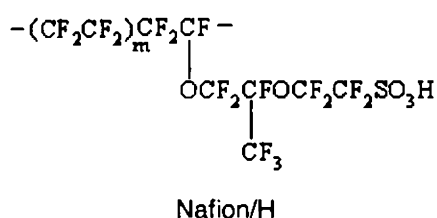
(II) Ionomers based on Poly (styrene)

Polystyrene-based ionomers are of two types: carboxylated derivatives and sulphonated derivatives. The first group includes poly (styrene - co - methacrylic acid)

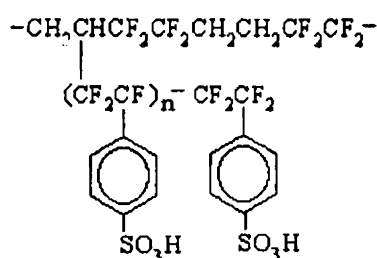
containing various amounts of metal carboxylate groups^{10,60,61}. Metal salts of sulphonated polystyrene, derived from the sulphonation of polystyrene are described in recent patents and publications. In this process, the molecular weight of the polymer back bone does not change significantly, but extremely strong, temperature-resistant ionic networks are created at low (0.5-3 mole %) ionic concentrations. The observed sulphonate ionic interactions are stronger than the corresponding carboxylate ionic interactions in a low polarity polymer matrix, because of the higher degree of polarity inherent in the sulphonate system and the consequent increase in the strength of the ion-pair associations^{34,35,62-67}.

(III) Ionomers based on poly (tetrafluoroethylene)

The ionomers based on polytetrafluoroethylene (PTFE) systems are an important class of ionomers; because they are extensively used as membranes in the chlor-alkali industry and in fuel cells¹⁹⁻²¹. The first commercial material of this class has the trade name of Nafion (E.I. Du Pont de Nemours & Co.)



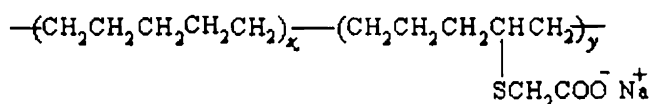
The other materials in this class are Flemion (Asahi Glass) and a short side chain system perfluorosulphonate ionomer (PFSI; Dow chemical). Nafion is thought to be too expensive for use in fuel cells for transportation. This situation can be solved by the introduction of new materials. One promising approach is that leading to Raymion² and found their performance in electrolysis cell to be substantially comparable.



Raymion

(iv) Polypentenamer

Polypentenamer is a noncrystalline polymer, where as its hydrogenated form is partially crystalline. A series of studies on hydrogenated functionalized polypentenamers were performed by Macknight's group using materials containing carboxylate, sulphonate and phosphate. The synthesis of the carboxylated polypentenamer and hydrogenation procedure were described by Sanui et al ^{128,129}. The sulphonated polypentenamers and their hydrogenated derivatives were prepared by Rahring et al ¹³².



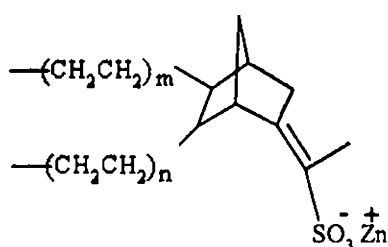
1.8.2 Elastomeric Ionomers

(I) Carboxylated elastomers

Carboxylated elastomers are prepared by incorporation of acrylic and methacrylic acids during free radical copolymerization. Typical examples of such systems are the metal salts of styrene butadiene acrylic acid, butadiene-acrylonitrile-acrylic acid, and butadiene-acrylic acid copolymers. Typically less than 6 % of carboxylated monomer is employed in order to preserve the elastomeric properties inherent in these systems¹¹⁷⁻¹²⁰.

(II) Sulphonated ethylene-propylene-diene terpolymers

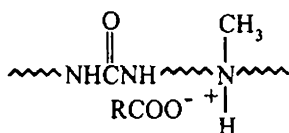
Sulphonate groups are introduced into the ethylene-propylene-diene monomer (EPDM) systems via electrophilic attack of the sulphonation reagent on the polymer unsaturation.



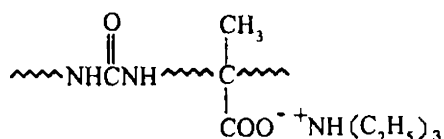
Neutralized sulphonated EPDM with few metal sulphonate groups is a thermally stable strongly associating ionomer with properties approaching those of the covalently crosslinked EPDM²⁸⁻³¹.

(III) Polyurethane Ionomers

The polyurethane based ionomers consist of large family of materials that shows much more complex behavior than do the styrene ionomers because of the heterogeneity of the backbone, i.e. the presence of both soft and hard segments. The synthesis and characterization of ionic polyurethane have been reported⁹²⁻⁹⁶. Typically the polyurethane zwitterionomers are prepared from a pre-polymer and a diisocyanate in the presence of a tertiary amine containing diol extender, such as N-methyl diethanolamine, dissolving the polyurethane produced in dimethyl acetamide and adding the appropriate amount of γ propane sultone. Reaction of zwitterionomer with the appropriate metal acetate results in a metal sulphonyl ion pair, and reduction to the tertiary amine of the ammonium ion, with the generation of methyl acetate.



Cationic urethane



Anionic urethane

1.8.3 Other Ionomers

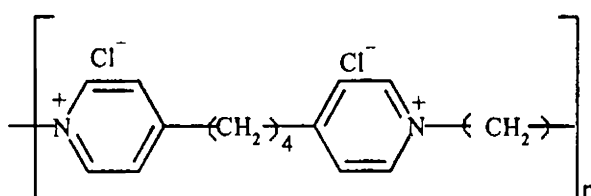
(I) Halato-telechelic Ionomers

In telechelic polymer systems, the acid functionality terminates both ends of the polymer chain^{121,122}. Teyssie and co-workers have converted carboxyl terminated polymers to salt forms, which they refer to as "halato-telechelic polymers", by neutralizing with metal alkoxides in appropriate solvents, commonly toluene¹²³⁻¹²⁵. Kennedy, Wilkes and co-workers¹²⁶⁻¹³⁰ have reported the synthesis of halato-telechelic polyisobutylene sulphonate ionomers. The sulphonation of linear telechelic polyisobutylene diolefins has been carried out in a solution in hexane at room

temperature with excess of acetyl sulfate generated in situ by the addition of sulphuric acid to acetic anhydride, and after reaction the neutralization is accomplished in THF solution with ethanolic sodium hydroxide.

(II) Ionenes

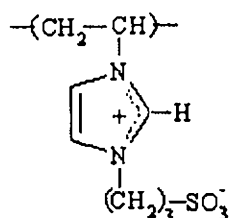
Ionenes are ionic polymers in which precise spacing of ionic groups along the backbone is possible, i.e., a quaternary ammonium or pyridinium ion is located on the backbone⁴⁰.



The structure contains aliphatic or aromatic sequences. High molecular weight analogs of these materials can also be made, i.e., materials in which the spacing between the ammonium groups are oligomers or low molecular weight polymers. Some ionenes have been studied for their bacteriostatic and bactericidal activity. The tetra methyl ionene has been evaluated for its pharmacological and antiheparin action. Ionenes with segments of polypropylene oxide in the backbone have been evaluated as thermoplastic elastomers³⁴. An important paper in the field of ionenes was published by Klun¹³¹ et al and a more recent study of ionenes came from Wilkes group¹³².

(iii) Zwitter Ionomers

In the zwitterionomers the anion and cation are attached to each other and to the main chain. Thus members of this class have similar behaviour in many respects. The first systematic study of a zwitterionomeric system was that of Graives et al.,¹³³⁻¹³⁴ who investigated copolymers of dimethylsiloxane and 4,7-diazaheptyl4,7-di(3-propane-sulfonate) methylsiloxane. Other zwitterionomers based on polyvinylimidazolium sulphobetaine) was studied by Salamone et al.¹³⁵



(iv) Polyelectrolyte complexes

It has been known for a long time that the mixing of aqueous solutions of anionic and cationic polyelectrolytes results in a complex of the two polymers with properties different from either. The polyelectrolyte complexes are generally insoluble, and behave like cross-linked non-ionic polymers^{136,137}. The molecular structure of polyelectrolyte complexes depends upon the special distribution of ions along the two contributing polymer chains, but for simplicity it may be visualized as ladder-like. These materials have potential applications in membrane processes where special permselective properties are required.

(v) Block Ionomers

Block ionomers are typically di or triblock in nature, i.e.; block copolymer in which one block consists of a completely nonionic material and the other segment or segments consisting of a random ionomer of relatively low ionic content, and also a different type

of block copolymer in which each of the groups in the ionic block is actually ionized^{138,139}. Gouin et al.¹⁴⁰ investigated the morphology of compression moulded poly4-vinylpyridinium methyl iodide-block polystyrene-block –poly4-vinyl pyridinium methyl iodide by SAXS and SANS.

(vi) Glass ionomers

Most glass ionomers are based on calcium aluminosilicate glasses¹⁴¹. The aluminosilicate poly (alkenoic acid) (ASPA) ionomer is prepared by fusing a mixture of calcium oxide or fluoride, alumina and silica with aluminum phosphate and cryolite as flux at 1000-1500°C. Several methacrylate/glass ionomer hybrid materials are now available for clinical use as restorative filling materials. However, the long-term resistance of these materials to physical degradation in the humid oral environment is under investigation.

1.9. Properties of ionomers

1.9.1 Glass transition temperature

The glass transition temperature (T_g) is one example of a property influenced by the polymer's ionic character. T_g is related to the amount of ionic groups in the ionomer. The concentration of ionic groups present dictates the extent of area with restricted mobility. At low ion content, no overlap of the restricted mobility regions occurs and single T_g is expected. This is because the few multiplets inter-dispersed among the bulk exhibit characteristics similar to the bulk material; the multiplets act only as crosslinks and do not exhibit behavior independent from the bulk. For a polymer with high ion content a large overlap of the restricted mobility regions is apparent and thus two T_gs are expected, one for the multiplet domains and one for the bulk behavior¹⁴³.

1.9.2 Influence of aggregate formation on mechanical properties

The aggregate formations, whether multiplets or clusters, give rise to novel physical properties in ionomers. At room temperature ionic thermoplastic elastomers show higher modulus and tensile strength than their base material owing to the presence of ionic domains, which act as physical crosslinks¹⁴⁴⁻¹⁴⁶.

1.9.3 Reinforcement and plasticisation

The effect of fillers on the mechanical properties of ionic elastomers is of great importance because fillers could be used very effectively to enhance the physical properties such as tensile strength, modulus, and tear strength. Fillers such as HAF, silica and zinc stearate could improve stress-strain properties and melt viscosity. Incorporation of fillers seems to strengthen the physical crosslinks arising from the ionic aggregates. There are two possibilities for plasticization of ionomers namely the plasticization of ionic phase, and plasticisation of hydrocarbon phase (backbone). In a study by Kurian et al reported that paraffinic oil is plasticiser for the hydrocarbon phase and zinc stearate is known to act as a plasticiser for ionic phase of zincsulphonated EPDM containing HAF black¹⁴⁷

1.9.4 Dielectric properties

The dielectric behaviour of a polymer is determined by the charge distribution and the statistical thermal motion of polar groups¹⁴⁸. It is therefore evident that the chemical structure should be the basic factor for the determination of dielectric behavior. Polymers that have polar bonds in their chains would be expected to have high dielectric constants.

1.9.5 Blends and Compatibilization

A wide range of ionic interactions enhances compatibility of the blend components. Ionic groups in the polymers are capable of creating specific interactions between the

polymers in the blend¹⁴⁹. Several different types of ionic interactions can be used to control miscibility. They are ion-ion, hydrogen bond-assisted ion-ion, complimentary ion pair-ion pair, identical ion pair-ion pair, ion-dipole, and ion-coordination. The strongest interaction may lead to a homogeneous material at a relatively low ion content¹.

1.9.6 Reprocessability

Ionic elastomers have the unique ability to behave as crosslinked elastomers at ambient temperatures and to melt and flow at elevated temperatures like thermoplastics. However, the ionic crosslinks are thermoreversible, particularly under shear, by the ion-hopping mechanism, which allows the viscosity of ionomers to be decreased to such a level that they could be easily processed¹⁵⁰. The ionic elastomers can be reprocessed by mechanical recycling without deterioration in their properties.

1.10. Application of Ionomers

Ionomers are used in a wide range of applications at present and many more are being developed for the future.

1.10. 1 Elastomers

Ionic elastomers with enhanced elastomeric green strength provides a new class of thermoplastic elastomers. The ionic elastomer based on metal sulphonated EPDM could be compounded to enhance its suitability in many applications^{1,4}. At high temperatures, the ionic interactions within the multiplets are loosened; the addition of zinc stearate reduces viscosity of the melt even further and allows the material to be injection molded. On cooling the ionic crosslinks were re-established. These materials

can be extended with usual additives, such as carbon black and oil¹⁵¹. These materials are widely used as roofing membranes.

1.10. 2 Plastics

Ionomers have wide applications as bulk plastic materials. Examples of such applications include golf ball covers, bowling pin covers, bumper guards, side molding strips and shoe parts, especially for the athletic footwear¹⁵². In all of these applications two of the required properties are moldability and toughness. Furthermore, by appropriate use of both zinc and sodium ionomers in a blend form, the cold crack problem encountered in the sodium ionomer and low rebound problem encountered in the zinc ionomers have been effectively eliminated.

1.10. 3 Adhesives

Ionomers such as carboxylated and sulphonated systems have been used as adhesives¹⁵³. Both solvent-based and pressure-sensitive type have been commercialised. The butylene ionomers and EPDM-based systems are frequently used.

1.10. 4 Magnetic recording media

Polyurethane ionomers are extensively used in magnetic recording media¹⁵⁴. Ionic urethanes are prepared as aqueous dispersions; they serve both as a binder and as a dispersing agent in magnetic tape formation.

1.10. 5 Imaging systems

Ionomers found wide applications in the area of imaging systems. They are used as antistatic agents in silver halide photography to protect light sensitive emulsion layers¹⁵⁵. Electrophotography makes use of ionomers primarily as a binder for

pigments in the toners, in which they act as compounds that determine the charge of the toner during contact charging¹⁵⁶.

1.10. 6 Floor polish

Based on the idea of ionic cross-linking of water-soluble polymers or emulsions several floor polishes have been developed. Zinc carboxylated copolymers provide a stable and durable floor wax¹⁵⁷.

1.10. 7 Packagings

The applications of ionomers in packaging are currently extensive¹⁶². The advantages of ionomers, especially ethylene ionomers, as packaging materials are their oil and chemical resistance, flex resistance, resistance to impact, ability to be heat sealed under a broad range of conditions, adhesion to wide range of substrates, excellent optical properties, and their high melt strength.

1.10. 8 Coatings

One application of ionomers involves the direct coating on to glass objects to reduce the danger of breakage. A wide range of applications involves polyurethane emulsions. Ionomers can also be used as coatings in fertilizer industry, in which zincsulphonated EPDM is used as a coat for microspheres of urea¹⁵⁸, and the deposition of the ionomer on the fertilizer particle can be arranged to produce maximum release at the height of the growing season when it is needed.

1.10. 9 Membranes and thin films

One of the most important applications of ionomers has been as membranes exhibiting superpermselectivity^{4, 159}. Perfluorosulphonates, and perfluorocarboxylates are typical examples. These materials show exceptional stability, resembling that of PTFE, in both

thermal and electro-chemical applications. Sulphonated form of perfluorinate ionomer is used in the fuel cell as a solid polymer electrolyte that keeps oxygen and hydrogen apart.

1.10. 10 Catalysts

Olah's group¹⁶⁰ found that the acid form of the perfluorosulphonic acid can be used as superacid catalyst. For example, perfluorosulphonic acid can act as a catalyst in some organic reactions such as pinacol rearrangement, deacetylation, and decarboxylation of aromatic rings.

1.10. 11 Asphalt Ionomers

The asphalt ionomers prepared by modification of asphalt are useful as road paving materials that retain a very high fraction of their strength when wet. The ionomers and their original acid copolymers and derivatives can be combined with asphalts and other components such as aggregates (rock) and reclaimed rubber. The use of relatively small amounts of ethylene acrylic acid copolymers and their ionomers can be improve adhesion of rock and asphalt (bitumen)¹⁶¹. Marzocchi and coworkers used organic polyacrylic acid as crosslinking agents between asphalt and rubbery polymer containing reclaimed rubber¹⁶²

1.11 Recent studies on ionomers

Development on ionomers is a promising and challenging area of modern polymer science and technology. Some important studies in the field of ionomers, during the year 2001, include the synthesis and characterization of ion-conducting polymer systems based on EPDM blends¹⁶³, synthesis and characterization of styrene grafted NR ionomers¹⁶⁴, and kinetic study and characterization of sulphonated poly (etheretherketone) (PEEK)¹⁶⁵. The current year has been witnessing a large number

of studies on ionomer systems. The influence of carboxylic group content on properties of ionic elastomers based on carboxylated nitrile rubber (XNBR) and zinc peroxide¹⁶⁶, ion aggregation in the polysiloxane ionomers bearing pendant quaternary ammonium groups¹⁶⁷ are some of the most recent publications. Wetting properties of polystyrene ionomers treated with plasma source ion implantation¹⁶⁸ and simulation study on molecular relaxation in ionomer melts¹⁶⁹ also have been reported of late.

1.12 Scope and objective of the work

The investigations on the ionomers present a promising and challenging area of modern polymer science and technology. Though ionomers are emerging as important commercial polymers; they have many intriguing scientific characteristics. The forgoing discussion shows the growing interest in ionomers as materials with unique properties.

The ionic thermoplastic elastomers differ from conventional rubbers in that the presence of ionic aggregates provide strong physical crosslinks at ambient temperatures, but they become soft at elevated temperatures permitting melt processing. One of the major attractions of the materials is the possibility of reprocessability.

The main objective of the present investigations is to synthesis ionic thermoplastic elastomers based on styrene butadiene rubber (SBR), and high styrene rubber (HSR). The unique features of the new ionomers could be best appreciated by comparing their properties with those of base materials.

The effect of fillers on the properties of elastomers is of great interest because fillers could be used very effectively to enhance the physical properties. The effect fillers on the properties of ionic elastomer based on SBR is an aim of the present study.

There is a real need for better materials of intermediate conductivity (10^{-9} S/cm to 10^{-2} S/cm) for variety of applications. The evaluation of dielectric properties of materials is important in this aspect. The dielectric properties of the ionomer based on SBR in the microwave region have been studied.

The role of ionomers as a compatibiliser in blends is a new area of research. In the present investigation the compatibilising effect of new ionomer based on zinc sulphonated SBR in SBR/NBR blends have been studied.

1.13 Conclusion

Review of the literature revealed that ionic interactions have been used to modify the properties of polymers. Ionomeric associations dramatically modify polymer properties over a wide range of modulus, melt viscosity and transition temperatures. Multiple synthetic approaches to ionomeric elastomers exist and are commercially viable. Some of these have been discussed here.

1.14 References

1. Eisenberg, A., Kim, J-S., in Introduction to Ionomers. John Wiley & Sons, Inc. New York, 1998.
2. Tant, M.R., Mauritz, K.A., Wilkes, G.L., Eds.; Chapman and Hall: New York, 1997.
3. Jacob, S., Thommachan, X. and Kurian, T., *Progress in Rubber and Plastics Technology*, **16**, 1 (2000).
4. Schlick, S., "Ionomers: Characterization, Theory and Applications" (New York: CRC Press, 1996.
5. Pineri, M., Eisenberg, A., Eds. "Structure and Properties of Ionomers"; NATO ASI series C, 198; Reidel: Dordrecht, The Netherlands, 1987.
6. Salmen, L., Htun, M., Eds; "Properties of Ionic Polymers, Natural & Synthetic", STFI meddelande; Stockholm, 1991.
7. Khokhlov, A. R., Dormidontova E. E., *Physics - Uspekhi* **40**, 109 (1997).
8. Ibarra, M., Alzorritz, *J.Appl. Polym. Sci.*, **83**, 605-615 (2002).
9. Zuoxin Huang, Yunzhao Yu, Ying Huang, *J.Appl. Polym. Sci.* **82**, 3099-3104 (2001).

10. Burke, L. M., Khan, I. M., *Macro. Chem. and Phys.* **201**, 2228-33 (2000).
11. Jackson, D. A., Koberstein, J. T., Weiss, R. A., *J. Polym. Sci.: Polym. Phys.*, ; **37**, 3141 (1999).
12. Deimede, V.A.; Fragou, K.V.; Koulouri, E.G.; Kallitsis, J.K. and Voyiatzis, G.A.; *Polymer*, **41**, 9095 (2000).
13. Genies, C., Mercier, R., Sillion, B., Cornet, N., Gebel, G. and Pineri, M., *Polymer*, **42**, 359 (2001).
14. Tong, Z. and Gao, B.R., *Polymer*, **42**, 143 (2001).
15. Kalhor, M.S., Gabrys, B.J., Zajac, W., King, S.M. and Peiffer, D.G.; *Polymer* **42**, 1679 (2001).
16. Eisenberg A., *Macromolecules*, **3**, 147-154 (1970).
17. Fitzgerald, W. E., Nielsen L. E., *Proc. R. Soc. Ser. A.*, **282**, 137 (1964).
18. Ide, F., Kodama, T., Hasegaawa, A., Yamamoto, O., *Kobunshi Kagaku* **26**, 873 (1969).
19. Kim, J. -S., Jackman, R. J., Eisenberg, A., *Macromolecules*, **27**, 2789 (1994).
20. Kim, J. -S., Wu, G., Eisenberg, A., *Macromolecules*, **27**, 814 (1994).
21. Hird, B., Eisenberg, A., *Macromolecules*, **25**, 6466 (1992).
22. Gauthier, M., Eisenberg, A., *Macromolecules*, **23**, 2066 (1990).
23. Rigdal, M., Eisenberg, A., *J. Polym. Sci. Polym. Phys. Ed.*, **19**, 1641 (1981).
24. Lundberg, R. D., Makowski, H. S. Eisenberg, A., Ed., " Ions in Polymers", *Advances in chemistry* **187**, American Chemical Society: Washington, DC, chapter 2, 1980.
25. Weiss, R. A., Fitzgerald, J. J., Kim, D., *Macromolecules*, **24**, 1071 (1991).
26. Hara, M., Jar; Sauer, J. A., *Polymer*, **32**, 1622 (1991).
27. Clas, S. -D., Eisenberg, A., *J. Polym. Sci. B Polym. Phys.*, **24**, 2743 (1986).
28. Makowski, H. S. , Agarwal, P. K., Weiss, R. A., and Lundberg, R. D. , *Polym. Prepr.* **20**, 281 (1979).
29. Agarwal, P. K., and Lundberg, R. D., *Polym. Prepr.*, **23**, 58 (1982).
30. Lundberg, R. D., Agarwal, P. K., and *Polym. Prepr.* **23**, 61 (1982).
31. Noshay, A., and Robeson, L. M., *J. Appl. Polym. Sci.*, **20**, 1885 (1976).
32. Rahrig, D., MacKnight, W. J. and Lenz, R. W. , *Macromolecules*, **12**, 195 (1979).
33. Earnest, T. R. , Jr. Higgins, J. S. , Handlin, D. L. and MacKnight, W. J. *Polym. Prepr.* **22**, 324 (1981).
34. Chakravarthy, D., Mal, D; Konar, J. and Anil K. Bhowmick, *J. Elastomers and Plastics*, **32** (2000).
35. Xavier, T., Jacob Samuel, K. B. Manjooran and T. Kurian, *Journal of Elastomers and Plastics* **34**, 91 (2002).
36. Lundberg, R. D., Singhal, G. H., Makowski, H. S., (to Exxon Research Engineering Co). U.S. Pat.

- 3, 870, 841, 1975.
37. Eisenberg, A., and Yeo, S. C. , *J. Appl. Polym. Sci.* **26**, 1027 (1981).
38. Rees, R. W. , Vaughan, D. J., *Polym. Prepr. Am. Chem. Soc. Div. Polym. Chem.*; **6**, 287-295 (1965).
39. Littman, E. R. Marvel C.S. *J. Am. Chem. Soc. Div. Polym. Chem.* **6**, 287-295 (1965).
40. Rembaum, A., Baumgartner, W., Eisenberg, A. *J. Polym. Sci. Polm. Lett.* **6**, 159- 171 (1968)
41. Fr. Patent assigned to I. G. Fathen Ind. A. G. 701 102, 1933.
42. Bacon, R. G. R., Farmer, E. H. *Rubber Chem. Technol.* **12**, 200-209 (1939).
- 43 Cowan, J. C. Teeter, H. M. *Ind. Eng. Chem.* **36**,148-152 (1944).
44. Erdi N. Z., Morawetz, H. *J. Colloid Sci.* **19**, 708-721 (1964).
45. Dietrich, D., Muller, E., Bayer O., Peter J. Bayer (A. G.) DB patent 1, 495, 693 1962.
46. Rees, R. W., U. S. Patent 3 264 272, 1966.
47. Tobolsky, A. V., Lyous P F Hata, N., *Macromolecules*, **1**, 515-519 (1968).
48. Dasgupta, A.M., David, D.J., Misra, A., *J. Appl. Polym. Sci.*, **44**, 1213 (1992).
49. Mathis, A., Zheng, Y.L., Galin, J.C., *Polymer* **32**, 3080 (1991).
50. Chen, -show-An; Hsu, --Jen-sung. *Polymer* **34**, 2776 (1993).
51. Chen, -Yun, Chen, -yun-Hsiu, *J. Appl. Polym. Sci.* **57**, 255 (1995).
52. Pilati,-F.; Manaresi,-P.; Ruperto,-M.G.; Bonora,-V.; Munari,-A.; Fiorini,-M. *Polymer* **34**, 2413 (1993).
53. Lei Chen, Xuehai Yu, Changzheng Yang, Qingchao Gu *J.Polym.Sci. Part B. Polym. Phys.* **35**, 799-806 (1997).
54. Rees, R. W.; Vaughan, D.J. *Polym. Prepr. Am. Chem. Soc. Div. Polym. Chem.*, **6**, 287-295 (1965).
55. Eisenberg, A.; Rinaudo, M. *Polymer Bull.*, **24**, 671 (1990).
56. Jerome, R.; Mazurek, M. In *Ionomers: Synthesis, Structure, Properties, and Applications*;
Tant, M.R., Mauritz, K.A., Wilkes, G.L., Eds.; Chapman and Hall: New York, 1997.
57. Lundberg, R. D., in *Encyclopedia of Polymer Science and Engineering*, **8**, Mark, H. F. Bikaler, N.M.
Overberger , c. G. and Menger, G. (Eds) John wiley and sons, NewYork, 1987.
58. Weiss, R. A. , Lundberg R.D., Werner, A., *J. Polym. Sci. Polym. Chem.* **18**, 3427 (1980).
59. Weiss, R. A. ; Turner S. R., Lundberg R.D. *J. Polym. Sci. Polym. Chem.* **23**, 525 (1985).
60. Turner, S. R., Weiss R. A., Lundberg, R.D. *J. Polym. Sci. Polym. Chem.* **23**, 535 (1985).
61. Weiss R. A., Turner S. R., Lundberg R.D. *J. Polym. Sci. Polym. Chem.* **23**, 549 (1985).
62. Allen R.D. Yilgor, I., Mcgrath, J.E., In "Coloumbic interactions in macromolecular systems":
Eisenberg A. Bailey, F.E. Eds.; ACS Symposium series no.302 American Chemical Society: 1986.

63. Salamone, J. C. Watterson, A. C., Hsu, T.D. Tsai, C. C., Mahmud, M. U. *J. Polym. Sci. : Polym. Chem.*, **15**, 487 (1977).
64. Salamone, J. C. Watterson, A. C., Hsu, T.D. Tsai, C. C.; Maumud, M. U. Wisniewski, A. W. Israel, S.C. *J. Polym. Sci. : Polym. , Symposium*, **64**, 229 (1978).
65. Salamone, J. C., Tsai, C. C.; Watterson A. C. *J. Macromol. Sci. : Chem.* **A13**, 665 (1979).
66. Salamone, J. C., Tsai, C. C., Allen, S.P., Watterson, A. C. *J. Polym. Sci. : Polym. Chem.*, **18**, 2983 (1980).
67. Salamone, J. C., Tsai, C. C., Watterson A. C., Olson, A.P. In *Polymer Amines and Ammonium Salts*; Geothals, E. J. Ed., Pergamon: Oxford, 1980.
68. Salamone, J. C., Mahmud, N. A., Maumud, M. U., Nagabhushanm, T.; Watterson, A. C., *Polymer*, **23**, 843 (1982).
69. Makowki, H. S., Lundberg R. D. , Singhal, G.H., US Patent 3 870 841, 1975.
70. Bishop, M. T. , Karasz, F.E., Russo, P.S. Langley, K. H., *Macromolecules*, **18**, 86 (1985).
71. Zhou, Z. L., Eisenberg, A., *J. Polym. Sci. Polym. Phys.*, **27**, 657 (1982).
72. Rahring, D., MacKnight, W. J. , Lenz, R. W. , *Macromolecules*, **12**, 195 (1979).
73. Peiffer, D. G., Lundberg, R. D., Duvdevani, I., *Polymer* **27**, 1453 (1986).
74. Hwang, K. K. S., Yang, C. Z., Cooper, S. L., *Polym. Eng. Sci.* **21**, 1027 (1981).
75. Miller, J. A. , Hwang, K. K. S., Cooper, S. L., *J. Macromol. Sci. : Chem.* **B22**, 321 (1983).
76. Kennedy, J. P. , Storey, R. F. Mohajer, Y. Wilkes, G. L. Proc. IUPAC, Macro **82** , 905 (1982).
77. Kennedy, J. P., Ross, L. R. Lackey, J. E., Nuyken, O. *Polym. Bull.* **4**, 67 (1981).
78. Kennedy, J. P., Storey, R. F. Am. Chem. Soc. ' *Prepr. Div. Org. Coat. Appl. Polym. Sci.*, **46**, 182 (1982).
79. Omeis, J. Muhleisen, E., Moller, M. *Polym. Prepr.* **27**, 213 (1986).
80. Siadat, B., Lundberg, R. D. and Lenz, R. W. ; *Polym. Eng. Sci.*, **20**, 530 (1980).
81. Yarusso , D.J. and Copper, S.L., *Polymer*, **26**, 371 (1985).
82. Longworth , R., in " Ionic Polymers " , Holliday, L. (ed.) , Applied Science , London , 1975 .
83. Roche , E.J., Stein, R. S., MacKnight , W. J., *J. Polym. Sci. , Polym. Phys. Ed.*, **18**, 1035 (1980).
84. Earnest, T.R., Higgins, J.S., Handlin, D.L. and MacKnight, W. J., *Macromolecules*, **14**, 192 (1981)
85. Phillips, P.J., and Macknight, W.J., *J. Polym. Sci. Polym. Phys. Ed.*, **8**, 727 (1970).
86. Shohamy, E. and Eisenberg, A., *J. Polym. Sci. Polym. Phys. Ed.*, **14**, 1211 (1976).
87. Hodge, I.M., and Eisenberg, A., *Macromolecules*, **11**, 283 (1978).

88. Hird, B., and Eisenberg, A., *J. Polym. Sci. Polym. Phys. Ed.*, **b**, 1665 (1990).
89. Brockman, N. L. and Eisenberg, A., *J. Polym. Sci. Polym. Phys. Ed.*, **23**, 1145 (1985).
90. Rigdahl, M. and Eisenberg, A., *J. Polym. Sci. Polym. Phys. Ed.*, **19**, 1641 (1981).
91. Hara, M., Jar, P., and Sauer, J. A., *Polymer*, **32**, 1622 (1991).
92. Weiss, R. A., Fitzgerald, J.J., and Kim, D., *Macromolecules*, **24**, 1071 (1991).
93. Pineri, M., Duplessix, R., Gauthier, S., and Eisenberg, A., in Chapter 18 of " Ions in Polymers " ,
Adv. Chem.Ser. 187, ACS, Washinton D.C. 1980.
94. Forsman, W.C., *Macromolecules*, **15**, 1032, (1982).
95. Datsy, V.K. and Taylor, P.L., *Macromolecules*, **18**, 1479 (1985).
96. Visser, S.A. and Cooper, S.L., *Macromolecules*, **24**, 2584 (1991).
97. Utracki, L.A. and Weiss, R.A. (Eds.) in Multiphase polymers: Blends and Ionomers, ACS
Symposium Series, ACS, Washington, DC, 395 p.21 1989.
98. Li, C., Register, R. A. and Cooper, S. L., *Polymer* **30**, 1227-1233 (1989).
99. Roche, E. J., Stein, R. S., Russel, T. P., MacKnight, W. J., *J. Polym. Sci. Polym. Phys.*, **18**, 1497-1512
(1980).
99. Graiver, D., Litt, M., Baer, E., *J. Polym. Sci. Polym. Chem.*, **17**, 3573-3587 (1979).
100. Broze, G.; Jerome, r.; Teyssie, P.; *J. Polym. Sci. Polym. Lett. B*, 415-418 (1981).
101. Feng, D.; Wilkes, G. L.; Leir, C. M. ; Stark, J. E. ; *J. Macromol. Sci. Chem. A26*, 1151-81 (1989).
102. Hashimoto, T., Sakurai, S., Morimoto, M., Nomura, S., Kohjiya, S., S. Kodaria, T., *Polymer*, **35**,
2672-2678, (1994).
103. Aldebert, P., Dreyfus, B., Gebel G., Nakamura, N., Pineri, M., Volino, F., *J. Phys. France*, **49**, 2101
(1988).
104. Aldebert, P., Dreyfus, B., Pineri, M., *Macromolecules*, **19**, 2651-2653 (1986).
105. Eisenberg, A., Hird, B., Moore, R.B., *Macromolecules*, **23**, 4098 (1990).
106. Delf, B. W., MacKnight, W. J., *Macromolecules*, **2**, 309-310 (1969).
107. Marx, C. L., Caulfield, D. F., Cooper, S. L. *Macromolecules*, **6**, 344 -353 (1973).
108. Binsbergen, F. L. ; Kroon, G. F. *Macromolecules*, **6**, 145 (1973).
109. Yarusso, D. J., Cooper, S. L., *Macromolecules*, **16**, 1871-1880 (1983).
110. MacKnight, W. J., Taggart, W. P. Stein, R. S. *J. Polym. Sci. Symp.* **45**, 113-128 (1974).
111. Eisenberg, A., Hird, B., Moore, R.B., *Macromolecules*, **19**, 2651-53 (1990).

112. Nyrkova, I. A., Khokhlov, A. R., Doi, M., *Macromolecules* **26**, 3601-3610 (1993).
113. Forsman, W. C., *Macromolecules* **15**, 1032-1040 (1982).
115. Rees, R.W. (to E.I.DuPont de Nemours and Co.), U.S.Patent 3,264,272 1966
116. Rees, R. W. (to E.I.DuPont de Nemours and Co.), U.S.Patent 3,404, 134 1968
117. Dolgoplosk, B. A., Reikh, V.N., Tinyakoa, E.I., Kalas, A.E., Koryushenko, Z. A. and Sladkevich, E.G., *Rubber Chem. Technol.*, **32**, 328 (1959).
118. Cooper, W., *J. Polym. Sci.*, **28**, 195 (1958).
119. Jenkins, D.K. and Duck, E.W., in " Ionic Polymers ", Holliday, L. (ed.) , Applied Science, London, 1979.
120. Navaratil, M. and Eisenberg, A., *Macromolecules*, **7**, 84 (1974).
121. Xue, H., Bhowmik , P. and Schlick ,S., *Macromolecules* , **26**, 3340 (1993).
122. Geothals , E. (ed.) " *Telechelic Polymers : Synthesis and Applications* " , CRC Press , Boca Raton , FL , 1989.
123. Broze, G., Jerome, R. and Teyssie, P., *J. Polym. Sci., Polym. Lett. Ed.*, **19**, 415 (1981).
124. Broze , G., Jerome, R. and Teyssie, P., *Macromolecules* , **14**, 224 (1981).
125. Broze , G., Jerome, R. and Teyssie, P., *Macromolecules* , **15**, 920 (1982).
126. Kennedy, J.P. and Storey , R.F., *Organic Coating and Appl. Polym. Sci. Proceedings*, **46**, 182 (1982).
127. Mohajir, Y., Tyagi, D., Wilkes, G.L., Storey, R.F. and Kennedy, J.P., *Polym. Bull.*, **8**, 47 (1982).
128. Bagrodia , S., Mohajir, Y., Wilkes, G.L., Storey, R.F. and Kennedy, J.P., *Polym. Bull.*, **9**, 174 (1983).
129. Bagrodia , S., Wilkes, G.L., and Kennedy, J.P., *J. Rheol.*, **28**, 47 (1983).
130. Mohajir, Y., Bagrodia ,S., G.L. Wilkes,, Wilkes, Storey, R . F. and Kennedy, J.P., *J. Appl. Polym. Sci.*, **29**, 1943 (1984).
131. Klun, T.P., Wendling, L. A., Van Bogart, J. W. C., Robbins, A. F., *J. Polym. Sci. A Polym.Chem.* **25**, 87 (1987).
132. Feng, D., Wilkes, G. L., Leir, C. M., Stark, J. E., *J. Macromol. Sci.Chem.*, **A26**, 1151 (1989).
133. Graiver, D., Baer, E., Litt, M., Baney, R. H., *J. Polym. Sci. Polym. Chem. Ed.*, **17**, 3559 (1979).
134. Gravier, D., Litt, M., Baer, E., *J. Polym. Sci. Polym. Chem. Ed.*, **17**, 3573 (1979).
135. Salomone, J. C., Volksen, W., Olson, A. P., Israel, S. C., *Polymer* 1978, **19**, 1157 (1979).
136. Michaels, A.S., Mieka, R.G., *J. Phys. Chem.* **65**, 1765 (1961).

137. Tsuchida, E., Abe, K., *Adv. Polym. Sci.* **45**, 1 (1982).
138. Weiss, R.A., Sen, A., Willis, C.L., Pottick, L. A., *Polymer* **32**, 1867 (1991).
139. Selb, J., Gallot, Y., *J. Polym. Sci. Polym. Lett. Ed.*, **13**, 615 (1975).
140. Gouin, J. P., Williams, C. E., Eisenberg, A., *Macromolecules*, **22**, 4573 (1989).
141. Wilson, A.D. and Kent, B.E., *J. Appl. Chem.* **21**, 313 (1971).
143. Visser, S. A., and Cooper, S. L., *Macromolecules*, **24**, 2584 (1990).
144. Macknight, W., and Lundberg, R. D., *Rubber Chem. Technol.* **57**, 652 (1984).
145. Xie, H. Q., Xu, J., and Zhou, S., *Polymer* **32**, 95 (1992).
146. Paeglis, A. U., and O' Shea, F. X., *Rubber Chem. Technol.* **61**, 223 (1988).
147. Kurian, T.K.; De, P.P.; Khastgir, D.; Tripathy, D.K.; De, S.K.; Peiffer, D.G. *Polymer*, **36**, 3875 (1995).
148. Romen, D., *Poly. Eng. Sci.* **36**, 1065-1070 (1996).
149. Halimatudahliana, H. Ismail, M. Nasir *Polymer Testing*, **21**, 163-170 (2002).
150. Tobolsky, A. V., *Properties and structure of polymers*, John Wiley and Sons, New York, chap5. 1960.
151. Paeglis, A. U., O' Shea, F. X. *Rubber Chem. Technol.* **61**, 223-237 (1988).
152. Statz, R. *J. Polym. Prepr. Am. Chem. Soc. Div. Polym. Chem.*, **29**, 435-437 (1989).
153. Lundberg, R. D. In *structure and properties of Ionomers*; Pineri, M.; Eisenberg, A.; Eds. NATO ASI series C: Mathematical and Physical Sciences 198, Reidel: Dordrecht, p. 429-438, 1987.
154. Tan, J. S. In *structure and properties of Ionomers*; Pineri, M.; Eisenberg, A.; Eds. NATO ASI series C: Mathematical and Physical Sciences 198, Reidel: Dordrecht, p. 439-451, 1987.
155. von Bonin, W., et al., U. S. Patent 3, 791, 831, 1975.
156. Erhardt, P. F. et al., U. S. Patent 3, 903, 320, 1980.
157. Rogers, J. R., Randall, F. *J. Polym. Prepr. Am. Chem. Soc. Div. Polym. Chem.* **29**, 432 (1989).
158. Drake, E. N.; *J. Polym. Prepr. Am. Chem. Soc. Div. Polym. Chem.* **35**, 14 (1994).
159. Eisenberg, A., Yeager, H. L., Eds. In *Perfluorinated Ionomer Membranes*; ACS symposium Series American Chemical Society: Washington DC, 1982.
160. Olah, G. A., Laali, K., Mehrota, A. K., *J. Org. Chem.* **42**, 4187-4191 (1977).
161. Chang, et. al, U. S. Patent 4, 839,404 (1989).
162. Marzocci, A. et.al, U. S. Patent 4, 301,051.
163. Bashir, H., Linares, A., Acosta, J. L. *J. Appl. Polym. Sci.*, **82**, 3133- 3141 (2001).
164. Thommachan X., Jacob, S., Thomas Kurian, *Macromolecular Materials and Engineering*, **286**,

- 507 (2001).
165. Huang, OR. Y. M., Pinghai Shao, Burns, C. M., Feng, X., *J. Appl. Polym. Sci.*, **82**, 2651-2660 (2001).
166. Ibarra, L., Alzorriz, M., *J. Appl. Polym. Sci.*, **84**, 605-615 (2002).
167. Zuoxin Huang, Yunzhao Yu, Ying Huang; *J. Appl. Polym. Sci.*, **83**: 3099-3104 (2002).
168. Kim, J.-S., Min-Chul Hong, Yeon Hwa Nah, Yeonhee Lee, Seunghee Han, Hyun Eui Lim, *J. Appl. Polym. Sci.*, **83**, 2500-250 (2002).
169. Masubuchi, Akihiro Nishioka, Jun-ichi Takimoto, Kiyohito Koyama, *Polymer*, **43**, 239 (2002).

Chapter 2

Experimental

2.1 *Materials*

2.2 *Methods*

2.2.1 *X-ray fluorescence spectroscopy*

2.2.2 *Fourier transform infrared spectroscopy*

2.2.3 *Fourier transform nuclear magnetic resonance spectroscopy*

2.2.4 *Thermogravimetric analysis (TGA)*

2.2.5 *Differential Scanning calorimetry (DSC)*

2.2.6 *Dynamic Mechanical analysis (DMA)*

2.2.7 *Scanning electron microscopy*

2.2.8 *Compounding and moulding*

2.2.9 *Determination of cure characteristics*

2.2.10 *Compression Moulding of test sheets*

2.2.11 *Physical properties*

2.2.12 *Determination of reprocessability*

2.2.13 *Dielectric measurement*

2.3 *References*

2.1 Materials

2.1.1 Elastomers

(a) Styrene butadiene rubber (SBR)

Styrene butadiene rubber (Synaprene-1502) was obtained from Synthetics and Chemicals Ltd., U.P., India. The Mooney viscosity (ML (1+4) at 100°C) was 49.2.

(b) High Styrene Rubber

Styrene- butadiene rubber of high styrene content abbreviated as HSR (Powerene-958, bound styrene – 52%) was obtained from Apar Industries Ltd.

(c) Nitrile rubber (NBR)

Acrylonitrile butadiene rubber (NBR) was obtained from Apar Industries Ltd .; India. The sample used was N553 with 33% acrylonitrile content, and Mooney viscosity ML(1+4) at 100°C was 45.

2.1. 2. Reagents

1,2-dichloroethane (DCE), concentrated sulphuric acid, methanol, and isopropanol, were procured from E. Merck India Ltd., Mumbai. Acetic anhydride, and zinc acetate, were obtained from S.D. Fine Chemicals Ltd, Mumbai, India.

2.1.3. Rubber Chemicals

2.1.3. (a) Zinc oxide

Zinc oxide was procured from Meta zinc Ltd., Bombay. It had the following specifications:

Specific gravity	-	5.5
ZnO content	-	98%
Acid content	-	0.4% max.

Heat loss (2hrs at 100°C) - 0.5% max.

2.1.3 (b) Stearic acid

Stearic acid used in this study was supplied by Godrej soaps Ltd., Bombay and had the following specifications:

Melting point	-	50-69°C
Acid number	-	185-210
Iodine number	-	95 max.
Specific gravity	-	0.85 ± 0.01
Ash	-	0.1 max %

2.1.3 (c) Tetra methyl thiuram disulphide (TMTD)

TMTD was supplied by NICIL, Bombay. It had the following specifications:

Melting point	-	136°C
Specific gravity	-	1.4

2.1.3 (d) Sulphur:

Sulphur was supplied by Standard Chemical Company Pvt. Ltd., Chennai and had the following specifications:

Specific gravity	-	2.05
Acidity	-	0.01% max.
Ash	-	0.01% max.
Solubility in CS ₂	-	98% max.

2.1.3 (e) CBS

N-cyclo hexyl-2-benzthiazyl sulphonamide (CBS) used in the study was PIL cure CBS supplied by Polyoleffins Industries, Bombay, having the following specifications:

Ash	-	0.5% max
Moisture	-	0.5% max
Specific gravity	-	1.27

2.1.3 (f) Aromatic oil

Aromatic oil was supplied by Hindustan Petroleum Corporation Ltd. It had the following specifications:

Specific gravity	-	0.95-0.98
Aniline point	-	25°C
Flashpoint	-	245°C

2.1.4 Fillers

2.1.4 (a) HAF

High abrasion furnace carbon black (N330) was obtained from M/s. Carbon and Chemicals (India) Ltd., Cochin. It had the following specifications:

Iodine adsorption	-	80 mg/g
DBP absorption	-	105-cm ³ /100 g
Mean particle diameter	-	32 nm
Surface area	-	80 m ² /g
pH	-	7.6

2.1.4 (b) Silica

Precipitated silica manufactured by Degussa, Germany, had the following characteristics:

Surface area	-	234-m ² g ⁻¹
Oil absorption	-	240 g per 100 g
pH	-	6.0
Mean particle diameter	-	20 nm

2.1.4 (c) Zinc stearate

Zinc stearate of rubber grade was obtained locally

Melting point	-	128-130°C
---------------	---	-----------

2.2 Methods

2.2.1 X-ray fluorescence analysis (XRF)

The sulphur content of the ionomers was estimated as per ASTM D-4294 (1995) using Oxford Lab X-3000 bench-top X-ray fluorescence analyzer supplied by Oxford Instruments (Oxford, UK)¹. For the analysis, a sample is irradiated with x-rays generated in a high-intensity X-ray tube. This apparatus works on the principle of energy dispersive X-ray fluorescence (EDXRF). The EDXRF spectrometer has a single detector, which sees X-rays of all energies simultaneously. This advantage has to be used casually to ensure a maximum count rate of, typically, 30,000 counts per second, which the detector will accept. Helium purging is given for concentrations of sulphur up to 0.05%. The fluorescent beam traverses a significant thickness of the sample within which absorption and scattering can occur. The elements in the sample are excited by absorption of this primary beam and emit their own characteristic fluorescence X-rays. In the process of absorption of X-ray energy in the sample, electrons are dislodged from the innermost shells. An electron vacancy must be replaced from the next outer shell. This creates a new vacancy, which is filled from the next shell, and so on. The electrons move from higher to lower energy levels and as a result emit energy in the form of a characteristic X-radiation. The generated X-ray spectrum consists of a number of spectral lines, which must be separated and identified by wavelength or energy. The spectral lines produced are described in figure 2.1 using the classical Siegbahn system i.e., K_{α} , K_{β} etc. The wavelength is specific to the elements responsible for their production. Therefore, the X-rays are diffracted by a diffraction crystal with known spacing d under a specified angle and counted by an X-ray detector.

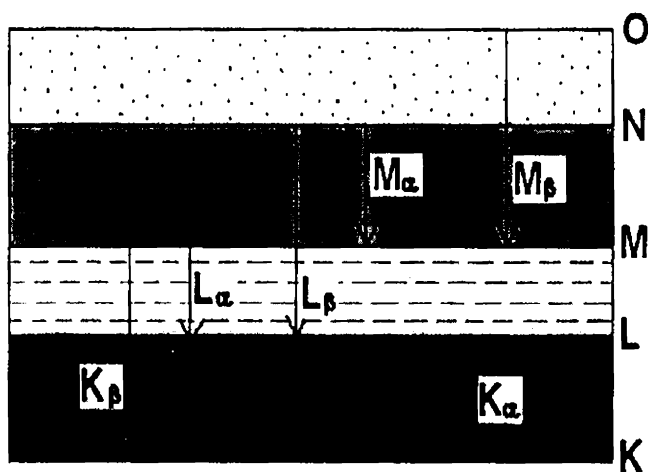


Figure 2.1 Representation of the various spectral lines; K_{α} and K_{β} are the most sensitive lines emitted as X-rays.

2.2.2 Fourier transform Infrared spectroscopy

Fourier transform Infra red spectra are generated by the absorption of electromagnetic radiation in the frequency range 400 to 4000 cm^{-1} by organic molecules. Different functional groups and structural features in the molecule absorb at characteristic frequencies. The frequency and intensity of absorption are indication of the bond strengths and structural geometry in the molecule. FTIR spectra of the compression moulded films of the samples were taken in Nicolet Avtar 360 ESP FTIR Spectrometer.

2.2.3 Nuclear magnetic resonance spectroscopy

NMR spectra samples were taken in a Bruker Avance DPX 300 FTNMR spectrometer (Bruker Instruments, Billerica, MA), operating at a proton resonance frequency of 300 MHz .

2.2.4 Thermogravimetric analysis (TGA)

Thermogravimetric analysis was carried out in a TGA Q50 (TA) at a heating rate of 5°C/minute. Thermograms were recorded from room temperature to 800°C. The onset of degradation temperature, the temperature at which the rate of weight loss is maximum (T_{max}), and the residual weight in percentage were evaluated. Sample sizes were between 5 and 10 mg.

2.2.5 Differential Scanning Calorimetry (DSC)

DSC is used to investigate thermal transitions, including phase changes, crystallization, melting, or glass-rubber transitions, of a material as a function of temperature. Heat flow, that is heat absorption (endothermic) or heat emission (exothermic), is measured, per unit time with the sample compared to a reference. TA Instrument (DSC Q 100) equipped with a RCS cooling system was used to study thermal transitions in the samples at a heating rate of 5°C/min. The sample size was between 7 and 10mg.

2.2.6 Dynamic Mechanical Analysis (DMA)

The dynamic mechanical analysis of the samples was performed in a dynamic mechanical thermal analyzer (DMTA-MK-II) at a frequency of 10 Hz, and a dynamic strain of 64 μ m. The measurements were carried out over a temperature range of -60 to +60°C at a heating rate of 3°C min⁻¹. A DMA is used to identify small and large-scale relaxations of materials in the solid state via an applied oscillatory stress. This is done by varying the sinusoidal stress applied to the polymer using frequency and temperature. Different geometries could be studied such as the single or double cantilever beam, tensile, or compression modes. When the stress is applied, its phase angle shift with resulting strain can be measured. The relationship between the stress

and the strain is a function of the material structure and can be analyzed in terms of the storage modulus (E') and the loss modulus (E''). Each modulus can be calculated from the measurement of the phase angle and oscillatory amplitudes as a function of time and temperature. The storage modulus for a viscoelastic polymer describes the polymer's ability to store energy upon deformation, an elastic behaviour. The loss modulus is proportional to the cyclic loss of energy, a viscous behaviour. $\tan\delta$ is defined as E''/E' . All of these measurements when plotted against time and temperature provide an enormous structural characterization of the polymer. From these measurements information is provided about chain motion, specifically when the main chains begin to rotate and disentangle (T_g).

2.2.7. Scanning electron microscopy

Scanning electron microscope (SEM) is very useful tool in polymer research for studying morphology². Scanning electron microscope, JEOL JSM-840 model-6211 (Oxford, England), having resolution of 1.38 μm was used to investigate the morphology of fractured surfaces. In this technique, an electron beam is scanned across the specimen resulting in back scattering of electrons of high energy, secondary electrons of low energy and X-rays. These signals are monitored by detectors (photo multiplier tube) and magnified. An image of the investigated microscopic region of the specimen is thus observed in cathode ray tube (CRT) and photographed using photographic film. The SEM observations reported in the present study were made on the fracture surface of tensile specimens. Thin specimen of the sample was prepared and mounted on a metallic stub with the help of a silver tape and conducting paint in the upright position. The stub with the sample was placed in an E-101 ion-sputtering unit for gold coating of the sample to make it conducting. Gold-coated sample was observed in the SEM.

2.2.8. Compounding and Mixing

2.2.8 (a) Using the Brabender plasticorder

The samples were masticated in a Brabender plasticorder model PL-3S. Mixing was done for five minutes at a rotor speed of 60 rpm, and at a temperature of 120°C.

2.2.8 (b) Using the mixing mill

Mixing and homogenization of elastomers and compounding were done on a laboratory size (15cm × 33cm) two-roll mill at a friction ratio of 1:1.2.

2.2.9 Determination of cure characteristics

The Goettfert Elastograph (model 67.85) was used in the determination of curing behaviour of rubber compounds. This is a rotorless cure meter and the torque time curve (vulcanization curve) is generated by the oscillation of the lower half of the cavity in which the rubber compound is charged. The reaction chamber is biconical in shape, so that the shear angle remains constant throughout the specimen. Further, by using a specimen of a defined size obtained by means of a special stamping press, the chamber can be filled completely restricting oxidative breakdown as well as ensuring greater reproducibility. The upper platen is brought to the lower by means of a ram actuated by compressed air.

ASTM D2084 describes in detail the test procedure. The relevant data that could be taken from the torque-time curve are;

Minimum torque (M_L): This is the torque attained by the mix after homogenizing at the test temperature before the onset of cure.

Maximum torque (M_H): This is the torque recorded after the curing of the mix is completed.

Optimum cure time (t_{90}): This is the time taken for attaining 90% of the maximum torque (90% vulcanization)

$$t_{90} \text{ (min)} = \text{minute to attain a torque of } (M_L + 90(M_H - M_L)/100)$$

Scorch time (t_2): This is the time taken for 2 units (0.02Nm) rise above the minimum torque (about 10% vulcanization).

2.2.10 Compression Molding of test sheets

The test specimens for determining the physical properties were prepared in standard moulds by compression moulding in an electrically heated hydraulic press having 30 cm×30 cm platens at a pressure of 10 MPa on the mould. The rubber compounds were vulcanized up to their respective optimum cure times at 150°C unless otherwise specified. At the end of the curing cycle mouldings were cooled quickly and stored in a cold and dark place for 24 hours and were used for subsequent physical tests. For samples having thickness more than 6 mm (compression set, abrasion resistance etc.) additional curing time based on the sample thickness was given to obtain satisfactory mouldings. The test specimens of ionomers were prepared by molding in an electrically heated hydraulic press for 5 minutes at 150°C and at a pressure of 10 MPa.

2.2.11 Physical properties

2.2.11 (a) Stress-Strain properties

The stress-strain properties such as tensile strength, modulus, elongation at break (%) were measured according to ASTM D 412 (1998a)³ at 25°C using dumb-bell specimens in an Instron Universal Testing Machine (UTM) model 4206. Samples were punched from compression-molded sheets parallel to the mill grain direction. The sample was held tight by the two grips, the upper grip of which was fixed. The rate of

separation of the power actuated lower grip was 500 mm/minute. The computer attached to the machine calculates the tensile strength and elongation at break and prints out these data after each testing.

2.2.11 (b). Tear strength

The tear strength was determined as per ASTM D 624 (1998)⁴ using unnicked 90° angle test pieces (die C) at 25 °C, using a crosshead speed of 500 mm/ minute in an Instron UTM, model 4206.

2.2.11 (c) Hardness

The hardness of the molded samples was tested using Shore A type Durometer hardness tester in accordance with ASTM D 2240 (1997)⁵.

2.2.11 (d) Compression set

The compression set was measured according to ASTM D. 395-71. The samples were compressed to give 25% deflection were kept in an air oven at 70°C for 22 h. After heating the compression was released, the samples were cooled to room temperature for half an hour and final thickness was measured. The compression set was calculated using the equation,

$$\text{Compression set (\%)} = (t_o - t_f / t_o - t_s) \times 100$$

Where t_o and t_f are the initial and final thickness of the specimen respectively, t_s is the thickness of the spacer bar

2.2.11. (e) Density

Density of the samples was measured as per ISO 2781 (method A). Samples weighing about 2.5 g with smooth surface were used. Weight of the specimen in the air and water was taken. Density of the sample was calculated as

Density	=	$W_1/W_2 \times D$	Where,
W_1	=	weight of the sample in air	
W_2	=	loss of weight in water	
D	=	density of water, (1 g/cm ³)	

2.2.12 Determination of Reprocessability

The reprocessability of the ionomer was studied by masticating the moulded samples in the Brabender Plasticorder PL - 3S for 5 min at a rotor speed of 60 rpm at 120°C. The sample was remoulded in an electrically heated hydraulic press for 5 min at 150°C, under a pressure of 10 MPa. The process of mastication and molding was repeated up to three cycles. The stress-strain properties of the molded specimen after each cycle were determined.

2.2.13 Dielectric measurement

Dielectric measurements of the samples at microwave region were determined by using Cavity perturbation technique⁶. A closed section of a wave-guide constitutes wave-guide cavity resonator.

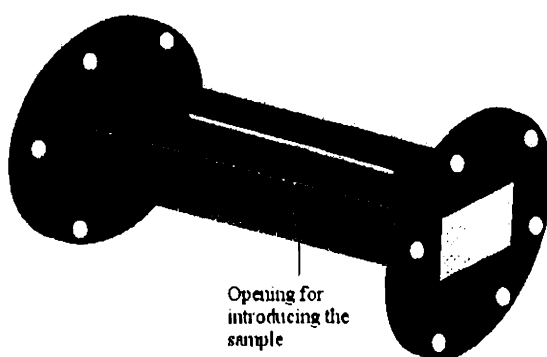


Figure 2.2 Schematic diagram of the transmission type cavity used in the cavity perturbation technique for the Microwave measurement.

The cavity resonator can be of transmission or reflection type. The electromagnetic energy is coupled to the cavity through coupling holes at the ends of the cavity. A non-radiating slot is provided at the broad wall of the cavity for the introduction of the sample. The cavity resonates at different frequencies depending on the dimensions of the cavity. The schematic diagram of the transmission type cavity is shown in figure 2.2. The basic principle involved in the technique is that the field within the cavity resonator is perturbed by the introduction of the dielectric sample through the non-radiating slot. The perturbation shifts the resonant frequency and the quality factor of the cavity. The shift in the frequency is a measure of dielectric constant and that in quality factor gives the loss factor. The conductivity of the sample can be found out from the loss factor.

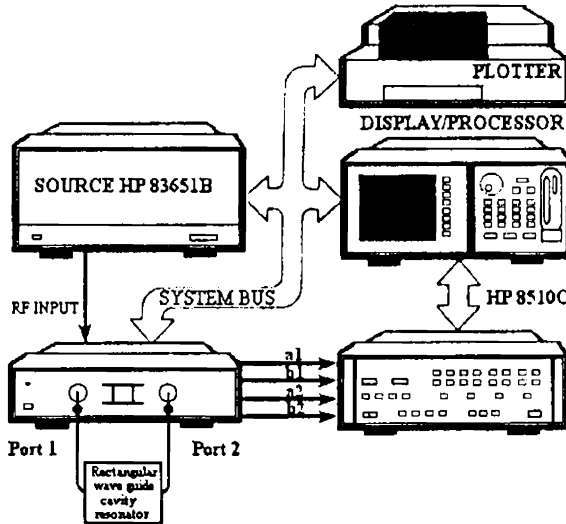


Figure 2.3. Schematic diagram of the experimental set-up consisting of a transmission type cavity resonator, HP 8510 C network analyzer and an interfacing computer.

The experimental set-up consists of a transmission type S-band rectangular cavity resonator, HP 8510 C network analyzer and an interfacing computer as shown in figure 2.3. A typical resonant frequency spectrum of the cavity resonator is shown in figure 2.4. Initially, the resonant frequency f_0 and the corresponding quality factor Q_0 of each resonant peak of the empty cavity were determined. Samples prepared in the form of thin strip were introduced into the cavity resonator through the non-radiating slot. One of the resonant frequencies of the loaded cavity was selected and the position of the sample was adjusted for maximum perturbation (i.e. maximum shift of resonant frequency with minimum amplitude for the peak). The new resonant frequency f_s , 3dB bandwidth and hence the quality factor Q_s were determined. The procedure was repeated for all other resonant frequencies.

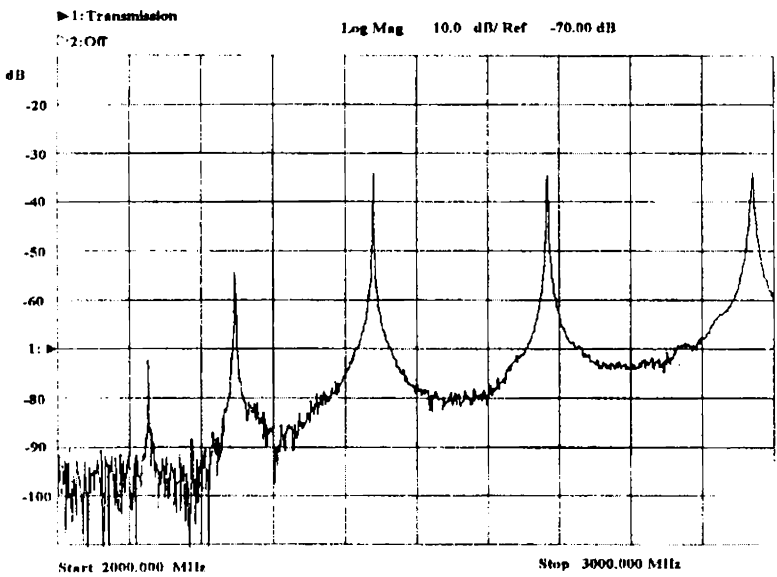


Figure 2.4 A typical resonant frequency spectrum of the cavity resonator

2.3 References

1. Annual Book of ASTM of Standards , D 4294, 05.02, 2000.
2. Sawyer, L.C.; Grub, D.T. 'Polymer Microscopy' Chapman & Hall, London, U.K. Second Edition (1996).
3. Annual Book of ASTM Standards, D 412, 09.01, 2000.
4. Annual Book of ASTM Standards, D 624, 09.01, 2000.
5. Annual Book of ASTM Standards, D 2240, 09.01, 2000.
6. Mathew, K. T., Raveendrannath, U., In: "*Sensors Update*" Baltes, H.; Gopel, W.; Hesse, J. Eds. WILEY-VCH (UK) 1998.

Chapter 3

Ionomers based on Styrene Butadiene Copolymers

o

- 3. Introduction
 - 3.1 Part A: Ionomer based on SBR
 - 3.1.1 Synthesis
 - 3.1.2 Estimation of sulphur
 - 3.1.3 Characterisation of ionic group by FTIR spectroscopy
 - 3.1.4 FTNMR spectroscopy
 - 3.1.5 Thermogravimetric analysis
 - 3.1.6 Differential scanning calorimetry
 - 3.1.7 Dynamic mechanical thermal analysis
 - 3.1.8 Physical properties
 - 3.1.9 Reprocessability studies
 - 3.2 Part B: Ionomer based on HSR
 - 3.2.1 Ionomer preparation
 - 3.2.2 Estimation of sulphur
 - 3.2.3 FTIR characterisation
 - 3.2.4 FTNMR spectroscopy
 - 3.2.5 Dynamic mechanical thermal analysis
 - 3.2.6 Physical properties
 - 3.2.7 Reprocessability studies
 - 3.3 Part C: Comparison of ionomers
 - 3.4 Conclusion
 - 3.5 References
-

3 Introduction

Ionomers could be considered as replacements for vulcanized elastomers to a great extent. One of the major attractions of these materials is the possibility of reprocessability and reuse of reject and waste. Many parts of the world face the serious problem of managing the waste rubber products, which are thermosetting materials. Since ionic elastomers could be recycled and reused, the present research work focuses on the development of reprocessable ionic elastomers based on conventional elastomers. Ionic elastomers have the unique ability to behave as cross-linked elastomers at ambient temperatures, and to melt and flow at elevated temperatures, like thermoplastics^{1,2}. The properties of ionomers are dependent on the type of polymer backbone, ionic content, type of cation and the degree of neutralization^{3,4}. The introduction of relatively low levels of zinc sulphonate groups into polymer yields ionomers with improved mechanical properties; which could be attributed to the very strong intermolecular association and relatively high stability of metal sulphonate groups^{5,6}. Since these materials could be processed by thermoplastic processing techniques avoiding a vulcanization step, they have the potential to emerge as important industrial polymers. In this chapter the synthesis and characterization of reprocessable ionic elastomers based on styrene butadiene rubber (SBR), and high styrene rubber (HSR) are discussed.

This chapter presents:

- (i) Introduction of ionic groups into styrene butadiene rubber (SBR) and high styrene rubber (HSR)
- (ii) Characterization of zinc sulphonated styrene butadiene rubber ionomer ((ZnS-SBR), and zinc sulphonated high styrene rubber (ZnS-HSR)
- (iii) Evaluation of the effects of ionic groups on the mechanical properties
- (iv) Study of the reprocessability of the new ionic elastomers

3.1 Part A: Ionomers based on SBR

3.1.1. Synthesis

The styrene butadiene rubber (SBR) was dried under vacuum at 50°C for 48 hours prior to use. 20 g of polymer was dissolved in 400 ml of 1, 2, Dichloroethane (DCE), and cooled below 10 °C. The sulfonating reagent (acetyl sulphate) was generated in a separate vessel by mixing acetic anhydride and sulfuric acid (98%) in the volume ratio of 4:1 at 0°C. Subsequently the reagent (acetyl sulfate) was diluted by DCE. The sulfonating reagent was added slowly; with stirring under nitrogen atmosphere below 10 °C. After complete addition the cooling system was removed and the solution was stirred vigorously for half an hour and then the reaction was terminated by adding 20 ml isopropanol. Stirring was continued and a stoichiometric amount of zinc acetate in methanol was added for the neutralization of the polymer sulfonic acid. The product was recovered by steam stripping, and was washed several times with deionised water (until reaching neutral pH). The zinc sulfonated styrene butadiene rubber was then vacuum dried at 50°C for 72 hours. SBR of various concentrations of sulfonic acid contents could be prepared. This ionic polymer is hereafter represented as x.y ZnS-SBR where x.y shows number of milliequivalents of sulfonic acid/100 g of styrene butadiene rubber (meq).

3.1.2 Estimation of sulphur

Figure 3.1.1 shows the variation of the level of sulphonation of SBR with the meq of sulfuric acid in the form of acetyl sulfate added at the experimental conditions as estimated using X-ray fluorescence spectroscopic analysis (XRF) method. The weight % of sulphur is directly obtained from XRF. The ionic content increases with increase in the concentration of sulfuric acid added. The reagent conversion at the level of 32 % was established through the estimation of sulphur, present in the sulphonic acid of the Zn-SBR using the XRF analysis. Table 3.1.1 shows the

number of milliequivalents of sulphonate content/100g polymer in each of the ionomer samples calculated using the relation,

Milliequivalents of sulphur = Weight % of sulphur \times 1000 / 32.

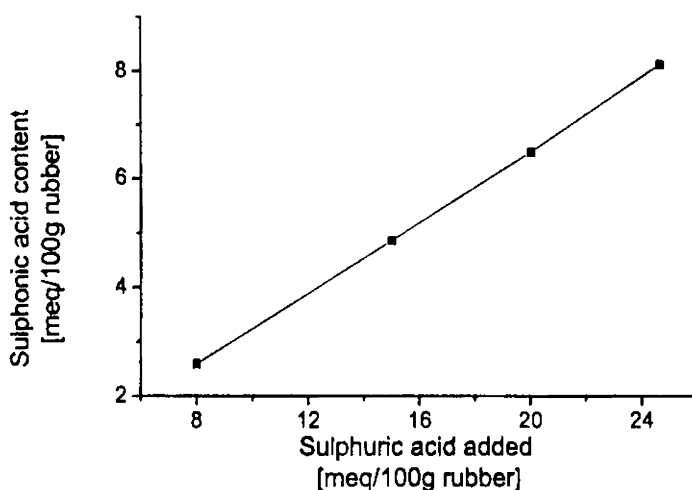


Figure 3.1.1 Level of sulphonation of SBR with the amount of sulphuric acid

Table 3.1.1 Results of XRF analysis of sulphur

Sample	Amount of sulphur (weight %)	Sulphonate content [meq (100g SBR) ⁻¹]
ZnS-SBR-1	0.326	10.2
ZnS-SBR-2	0.634	19.8
ZnS-SBR-3	0.985	30.7
ZnS-SBR-4	1.232	38.5

3.1.3 Characterisation of ionic groups using FTIR spectroscopy

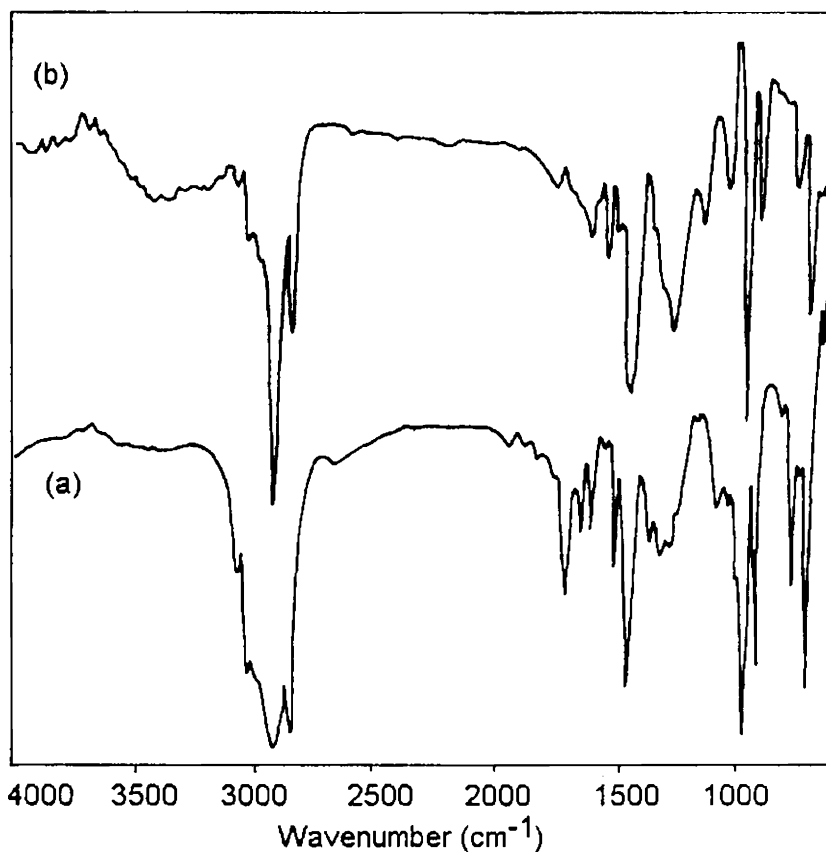
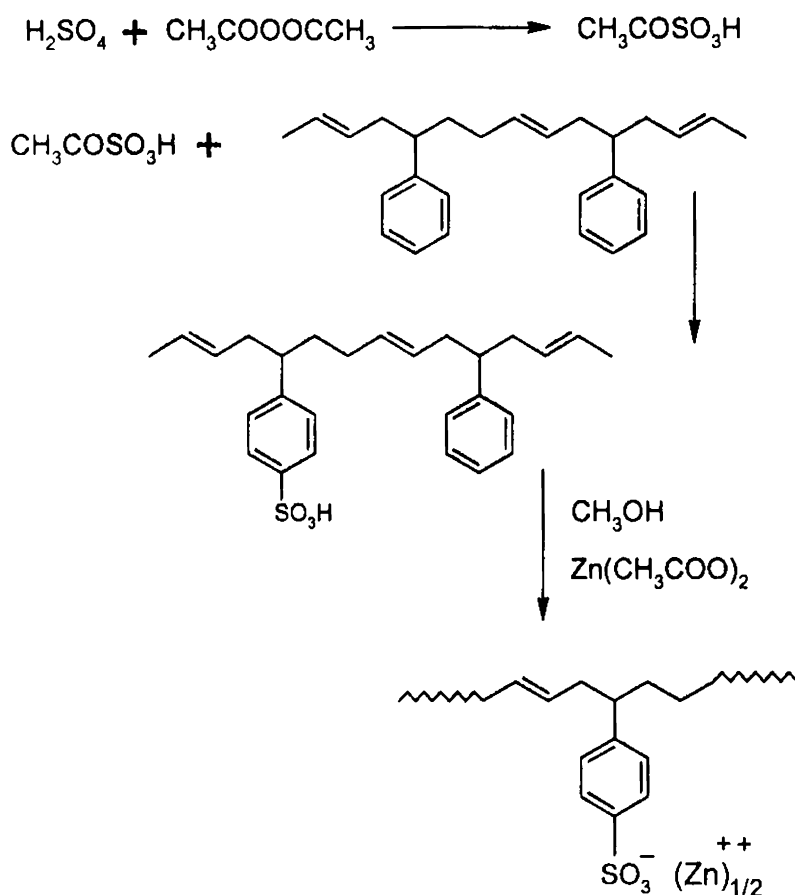


Figure 3.1.2 FTIR spectra of the (a) Control styrene butadiene rubber, and (b) Zinc sulphonated styrene butadiene rubber

The FTIR spectra of the (a) control SBR and the (b) ionomer (ZnS-SBR) prepared from it are shown in figure 3.1.2. The spectrum of SBR (figure 3.1.2a) shows band at 2912, corresponding to CH_2 group. The weak band around 1600 is characteristic of $\text{C}=\text{C}$ stretching in benzene ring. The band at 963 represents $\text{C}-\text{H}$ out of plane deformation of $\text{C}=\text{C}$ of butadiene units. In ZnS-SBR the bands at 2912, 1602, and 962 are also present. The FTIR spectrum of the ZnS - SBR shows a band at 1142

representing S=O stretching (asymmetric) (figure 3.1.2 b). The band at 1035 represents S=O symmetric stretching. The band at 1259 corresponds to ionic sulphonate groups attached to a phenyl ring⁷⁻⁹. Infrared spectroscopic analyses confirmed that sulphonation occurred almost exclusively¹⁰ in the styrene units as proposed in scheme 3.1.1.



Scheme 3.1.1 Chemical reaction involved in the preparation of zinc sulphonated styrene butadiene rubber

3.1.4 FTNMR spectroscopy

The FTNMR spectra of the (a) control SBR and (b) ZnS-SBR are shown in figure 3.1.3. In the spectrum of ZnS-SBR, the characteristic signals of SBR at 2, 5 and 7 ppm are retained. The environment of the phenyl units has been disturbed in the sulphonated polymer. The signals due to the aromatic protons are shifted on sulphonation¹¹. This is clear from the chemical shift of the signals corresponding to the aromatic ring. The peak at 7.005 and 7.26 in the base material shifted to 7.103 and 7.327 respectively.

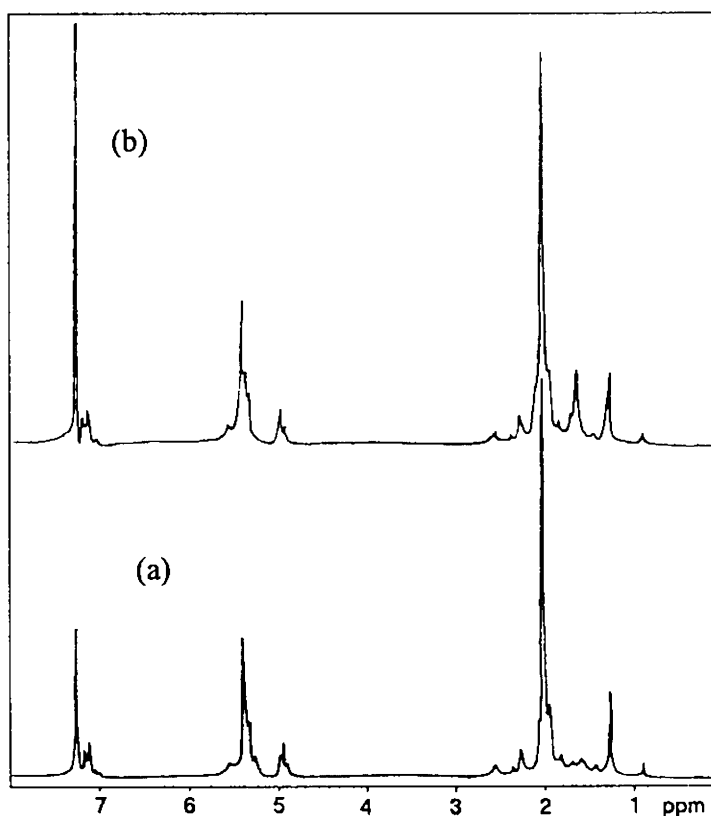


Figure 3.3 FTNMR spectra of (a) SBR, and (b) ZnS-SBR.

This shift in the resonance signals of phenyl ring confirms that a strong ionic group like $-(SO_3)_{1/2} Zn$ is attached to the benzene ring in SBR. The chemical shift of peaks in the modified polymer is due to the local conformational change, which arises due to the grafting of sulphonate units at the para position of the benzene ring in SBR^{11, 12}. It could therefore be considered as a supplementary evidence for the FTIR spectroscopic observation.

3.1.5 Thermogravimetric analysis (TGA)

Figures 3.1.4 represent both the TGA thermal profiles of base polymer, 38.5 ZnS-SBR. The onset of degradation and T_{max} values i.e., the temperature at which the rate of degradation is maximum are shown in the table 3.1.2. Incorporation of ionic groups improves the thermal stability. Increase in the concentration of the ionic content in the polymer influences their melt viscosity. The change in the viscosity may be affecting their T_{max} values⁵. The increased stability of the ZnS-SBR when compared to SBR could be due to the greater stability of the aromatic sulphonate derivatives.

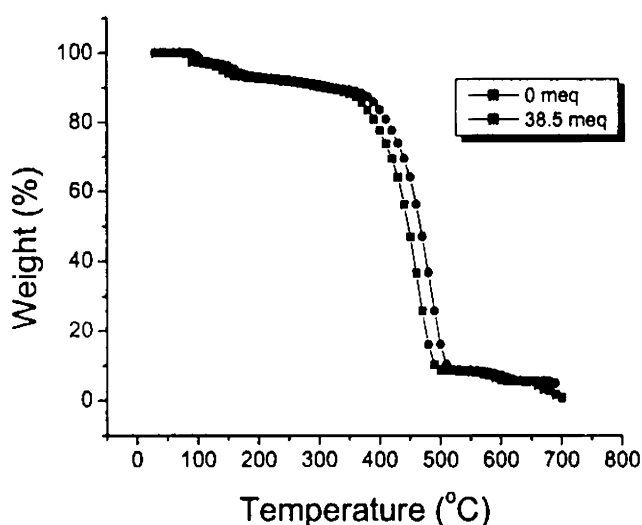
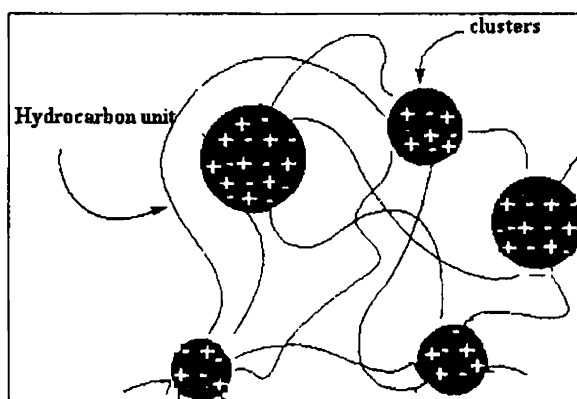


Figure 3.1.4 TGA thermograms of base polymer and ionomer

3.1.6 Differential scanning calorimetry (DSC)

Incorporation of zinc sulphonate groups into the base polymer produces changes in the matrix glass rubber transition temperature (T_g) of the resultant material. Changing the ionic concentration clearly provides an effective way of changing T_g . Figure 3.1.5 shows the DSC thermograms of samples with varying ion content and the results are summarized in table 3.1.3. These change in T_g shows that the ionic groups have affected the transition temperature of the soft rubbery phase. The glass rubber transition temperature increased with increasing ionic content. At the relatively low dielectric constant of the base polymer the ionic cross-linking imposes restriction towards the segmental mobility of the styrene butadiene rubber backbone increasing the T_g of the ionomers.



Scheme 3.1.2 Clustering of polar ionic groups

Incorporation of more ionic groups may increase the ionic interactions leading to the formation of stronger polar clustering as proposed in scheme 3.1.2. Apart from the low temperature thermal transitions, the ionomers show a second transition at higher temperature. The ionic cross-links, being thermo-labile, weakened at higher temperatures and contribute a relaxation towards the barrier to bond rotation around the polymer backbone and intermolecular constraints. These relaxations may produce volume shrinkage and the corresponding response

appears as a drop in temperature in DSC thermograms. Thus, Tg_2 depends upon the barrier to free rotation around the polymer backbone, which in turn depends on the ionic interactions (or electrostatic force).

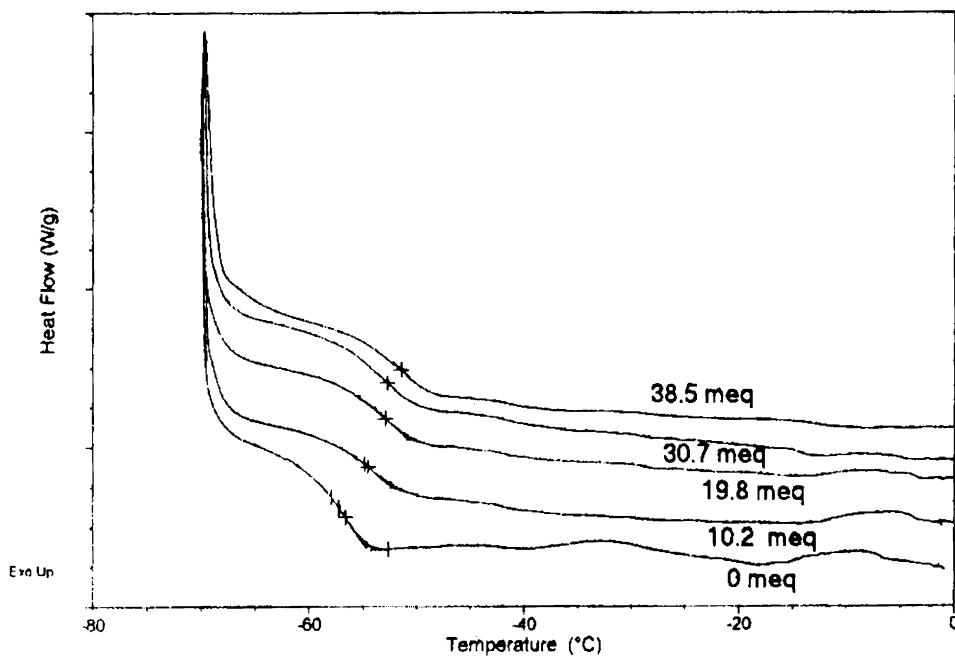


Figure. 3.1.5 DSC thermal profiles of base polymer and the ionomers

It has been reported¹³ that $Tg_2 \propto W_{ei}$, where W_{ei} is the electrostatic work of removing an anion or cation from its coordination sphere. The DSC observations suggest that the incorporation of the zinc sulphonate groups into the styrene butadiene rubber produces phase-separated regions corresponding to the soft rubbery phase, and the hard phase arising out of the clustering of the zinc sulphonate groups attached to the styrene units in the polymer. The dimension of the micro-phase clustering of polar groups in these ionomers may be falling within the size requirement to be detectable using DSC, as was reported in the case of other ionomers¹⁴⁻¹⁸.

Table 3.1.3 DSC results of base polymer, ionomers

Sample	Tg1(°C)
SBR	-56.52
ZnS-SBR-1	-54.55
ZnS-SBR-2	-52.97
ZnS-SBR-3	-52.10
ZnS-SBR-4	-51.33

3.1.7 Dynamic mechanical thermal analysis (DMTA)

Figures 3.1.6 shows the plot of loss tangent ($\tan\delta$) against temperature obtained from the dynamic mechanical thermal analysis of SBR (base polymer), and the ionomers. The glass-rubber transition (T_g) occurred around -48.13°C in the case of SBR. T_g occurred at higher temperatures in the case of ionomers, as compared to the base polymer. The glass-rubber transition temperatures of ionomers increased as the ionic content increased. The increase in the T_g 's of ionomers with increased ion content is due to the crosslinking effects of the ionic groups. The results show that the ionic cross-links are as efficient as the covalent cross-links in raising T_g .

The ionomers show (ZnS-SBR-3 and ZnS-SBR-4) another broad transitions in the temperature range of -19 to $+10^\circ\text{C}$ and -19 to $+19^\circ\text{C}$ respectively, which is ascribed to the transition due to the ionic aggregates (Ti)²⁰. Transition due to ionic aggregates has been found to occur in the same temperature range, as observed here, in the case of other rubbery ionomers²¹. The absence of clear ionic transitions in the case of 10.2 ZnS-SBR, and 19.8 ZnS-SBR

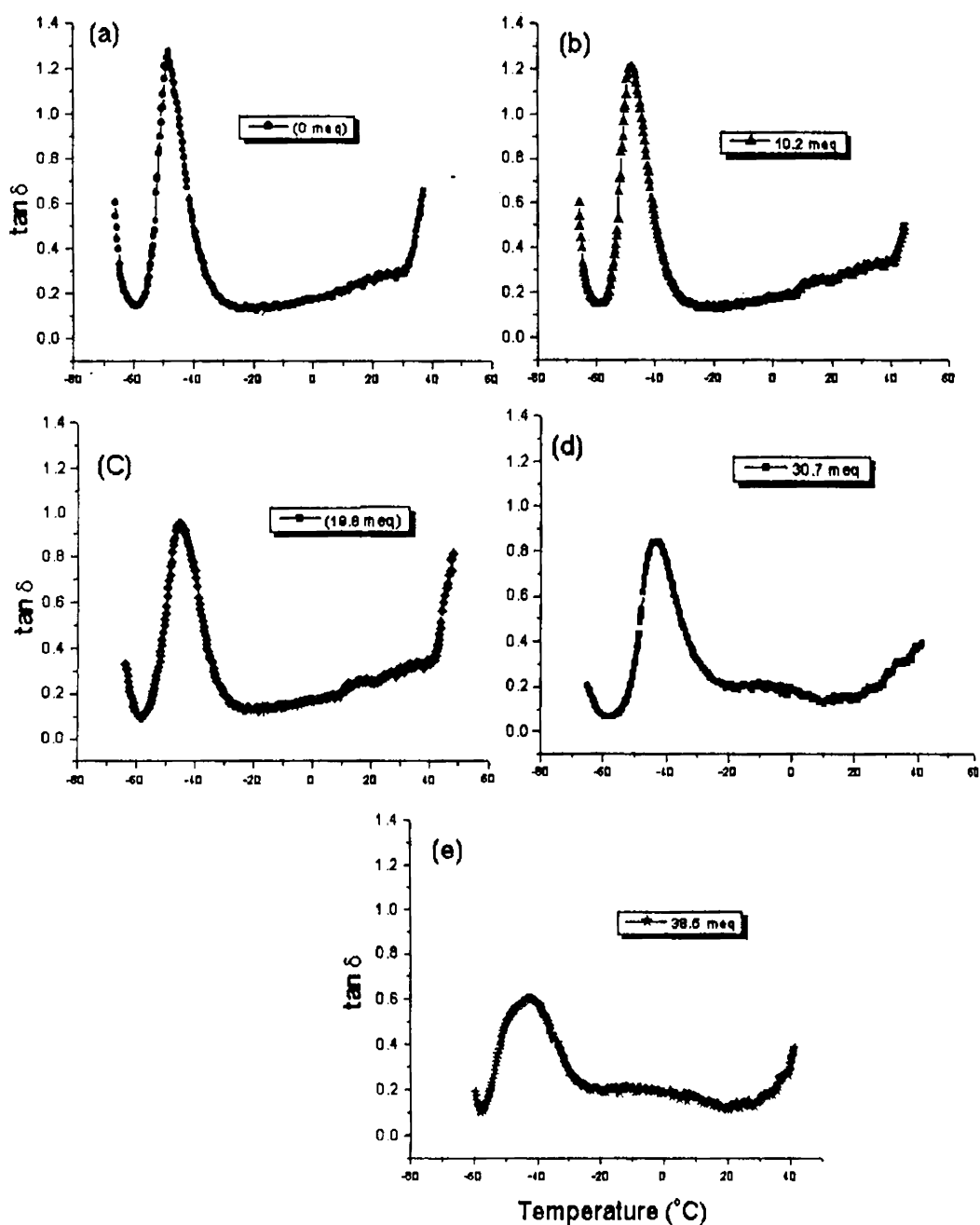


Figure 3.1.6 Variation of loss tangent with temperature of (a) SBR, (b) 10.2 meq (c) 19.8 meq, (d) 30.7 meq and (e) 38.5 meq

may be due to the low ion content. In the case of the base SBR, expectedly, the broad transition due to ionic aggregates has not been observed. The ionomers as they are not chemically cross-linked became soft at elevated temperatures⁵.

The $\tan \delta_{\max}$ (i.e., the $\tan \delta$ value at T_g) was higher for the base SBR, as compared to the ZnS-SBR ionomers. The lower $\tan \delta_{\max}$ of the ionomers is attributed to the stiffening of the matrix imparted by the ionic domains due to the strong polar – polar interaction involving the backbone chains. The results indicate that the ionic aggregates of ZnS-SBR's behave like ultrafine particles of a reinforcing filler. Incorporation of the ionic groups increased the storage modulus of SBR. The results of dynamic mechanical analyses are summarized in Table 3.1.4

Incorporation of zinc sulphonate groups in to the base polymer increased the storage modulus of zinc sulphonated SBR. The ionomers show higher storage modulus than the base polymer. An increase in the ionic concentration in ionomer further enhances the storage modulus. The increase in the storage modulus of the ionomers based on SBR may be due to the increase in the ion content, and the relative number of ionic associations in the matrix phase. The effects of these two different ionic environments on the ionic modulus are different.

Table 3.1.4 DMTA results of base polymer, and its ionomers

Ionic content	T_g ($^{\circ}\text{C}$)	$\tan \delta$ at T_g	Transition due to ionic aggregates T_i ($^{\circ}\text{C}$)	$\text{Log } E'(\text{Pa})$ at T_g
SBR	-48.294	1.2734	-	7.4586
ZnS-SBR-1	-47.934	1.2044	-	7.52
ZnS-SBR-2	-45.036	0.9447	-	7.714
ZnS-SBR-3	-43.024	0.8358	-19- +10	8.047
ZnS-SBR-4	-42.014	0.6030	-19- +19	8.150

3.1.8 Influence of ionic groups on physical properties

The physical properties of the SBR gum vulcanizate prepared as per the formulation listed in table 3.1.5 and the ionomer samples are given in the table 3.1.6. The tensile strength increased linearly with increase in the ion dosage. The elongation at break of the ionomer samples showed a reciprocative change with the sulphonation level. This is because of the fact that, ionic groups phase separate into spherical ion-rich domains, acting as physical crosslinks¹⁰. The modulus and hardness also increased as the level of sulphonation increased. Hardness is a measure of modulus of elasticity at low strain²². The increased modulus of elasticity brought about by the increased concentration of ionic aggregates in ZnS-SBR samples may be the reason for the higher hardness. The modulus at 100% elongation and tensile strength of the ionomer at a sulphonation level of 19.8 meq was equivalent to that of SBR gum vulcanizate. The tear resistance is increased with the level of sulphonation. Kraus et al have reported that the tear strength is enhanced by the factors, which tend to dissipate energy²³. The ionic domain of ZnS-SBR may be acting as tear deviators or arrestors. The enhancement in physical properties may be due to the presence of a small coherent second phase that acts as reinforcing filler and decreases the crack propagation^{24, 25}.

Table 3.1.5 Formulation of SBR gum compound

Component	Parts
SBR	100
Sulphur	2.0
MBT	1.25
TMTD	0.20
ZnO	3.0
Stearic acid	2.0
SP(antioxidant)	1.0

Table 3.1.6 Physical properties of SBR gum vulcanizate and zinc sulphonated SBRs

Sample	Modulus 100% (MPa)	Tensile strength (MPa)	Elongation at break (%)	Tear strength (kN/m)	Hardness (Shore A)
SBR	1.28	1.89	218	12.39	35
ZnS-SBR-1	0.98	1.10	518	11.79	26
ZnS-SBR-2	1.38	2.71	510	15.47	35
ZnS-SBR-3	5.37	5.38	205	20.5	54
ZnS-SBR-4	-	6.69	108	26.21	64

3.1.9 Reprocessability Studies

Table 3.1.7 shows that, the tensile properties of the ZnS-SBR ionomer remain almost constant even after three repeated cycles of mixing and molding. The morphology of ZnS-SBR is believed to be similar to that of conventional thermoplastic elastomers, that is, a combination of soft segments and hard domains²³⁻²⁴.

Table 3.1.7 Results of reprocessability studies of 38.5 ZnS-SBR ionomer

No. of Cycle	Elongation at break. (%)	Tensile strength (MPa)	Tear Strength (N/mm)
1	106	6.69	26.5
2	108	6.56	24.4
3	107	6.23	25

3.2 Part B: Ionomers based on HSR

3.2.1 Ionomer preparation

The high styrene rubber (HSR) was dried under vacuum at 50°C for 48 hours prior to use. 20 g of polymer was dissolved in 400 ml of 1, 2, dichloroethane (DCE), and cooled below 10°C. The sulfonating reagent (acetyl sulphate) was generated in a separate vessel by mixing acetic anhydride and sulfuric acid (98%) in the volume ratio of 4:1 at 0°C. Subsequently the reagent (acetyl sulfate) was diluted by DCE. The sulphonating reagent was added slowly; with stirring under nitrogen atmosphere below 10 °C. After complete addition the cooling system was removed and the solution was stirred vigorously for half an hour and then adding 20 ml isopropanol terminated the reaction. Stirring was continued and stoichiometric amount of zinc acetate in methanol was added for the neutralization

of the polymer sulfonic acid. The product was recovered by steam stripping, and was washed several times with deionised water (until reaching neutral pH). The zinc sulphonated high styrene rubber was then vacuum dried at 50°C for 72 hours. HSR of various concentrations of sulphonate content could be prepared by varying the acetyl sulfate concentrations.

3.2.2 Estimation of sulphur

The weight percentage of sulfur in the samples and the corresponding level of sulphonation in meq are shown in Table 3.2.1. The ionomer samples became harder as the level of sulphonation increased.

Table 3.2.1 Results of XRF analysis

Samples	Amount of sulphur (Wt. %)	Sulphonate content [meq/100g polymer]
ZnS-HSR-1	0.307	10.6
ZnS-HSR-2	0.653	20.4
ZnS-HSR-3	1.024	34.4

3.2.3 FTIR characterisation

The infrared spectra (2000-500 cm^{-1}) of neat HSR and the ionomer prepared from it are shown in Figure 3.2.1. The spectrum of HSR (a) shows a peak at around 1601 cm^{-1} that is characteristic of C=C stretching in benzene ring. The peak at 966 cm^{-1} corresponds to C-H out of plane deformation of C=C of butadiene units. Figure 3.2.1 (b) shows the IR spectrum of the ionomer based on HSR. The peak at 1041 cm^{-1} is assigned to the symmetric stretching vibration of the sulphonate anion attached to a phenyl ring, and the other peaks at 1156 and 1193 cm^{-1} correspond to the asymmetric stretching of the sulphonate groups⁷⁻¹⁰. The peak at

1541 cm^{-1} represents the disubstituted benzene ring⁷. There are two kinds of reactive sites in the HSR, (i) the phenyl rings in the styrene units, and (ii) the residual C=C in the rubber block. Infrared spectroscopic analyses confirmed that sulfonation occurred almost exclusively in the styrene units.

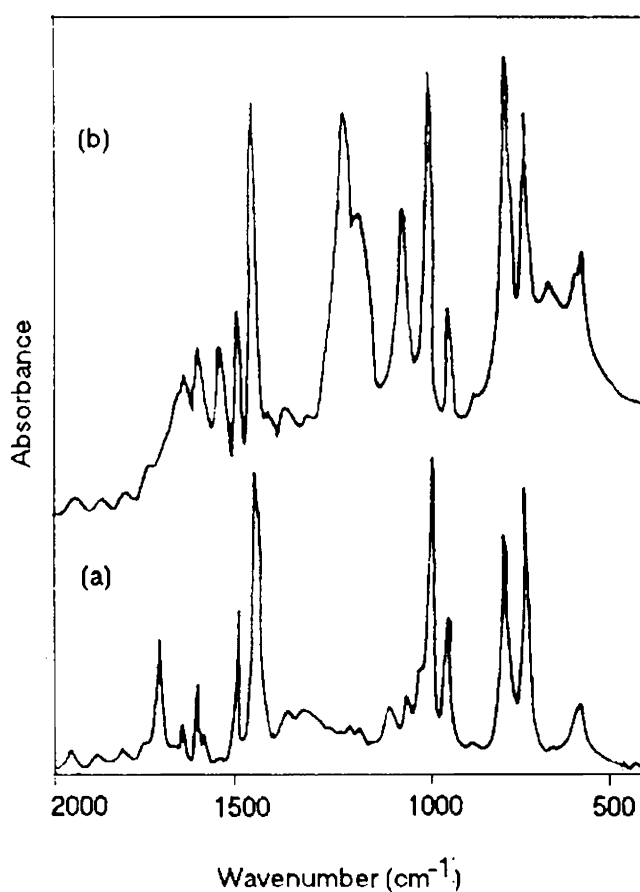


Figure 3.2.1 FTIR spectra of the control SBR (a), and (b) ZnS-SBR

3.2.4 FTNMR spectroscopy

The NMR spectra of the base (a) HSR and (b) ZnS-HSR are represented in Figure 3.2.3. In the spectrum of ZnS-HSR, the characteristic signals of HSR at 2 and 7

ppm are retained. The environment of the phenyl units has been disturbed in the sulfonated polymer. The signals due to the aromatic protons are shifted on sulphonation. This is clear from the chemical shift of the signals corresponding to the aromatic ring. . The peak at 7.13 and 7.26 (Figure 3.2.2a) in the base material shifted to 7.26 and 7.36 (Figure 3.2.2b) respectively. This shift in the resonance signals of phenyl ring confirms that a strong ionic group like $-(SO_3)_{1/2}Zn$ is attached to the benzene ring in HSR. The NMR spectra show supplementary evidence for the FTIR spectroscopic observation¹¹⁻¹².

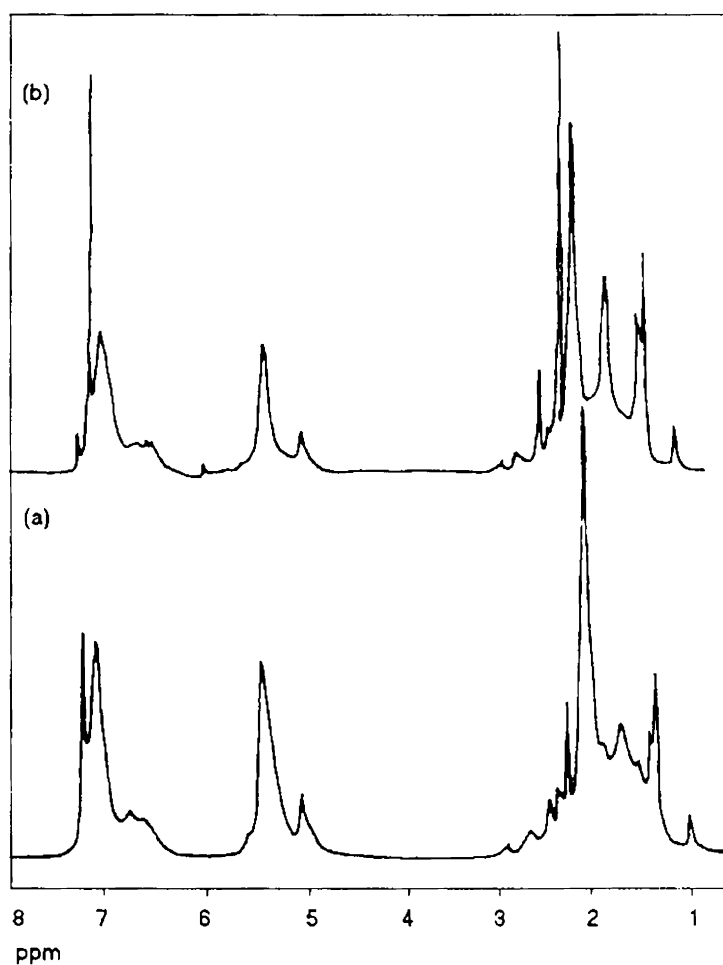


Figure 3.2.2 FTNMR spectra of (a) HSR, and (b) ZnS-HSR.

3.2.5 Dynamic mechanical analysis

Variation of dynamic mechanical properties with temperature gives information about different transition in polymers. Figure 3.2.3 shows the variation of log storage modulus ($\log E'$) vs. temperature for the base material and the ionomers. Compared with the base polymer the ionomers show a broad rubbery plateau with higher storage modulus due to physical crosslinking arising from ionic aggregates. It is believed that at room temperature ionic aggregates reinforce the matrix, resulting in higher E' .

Figure 3.2.4 shows the plot of loss tangent ($\tan\delta$) against temperature obtained from the dynamic mechanical analyses of neat HSR and its ionomers. The glass transition temperature (T_g) occurred around -39°C in the case of HSR. Incorporation of ionic groups causes a shift in the T_g towards higher side (-37°C). The $\tan\delta_{\max}$ (i.e., $\tan\delta$ value at T_g) was higher for HSR as compared to its ionomers. The lower value of $\tan\delta_{\max}$ of the ionomers may be attributed to the stiffening imparted by the ionic domains¹⁹.

The $\tan\delta_{\max}$ decreased as the concentration of ionic groups increased. 20.4ZnS-HSR and 34.4ZnS-HSR show additional transitions in the temperature range of -4°C to $+8^\circ\text{C}$, $+1^\circ\text{C}$ to $+30^\circ\text{C}$ respectively which may be ascribed to the presence of a second phase arising out of the immobile segments or due restricted mobility region adjacent to the ionic domains (T_i)²⁰. In the case of HSR, and 10.6ZnS-HSR as expected, the broad transition due to ionic aggregates was not observed. The absence of clear ionic transition in the case of 10.6 ZnS-HSR may be due to the low ion content. In the region of low ion concentration the ions are assumed to exist in the form of multiplets¹. The results of dynamic mechanical analysis are summarized in Table 3.2.2.

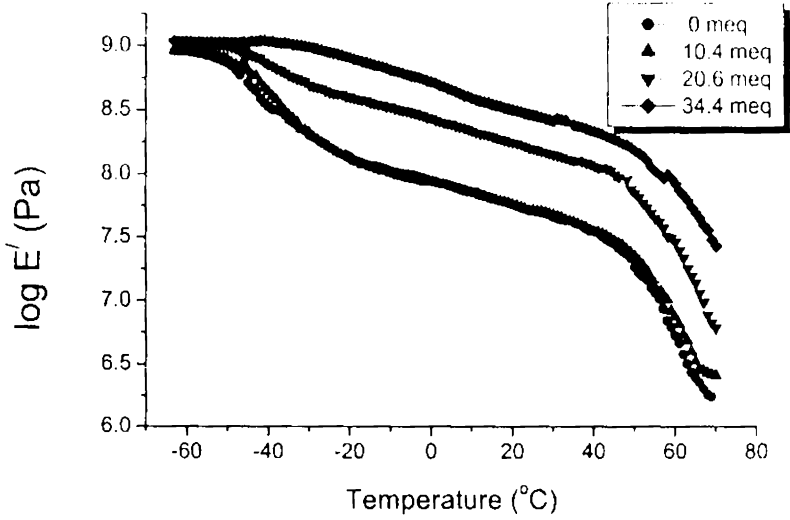


Figure 3.2.3 Variation of $\log E'$ against temperature for the HSR and its ionomers

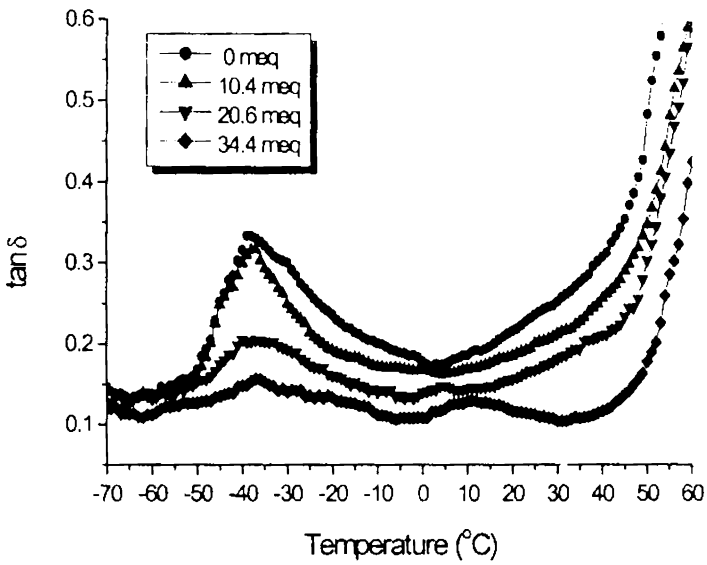


Figure 3.2.4 Variation of $\tan \delta$ against temperature for the HSR and its ionomers

Table 3.2.2 Results of dynamic mechanical analyses

Samples	T _g ^a (°C)	Tanδ at T _g	Transition due to ionic aggregates ^b T _i (°C)	Tanδ at T _i
HSR	-39	0.335	-	-
ZnS-HSR-1	-37	0.315	-	-
ZnS-HSR-2	-37	0.2050	-4 to +8	0.1486
ZnS-HSR-3	-37	0.15	+1 to +30	0.1306

^a From $(\tan \delta)_{\max}$ in the plot of $\tan \delta$ vs temperature

^b From $\tan \delta$ vs temperature plot

3.2.6 Physical properties

The physical properties of neat HSR and its ionomers are summarized in table 3.2.3. Incorporation of ionic groups caused a gradual increase in modulus, tensile strength and decrease in elongation at break. This is because of the fact that, ionic groups phase separate into spherical ion-rich domains, acting as physical crosslinks¹⁰. ZnS-HSR showed higher tear strength as compared to the base HSR. Tear strength values of ionomers increases with incorporation of ionic groups. Incorporation of ionic groups increased the hardness of ZnS-SBR. As expected hardness increased as the ionic content increased. Enhancement in mechanical properties is thought to arise from the presence of a small, coherent second phase that behaves like ultrafine particles of reinforcing filler in addition to acting as multifunctional crosslinks^{24,25}. Density of the samples increased with increasing ionic content.

Table 3.2.3 Physical properties at 25°C

Properties	Samples			
	HSR	10.6ZnS-HSR	20.4ZnS-HSR	34.4ZnS-HSR
Tensile Strength (MPa)	2.62	3.85	8.54	16.81
Modulus at 50% elongation (MPa)	2.43	3.36	8.18	14.98
Elongation at Break (%)	131.70	103.75	90.34	78.78
Tear Strength (N/mm)	15.48	22.49	57	106
Hardness (Shore D)	15	20	35	45
Density (g/cc)	0.9744	1.0828	1.1972	1.212

3.2.7 Reprocessability

Results of reprocessability studies are shown in Figure 3.2.5. It was observed that the stress-strain properties of the 34.4ZnS-HSR samples remained almost constant even after three cycles of processing. This shows that 34.4ZnS-HSR behaves as thermoplastic elastomer, and could be processed by mechanical recycling without deterioration in physical properties.

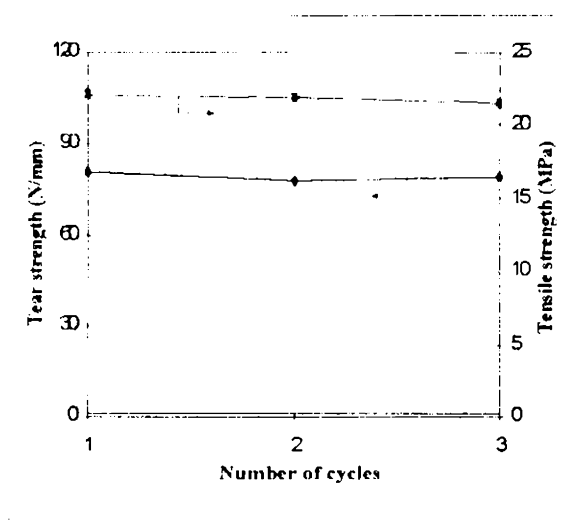


Figure 3.2.5 Variation of stress-strain properties of 34.4ZnS-HSR at different cycles of processing.

3.3 Part C: Comparison of ionomers

Ionomers based on styrene butadiene rubber and high styrene rubber has been prepared by direct method. Comparison of the physical properties of these ionomers (Table 3.3.3) has been done. Results show that the physical properties of 34.4 ZnS-HSR are higher than the 38.5 ZnS-SBR. Because of the presence of more styrene units in HSR, sulphonation preferentially occurred at the benzene ring, and more sulphonate groups are associate form multiplets.

Table 3.3.3 Physical properties of the ionomers based on SBR and HSR

Properties	Samples	
	38.5ZnS-SBR	34.4ZnS-HSR
Tensile Strength (MPa)	6.69	16.81
Elongation at break (%)	108	78.78
Tear Strength (N/mm)	26.21	106

3.4. Conclusion

Zinc sulphonated styrene butadiene rubber and high styrene rubber could be prepared. The ionic content could be estimated by using XRF. FTIR spectra show evidence for the sulphonation at the para position of the benzene ring in the styrene units of rubbers and also for the formation of zinc sulphonated rubber. NMR spectra confirm the presence of ionic groups in the modified rubbers, giving supplementary evidence to the FTIR spectra. Thermogravimetric results showed that thermo-oxidative stability of the base polymer improved upon ionomer modification. DSC results showed that the glass rubber transition temperature increased with increase in ionic content. Results of dynamic mechanical analysis show the occurrence of an ionic transition in the ionomers in addition to the glass-rubber transition. The modified rubbers showed higher physical properties as compared to the base polymer. The thermoplastic elastomeric nature of the newly synthesized ionomers is evident from the retention of the stress-strain properties even after three cycles of repeated mixing and moulding.

3.5 References

1. Adi Eisenberg, and Joon –Seop Kim, Introduction to Ionomers, John Wiley & Sons, New York, 1998.
2. P.K. Agarwal, H.S.Makowski, and R.D.Lundberg, *Macromolecules*, **13**, 1679 (1980).
3. W.J. Macknight, and R.D.Lundberg, *Rubber Chem.Technol.*, **57**, 652 (1984).
4. X.D.Fan, and C.G.Bazuin, *Macromolecules*, **26**, 2508 (1993).
5. Eisenberg, A. (ed.), *Ions in Polymers*, Advances in Chemistry Series 187, ACS, Washington D.C., 1980.
6. R. A. Weiss, J. J. Fitzgerald, and D. Kim, *Macromolecules*, **24**, 1064 (1991).
7. Dyer. J. R., *Applications of absorption spectroscopy of organic compounds*, Prentice-Hall of India, New Delhi, 1991.
8. R. A. Weiss, Ashish Sen, C.L.Willis, L.A. Pottick. *Polymer*, **32**, 1867 (1991).
9. S.R.Sandler, W. Karo, J. Bonsteel, E.M.Pearce, *Polymer Synthesis and Characterization*. SectionII, Expt.14, Academic Press California, USA, 1998.
11. R.A.Weiss, Ashish Sen, C.L.Willis, L.A. Pottick, *Polymer*, **32**, 1867 (1991).
12. Kemp, W. *Organic Spectroscopy*; Macmillan: Lon-don, 1991.
13. Xavier, T.; Samuel, J.; Kurian, T. *Macromol Mater Eng*, **286**, 507 (2001).
14. Tse, M.F. J. *Adhes. Sci. Technol.* **3**, 551 (1989).
15. Eisenberg, A.; In *Physical Properties of Polymers*; Mark, J.E.; Eisenberg, A.; Graessley, W.W.;
16. Mandelkern, L.; Samulski, E.T.; Koenig, J.L.; Wignall, G.D., Eds.; American Chemical Society: Washington, DC; Chapter 2 (1993).
18. Kanamoto, T.; Hatsuya, J.; Ohoi, M.; Tamaka, K. *Macromol. Chem.*; **176**, 3497-3500 (1975).
19. Maurer, J.J. In *Thermal Analysis: Proceedings of the Seventh International Conference on Thermal Analysis*, Vol. 2; Miller, B., Ed.; Wiley: New York; 1040-1049 (1982).
22. Tong, X.; Bazuin, C.G. *Chem. Mater.* **4**, 370-377 (1992).
23. Ehrmann, M.; Muller, R.; Galin, J.-C.; Bazuin, C.G. *Macromolecules* **26**, 4910- 4918 (1993).
24. P.P.A.Smith, *Rheol. Acta*, **5**, 277 (1966).
25. C.G. Bazuin, and A. Eisenberg, *Ind. Eng.Chem. Prod. Res. Dev.*, **20**, 271 (1981).
26. U.K. Mondal, D.K. Tripathy, and S. K. De, *Polymer*, **34**, 3832 (1993).

-
27. T.H. Ferrigno, *Hand Book of Fillers and Reinforcements for Plastics* (Eds. Katz H. S. & J.V
 28. Milewski) Van Nostrand Reinhold Company, New York, 1978.
 29. A.I. Medalia & G. Kraus, in *Science and Technology of Rubbers* (Ed. F.R.
 30. Eirich); Academic Press, New York, 1994.
 31. B. Hird, and A. Eisenberg *Macromolecules*, **25**, 6466 (1992).
 32. M. A. Bellinger, J. A. Sauer, M. Hara, *Polymer* , **35**, 5478 (1994).

Chapter 4

Effect of fillers on the properties of ZnS-SBR ionomers

- 4.1 *Introduction*
 - 4.2 *Differential scanning calorimetry*
 - 4.3 *Dynamic mechanical thermal analysis*
 - 4.4 *Physical properties of ionomer/filler compounds*
 - 4.4.1 *HAF*
 - 4.4.2 *Silica*
 - 4.4.3 *Zinc stearate*
 - 4.5 *Reprocessability studies*
 - 4.6 *Mechanism of filler reinforcement*
 - 4.7 *Comparison of the physical properties*
 - 4.8 *Conclusion*
 - 4.9 *References*
-

4.1 Introduction

The effect of fillers on the mechanical properties of elastomers is of great interest because fillers could be used very effectively to enhance the ultimate properties¹⁻⁴. While studying the effect of fillers on the properties of ZnS-SBR, we observed an improvement in the physical properties on incorporation of fillers. The two-phase morphology of ionomers, and the resulting differences in polarity of the two phases, provide possibilities of preferential interaction by different fillers. Evaluation of the effect of carbon black (HAF)⁵, silica⁶, and zinc stearate⁷ on the properties of EPDM based ionomers were published. The results of these studies our studies are discussed in terms of the multiplet-cluster and EHM model of ionomer microstructure^{8,9}. The effect of particulate fillers such as HAF black, silica, and zinc stearate on the thermal and physical properties of the 38.5 ZnS-SBR ionomers was discussed in this chapter.

4.2 Differential scanning calorimetry (DSC)

The DSC results of 38.5 ZnS-SBR ionomer and its compounds containing 30 phr HAF black, silica, and zinc stearate are presented in table 4.1 The DSC profiles as shown in figure 4.1 revealed that all these fillers slightly influenced the T_g of the 38.5 ZnS-SBR ionomer. The interaction of the active sites on the filler surface with both the matrix and the ionic domains in the ionomer may be responsible for the change in the glass rubber transitions on filler reinforcement.

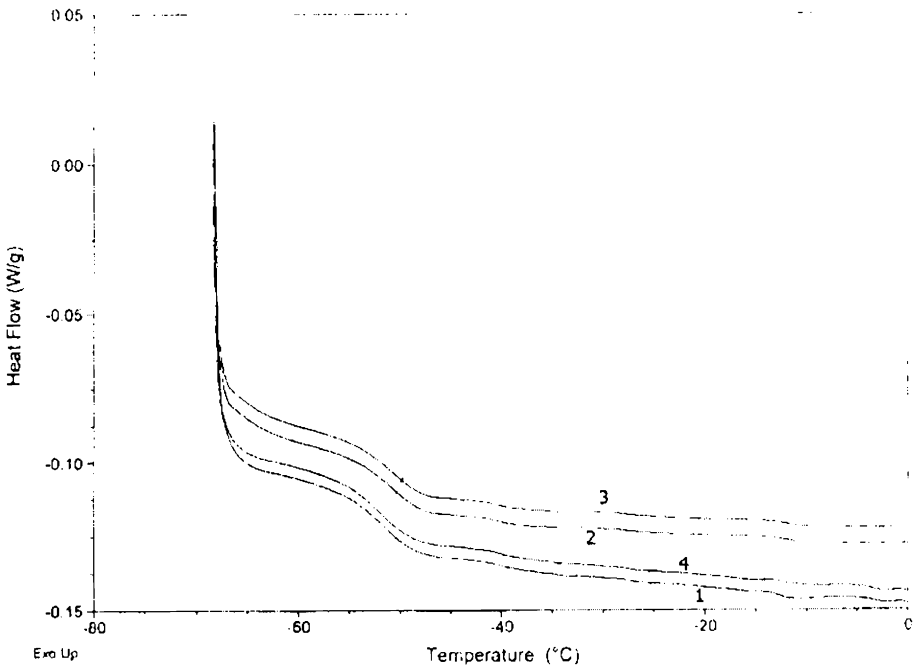


Figure 4.1 DSC profiles of the ionomer and its 30 phr filled compounds.

Samples are 1= neat ionomer; 2, 3, and 4, represent ionomer filled with 30 phr HAF black, Silica, and Zinc stearate respectively

Table 4.1 DSC results of ionomer/filler compounds containing 30 phr filler

Samples	Tg1(°C)
1	-51.33
2	-50.55
3	-50.97
4	-51.10

Samples are, 1 38.5 ZnS-SBR; 2, 3, and 4 represent 38.5 ZnS-SBR filled with HAF black, Silica, and Zinc stearate respectively

4.3 Dynamic mechanical thermal analysis

Results of dynamic mechanical thermal analyses for the 38.5 ZnS-SBR ionomer and their filled compounds (30 phr) are summarized in the table 4.2. Incorporation of (HAF) carbon black into the neat ionomer increased its T_g from -42.014°C to -41.654°C . But the change is significant in the case of silica filled system.

Table 4.2 Results of dynamic mechanical thermal analyses

Sample	T_g ($^\circ\text{C}$)	$\tan\delta$ at T_g	Transition due to ionic aggregates ^b T_i ($^\circ\text{C}$)	Log E' (Pa) at T_g
1	-42.014	0.6030	-19 to +19	8.150
2	-40.654	0.5720	-19 to +10	8.602
3	-38.754	0.5590	-19 to +20	8.701
4	-41.574	0.5965	-19 to +10	8.438

1=neat ionomer; 2=HAF black; 3 = Silica; 4 = Zinc stearate

As compared to the unfilled ionomer the $\tan\delta$ value of the filled compound is decreased. Reinforcement of the matrix is evident from the $\tan\delta$ value at T_g . The storage modulus is found to increase for the filled system. This is attributed to the strong interactions involving the backbone chains^{10, 11} and the clusters. Compared to HAF black incorporation of silica results in a further decrease in $\tan\delta$ presumably due to the formation of an adsorbed polymeric shell on the active filler surface. The incorporation of silica caused a slight increase in the T_g was also observed, which may be due to the stiffening of the backbone chain.

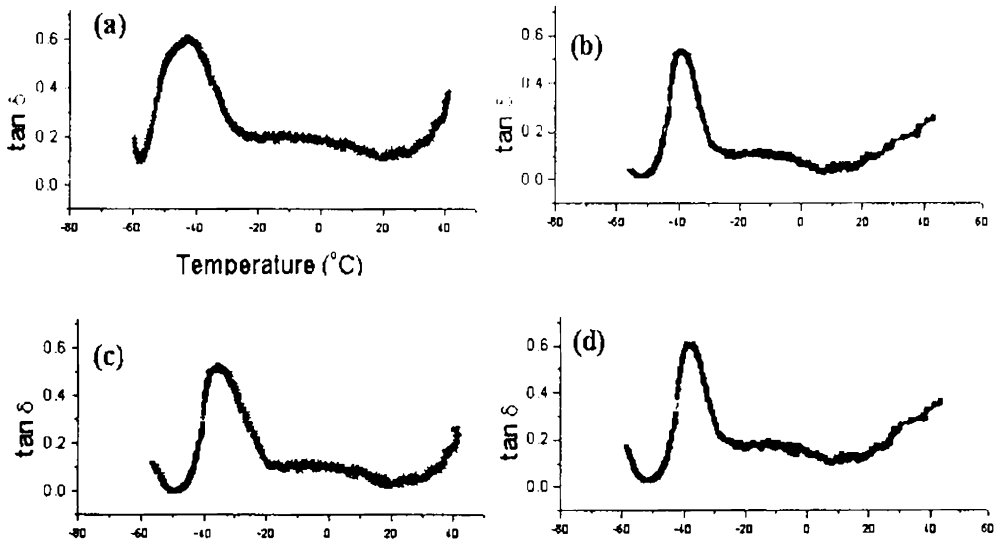


Figure 4.2 $\tan \delta$ plots of the 30 phr filled compounds of 38.5 ZnS-SBR ionomer.

a= 38.5 ZnS-SBR, b= HAF black; c= Silica;

and d=Zinc stearate.

The incorporation of zinc stearate in to 38.5ZnS-SBR ionomer also increases its glass-rubber transition (T_g). In the case of zinc stearate filled ionomer based on SBR, zinc stearate has a dual effect. The dual role exhibited by zinc stearate in ionomers based on SBR may be evident from the intensity of $\tan \delta$ peak at T_{g2} (Table 4.2). The $\tan \delta$ values at the T_{g2} are higher than the other filled systems. Zinc stearate acts as reinforcing filler and also it plasticises the ionic domains. The thermal profile of the zinc stearate filled SBR ionomer resembles the investigations of Weiss¹². Appearance of multiple transitions for the zinc stearate compound of the SBR ionomer along with the detection of the anomalous melting behavior of the zinc stearate in the thermal profiles may be considered as evidence of interactions between zinc stearate and sulphonate groups in SBR ionomers. Appearance of both the low temperature as well as high temperature transitions for the filled zinc sulphonated ionomer samples, similar to the neat ionomer ZnS-SBR, is considered as an evidence for the retention of the micro phase and the “physical cross-links” as characteristic of ionomers.

4.4 Physical properties

4.4.1 HAF black

The physical properties of the 38.5 ZnS-SBR and its HAF carbon black filled compounds are summarized in Table 4.3. As expected hardness increased as the loading of carbon black increased. Hardness is a measure of modulus of elasticity at low strain ¹¹. Incorporation of carbon black caused a gradual increase in tensile strength and decrease in elongation at break. Tear strength values of 38.5ZnS-SBR increases with incorporation of HAF carbon black. It is known that tear strength is enhanced by factors, which tend to dissipate energy ¹².

Table 4.3 Physical properties of HAF filled 38.5 ionomer at 25°C

Sample	Hardness (Shore A)	Tensile strength (MPa)	Elongation at break (%)	Tear strength (kN/m)
ZnS-SBR-4	64	6.69	108	26.21
ZnS-SBR-4+ 10 phr HAF	70	10.38	100.30	28.12
ZnS-SBR-4+ 20 phr HAF	81	12.90	70.95	30.21
ZnS-SBR-4+ 30phr HAF	85	16.41	38.75	33.90

The carbon black filler particles strengthen the physical crosslinks arising from the ionic aggregates there by increasing the strength properties.

4.4.2 Silica

Measurement of the physical properties of the ionomer and its compounds containing 10, 20 and 30-phr silica showed that the physical properties of the base ionomer increased with filler loading (Table 4.4). The tensile strength increased with the silica loading. The incorporation of filler caused a gradual increase in tensile strength and a decrease in the elongation at break. The higher tear strength of the silica filled ionomer may be due to the reinforcement of the matrix with the silica particles. The interaction between free – OH groups on silica with the polar centers of the ionomer may be the reason for the reinforcement.

Table 4.4 Physical properties of silica filled 38.5 ionomer at 25°C

Sample	Hardness (Shore A)	Tensile strength (MPa)	Elongation at break (%)	Tear strength (kN/m)
ZnS-SBR-4	64	6.69	108	26.21
ZnS-SBR-4+ 10 phr silica	72	9.58	90.30	26.92
ZnS-SBR-4+ 20 phr silica	80	12.65	78.95	31.91
ZnS-SBR-4+ 30phr silica	86	14.25	45.75	34.23

4.4.2 Zinc stearate

The results of stress-strain properties are given in table 4.5. The addition of zinc stearate increased the hardness. The tensile strength and tear strength also

increased as the filler loading increased. The elongation at break also increased with increase in filler loading. Zinc stearate acts as a reinforcing filler at ambient temperature where as at the higher temperature it plasticises the ionic domains.

Table 4.5 Physical properties of 38.5 ionomer filled with zincstearate at 25°C

Sample	Hardness (Shore A)	Tensile strength (MPa)	Elongation at break (%)	Tear strength (kN/m)
ZnS-SBR-4	64	6.69	108	26.21
ZnS-SBR-4+ 10 phr Zinc stearate	76	7.38	150.30	26.52
ZnS-SBR-4+ 20 phr Zinc stearate	78	8.90	185.95	28.91
ZnS-SBR-4+ 30phr Zinc stearate	80	10.41	206.50	30.23

4.5 Reprocessability studies

It has been observed that (Table 4.6), the stress-strain properties of the filled ionomer compounds at all the filler loadings under study remain almost constant even after repeated cycles of mixing and molding. This shows that the ionomer composites behave as thermoplastic elastomers and it could be reprocessed by mechanical recycling without deterioration in its physical properties.

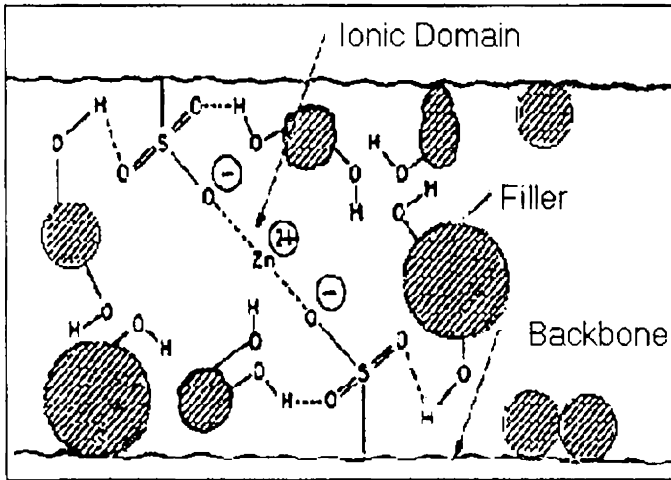
Table 4.8 Results of reprocessability studies ionomer / 30 phr filler compounds

Samples	E.B. at cycles (%)			Tensile strength at cycles (MPa)		
	1	2	3	1	2	3
1	108	110	104	6.69	6.56	6.23
2	38.75	41.7	39.5	16.41	16.50	16.20
3	45.75	44.1	44.5	14.25	14.0	13.8
4	206.5	210	205	10.41	10.60	10.10

1- neat ionomer; 2, 3, and 4 show ionomers filled with 30 phr each of HAF black, Silica, and Zinc stearate respectively

4.6 Mechanism of filler reinforcement

The interaction of the filler and the ionomer imparts an increase in stiffness and strength to the ionomer. In order to produce significant reinforcement, particle size must be less than about a micron. As specific surface area increases (i.e., as particle size decreases), strength of filled vulcanizates generally increases. Based on the results of thermal, and physical, studies it was deduced that the fillers act as facilitators for a stronger inter cluster attraction, which results in an increase in the glass transition temperature and thus decreasing the corresponding $\tan \delta$ and assumed that the polymer – filler interactions in the case of filled ZnS-SBR are of two types: (i) filler–nonpolar polymer backbone, which is similar to the interaction involving diene rubbers and reinforcing fillers, and (ii) ionic groups of the ionomer–polar groups present on the surface of the filler particles (- OH, >C=O, etc.), as proposed in scheme 4.1. While the rubber–filler interaction involving the non-polar polymer backbone is of weak van der Waals type; the same due to ionic aggregates can be of much stronger type. The increase in the T_g for the filled compounds of ZnS-SBR showed that carbon black, silica, and zincstearate act as reinforcing fillers.



Scheme 4.1 Proposed model showing the filler- ionomer interaction

4.7 Comparison of the physical properties

Among the fillers properties were observed to be in the order HAF black > silica > zinc stearate. The tensile strength was higher for the HAF filled ionomer and minimum for the zinc stearate/ionomer system (Figure. 4.3).

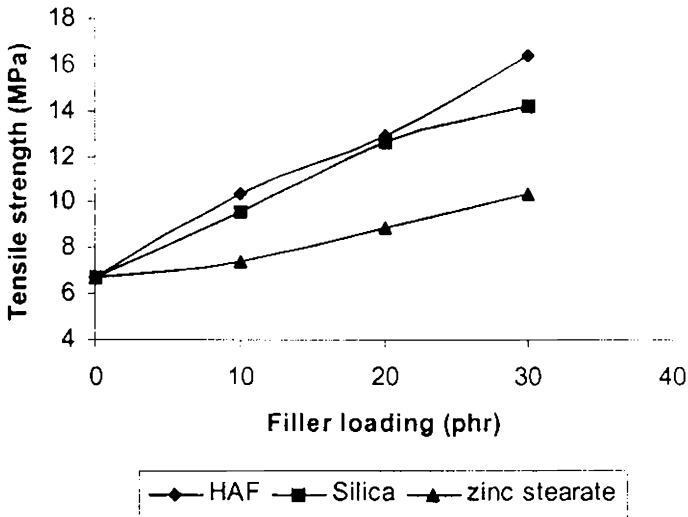


Figure. 4.3 Comparison of the tensile strength ionomer filled with (1) HAF black (2), silica and (3) zinc stearate

The elongation at break (Table 5.7), however, had its lowest value for the HAF filled system and highest for the zincstearate system. Both HAF and silica filled systems have shown higher tear strength. The shore A hardness of the silica reinforced compounds was higher than the other filled compounds of ionomers.

4.8 Conclusion

DSC AND DMTA results showed that the glass transition temperature was affected by filler incorporation. The $\tan\delta$ value of the thermal transitions suggests that all the fillers reinforce the backbone chain. The filled systems showed improvement of mechanical properties over the neat ionomer. Reprocessability studies revealed that the filler reinforced ionomer behave as thermoplastic elastomers and it could be reprocessed by mechanical recycling without deterioration in its physical properties. Particulate fillers such as HAF black, silica, and zinc stearate reinforce with the ionomers based on styrene butadiene rubber.

4.9 References

1. Meiccke, E.A.; Taftaf, M.I. *Rubber Chem. Technol.* **61**, 534 (1988).
2. Medalia, A.I. *Rubber Chem. Technol.* **60**, 45 (1987).
3. Ludberg, R.D.; Makowski, H.S.; Westerman, L. *Adv. Chem. Ser.* **187**, 67 (1980).
4. Ma, X.; Sauer, J.A.; Hara, M. *Polymer* **38**, 4425 (1997).
5. Kurian, T.; De, P.P.; Khastgir, D.; Tripathy, D.K.; De, S.K.; Peiffer, D.G. *Polymer*, **36**, 3875 (1995).
6. Kurian, T.; Khastgir, D.; De, P.P.; Tripathy, D.K.; De, S.K.; Peiffer, D.G. *Polymer*, **37**, 5597 (1996).
7. Kurian, T.; Bhattacharya, A.K.; De, P.P.; Tripathy, D.K.; De, S.K.; Peiffer, D.G. *Plast. & Rubber Proc. & Applications* **25**, 2075(1995).
8. Eisenberg, A.; Hird, B.; Moore, R.B. *Macromolecules* **23**, 4098 (1990).
9. Thommachan Xavier; Samuel, J.; Kurian, T. *Macromol. Mater. Eng.* **286**, 507 (2001).
10. Gauthier, C.; Chauchard, J.; Chabert, B.; Trotignon, J.P.; Battegay, G.; Lamblin, V. *Plast. & Rubber Proc. & Applications* **20**, 77(1993).
11. O'connor, J.E. *Rubber Chem. Technol.*, **50**, 945 (1977).
12. Weiss, R.A. *J. Appl. Polym. Sci.*, **28**, 3321(1983).

Chapter 5

Dielectric properties of ZnS-SBR ionomers

- 5.1 *Introduction*
 - 5.2 *Dielectric measurement-theory*
 - 5.3 *Dielectric properties of ionomers*
 - 5.3.1 *Complex permittivity*
 - 5.3.2 *Complex conductivity*
 - 5.3.3 *Loss tangent*
 - 5.3.4 *Microwave heating coefficient*
 - 5.3.5 *Absorption coefficient*
 - 5.3.6 *Penetration depth*
 - 5.4 *Conclusion*
 - 5.5 *References*
-

5.1 Introduction

Properties of polymeric materials are influenced by the presence of ionic groups. Besides modifying the mechanical properties, the presence of ionic groups in polymers is also found to affect their dielectric properties¹⁻⁵. Incorporation of ionic groups into polymers leads to the increase of the conductivity to the level, which is of practical interest. The electric conductivity may also be improved by blending conducting low molecular weight material into the polymer matrix. This chapter presents the studies of dielectric properties of zinc sulphonated styrene butadiene rubber ionomers.

Dielectric properties are one of the most widely varying physical properties known. The dielectric behaviour of a polymer is determined by the charge distribution and the statistical thermal motion of polar groups. It is therefore evident that the chemical structure should be the basic factor in the determination of dielectric behaviour. Polymers that have polar bonds in their chains would be expected to have high dielectric constants. Understanding of the electrical properties of polymers is important in two areas, (i) generation of high performance electrical insulators, and (ii) the synthesis of metallically conducting polymers. For purely practical reasons, there is always a need to produce material with lowest conductivity, than are currently available for high-quality communication cables, optical fibers, and low-loss power cables. There is also a need for better materials of intermediate conductivity (10^{-9} S/cm to 10^{-2} S/cm) to eliminate static charges from conveyor belts, carpeting, clothing, bushings, and satellite antennas. Generation of high conducting polymers with conductivity equal to the best of metals and organic super conductors with high transition temperatures are also vibrant areas of research nowadays.

Microwave properties of many polymers and their compounds are of growing interest due to their potentially wide range of applications like dielectric wave guides, lenses, dielectric resonators and microwave integrated circuit (MIC). Estimation of the heating response of lossy material is also important in microwave heating

applications^{6,7}. The dielectric data, at these frequencies besides being useful on lossy ceramics for their use as microwave absorbers; lossy pastes for the design of new food packages, for heating in microwave ovens and on biological materials for diathermy also serve as a tool for investigating the intermolecular and intramolecular mechanisms of compounds. It has also been useful to estimate the amount of moisture in wood, sand and agricultural products.

Microwaves constitute only a small portion of the electromagnetic spectrum, but their uses have paramount importance in the material characterization for Industrial Scientific and Medical applications (ISM)⁸. Under a suitable microwave frequency, the ionic centers of ionomers may be polarized. Hence, it seems worthwhile to investigate the dielectric properties of the ionomers at the microwave region. In spite of the relatively extensive effort on the investigations on the microwave dielectric properties of many conductive polymers, very little work has been conducted in dielectric characterization of ionomers⁹⁻¹³. As the dielectric properties aid the calculation of internal electric fields resulting from the exposure to the nonionising electromagnetic (EM) fields, it has excellent medical applications. The real part of the relative complex permittivity (dielectric constant) can vary from a value of about two to few thousands while the imaginary part of the relative complex permittivity (dielectric loss) vary from a small fraction to about hundreds for some materials.

The present study envisages a new and convenient microwave method called cavity perturbation technique, where the samples can be used in the pellet, powdered, solution, bulk, or in other desired forms. Cavity perturbation technique is used for the evaluation of the dielectric properties of the materials¹³ at microwave frequencies. The experimental set-up consists of a transmission type rectangular cavity resonator, HP 8510 C network analyzer and an interfacing computer. The experimental set-up has been described in detail in the section 2.7 of chapter 2. The

test specimens were moulded in an electrically heated hydraulic press for 5 minutes at 150°C, under a pressure of 10 MPa. Strip shaped test specimens were introduced into the cavity resonator through non-radiating slot for measurement.

The four key parameters – dielectric constant (ϵ'), dielectric loss (ϵ''), tangent of dielectric loss angle ($\tan\delta$), and dielectric conductivity (σ') of the ionomers based on SBR at S band (2-4 GHz), C band (5-7 GHz), and X band (8-12 GHz) of the microwave region were measured. The other related parameters such as microwave heating coefficient and absorption coefficient are also discussed. The resonant frequencies and the corresponding quality factors of the unloaded cavity resonators are given in Table 5.1.

Table 5.1. Characteristic features of the cavity resonators

Type of cavity	Resonant frequency (GHz)	Unloaded Q - factor
S - band cavity (TE ₁₀₃ - TE ₁₀₇)	2.4401	7781
	2.6850	7140
	2.9712	6548
	3.2875	7245
	3.6257	5162
	3.9797	5097
C - band cavity (TE ₁₀₃ - TE ₁₀₇)	5.0892	2347
	5.6321	2215
	6.2497	2046
	7.6580	2281
X- band cavity (TE ₁₀₅ - TE ₁₀₉)	8.5585	1670
	9.3085	1372
	10.1180	1303
	10.9780	840
	11.8820	706

5.2 Dielectric measurement- theory

The measurements were made in the frequency range from 2 to 12 GHz using cavity perturbation method. Cavity perturbation technique is a highly sophisticated method for the evaluation of dielectric properties of the materials. According to the theory of cavity perturbation, the complex frequency shift during perturbation by a sample is:

$$-\frac{d\Omega}{\Omega} \approx \frac{(\bar{\epsilon}_r - 1)\epsilon_0 \int_{V_s} E \cdot E_0^* dV + (\bar{\mu}_r - 1)\mu_0 \int_{V_s} H \cdot H_0^* dV}{\int_{V_c} (D_0 \cdot E_0^* + B_0 \cdot H_0^*) dV} \quad (1)$$

When the dielectric sample is introduced at the position of maximum electric field; the above equation is reduced to:

$$\frac{-d\Omega}{\Omega} \approx \frac{(\bar{\epsilon}_r - 1) \int_{V_s} E \cdot E_{0\max}^* dV}{2 \int_{V_c} |E_0|^2 dV} \quad (2)$$

Where $d\Omega$ is the complex frequency shift, E and H are the electric and magnetic fields in the perturbed cavity, and E_0 and H_0 are that inside the unperturbed cavity respectively, $\bar{\epsilon}_r$ is the relative complex permittivity of the sample

If Q_0 is the quality factor of the empty cavity and Q_s as that of object loaded cavity, the frequency shift can be represented as:

$$\frac{d\Omega}{\Omega} = \frac{d\omega}{\omega} + \frac{j}{2} \left(\frac{1}{Q_s} - \frac{1}{Q_i} \right) \quad (3)$$

Equating (2) and (3) and separating real and imaginary parts, and assuming $E = E_0$, we get

$$\epsilon_r' - 1 = \frac{f_o - f_s}{2f_s} \left(\frac{V_c}{V_s} \right) \quad (4)$$

$$\epsilon_r'' = \frac{V_c}{4V_s} \left(\frac{Q_o - Q_s}{Q_o Q_s} \right) \quad (5)$$

Where ϵ_r' is the real part of the relative complex permittivity, which is usually known as dielectric constant and ϵ_r'' , the imaginary part of the relative complex permittivity, which is associated with the dielectric loss of the material. While f_o and f_s represent the resonant frequencies of the cavity without and with sample. V_s and V_c are the volumes of the sample and the cavity resonator respectively.

The relative complex permittivity (ϵ_r^-) can be related as

$$\epsilon_r^- = \epsilon_r' - i\epsilon_r'' \quad (6)$$

The complex conductivity is expressed in terms of complex permittivity as given as

$$\sigma^* = i\omega \epsilon_0 \epsilon_r^- = i\omega \epsilon_0 (\epsilon_r' - i\epsilon_r'') \quad (7)$$

If σ^* is expressed in terms of its real and imaginary components of conductivity;

$$\sigma^* = \sigma' + i\sigma'' \quad (8)$$

Where σ' is the real part of complex conductivity and σ'' is the imaginary part of complex conductivity and they are related by the following equations.

$$\text{i.e.: } \sigma' = \omega \epsilon_0 \epsilon_r'' = 2\pi f \epsilon_0 \epsilon_r'' \quad (9)$$

$$\sigma'' = \omega \epsilon_0 \epsilon_r'' = 2 \pi f \epsilon_0 \epsilon_r'' \quad (10)$$

The complex refractive index can be related to the complex dielectric permittivity,

$$n^* = (\epsilon_r^-)^{1/2}$$

The loss tangent ($\tan \delta$) is given by the equation

$$\begin{aligned} \tan \delta &= \text{loss current} / \text{charging current} \\ &= \epsilon_r'' / \epsilon_r' \end{aligned} \quad (11)$$

The efficiency of heating is usually compared by means of a comparison coefficient J, which is defined as

$$J = 1 / (\epsilon_r^- \tan \delta) \quad (12)$$

The transparency of the sample to microwave is defined by the parameter, absorption coefficient (α_f), which is given by the equation

$$\alpha_f = \pi \epsilon'' f / n^* c \quad (13)$$

Where n is the real part of the refractive index, c is the velocity of light.

The penetration of waves is governed by δ_f , called the penetration depth or skin depth. However, for most real situations the penetration of waves is smaller than δ_f .

$$\delta_f = 1 / \alpha_f \quad (14)$$

5.3 Dielectric properties of ionomers

5.3.1 Complex permittivity

5.3.1.1 Real part of the complex permittivity (dielectric constant)

The real part of the complex permittivity of the base polymer and the ionomers are probed at S, C and X bands of microwave region. Figures 5.1 to 5.3 demonstrate the dependence of dielectric constant for the ionomers in the S, C and X bands respectively, in the frequency region. It was observed that introduction of ionic groups into the base polymer improves its dielectric constant. This improvement with ionic content may be due to the increase in the polar centres such as unassociated ionic moieties, multiplets, ionic clusters and zinc metal ions in the polymer matrix. The microwave responses of these charge moieties may be contributing towards the dielectric constant. The physical state of polymers may also influence their polarity. At the microwave region orientation polarization takes place. The dipole orientation polarization comes only from the movement of polar groups itself. It is therefore evident that the chemical structure should be the basic factor in the determination of the dielectric behaviour¹⁴.

At high ion content the probability of occurrence of nearest-neighbour ion pairs is high. This probably leads to an enlargement of the multiplets. It was believed that if the dielectric constant is very high the multiplets or cluster formation would not be expected⁵. The dielectric constant changes marginally as the concentration of ionic groups increased from 0 meq to 38.5 meq. At higher ionic content as the ionic groups associated to form clusters; chain segmental movement is restricted.

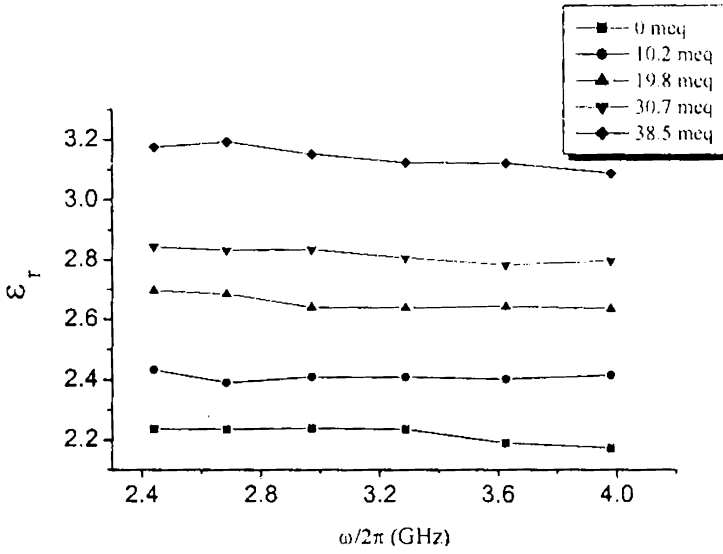


Figure 5.1 Plot of ϵ' with frequency for various ion content at the S band

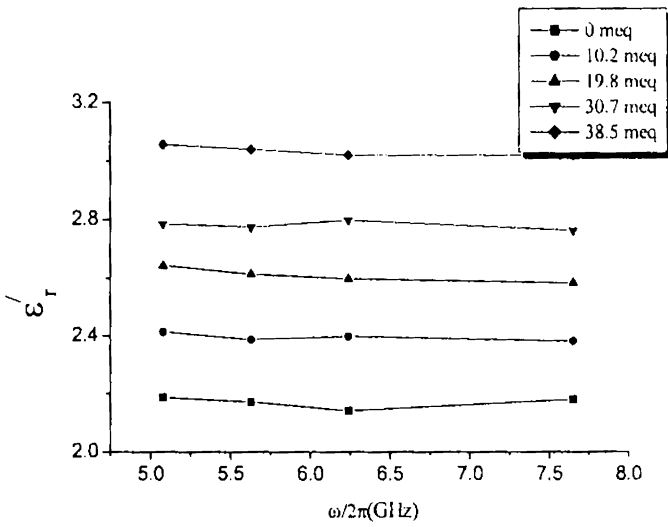


Figure 5.2 Plot of ϵ' with frequency for various ion content at the C band

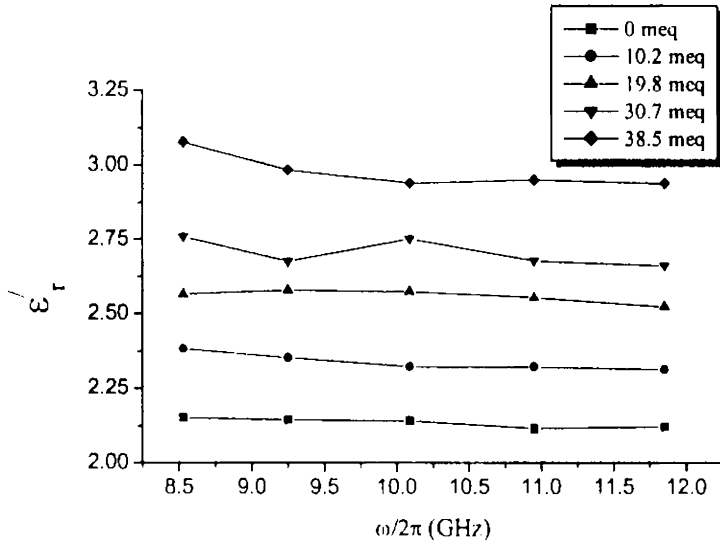


Figure 5.3 Plot of ϵ' with frequency for various ion content at X band

Symmetry and crosslinking tend to decrease the dipole moment¹⁴. Due to the orientation polarization of the dipoles, the possibility of dielectric relaxation cannot be ruled out at higher frequencies. This dipole polarization may be related to the "frictional" losses caused by the rotational displacement of molecular dipoles under the influence of the alternating microwave field. At low frequencies the interfacial polarization is caused by the alternating accumulation of charges at interface between different phases of the material¹⁵. At higher frequencies, the interfacial polarization is caused by the polarization with dipole orientation. This might result in the decrease of ϵ_r' with frequency. The rotatory motion of the molecules may not be sufficiently rapid for the attainment of equilibrium at higher frequency.

5.3.1.2 Imaginary part of the complex permittivity (dielectric loss)

Figures 5.4 - 5.6 shows the log plots of imaginary part of the relative complex permittivity at different bands of microwave frequency. The dielectric loss factor (ϵ_r'') is observed to increase with increasing ionic content. At S band the loss value initially increased until 2.68 GHz and then decreases with frequency. The $\log \epsilon_r''$ plots shows a slow decrease with the value of ϵ_r'' on further increasing frequency (at C and X bands). The dielectric loss becomes large at low frequencies due to free charge motion within the material¹⁶. These values do not correspond to bulk dielectric processes. For very low frequencies there is particularly time for charges to build up at the interfaces before the field changes the direction and this contributes to higher values of ϵ_r'' .

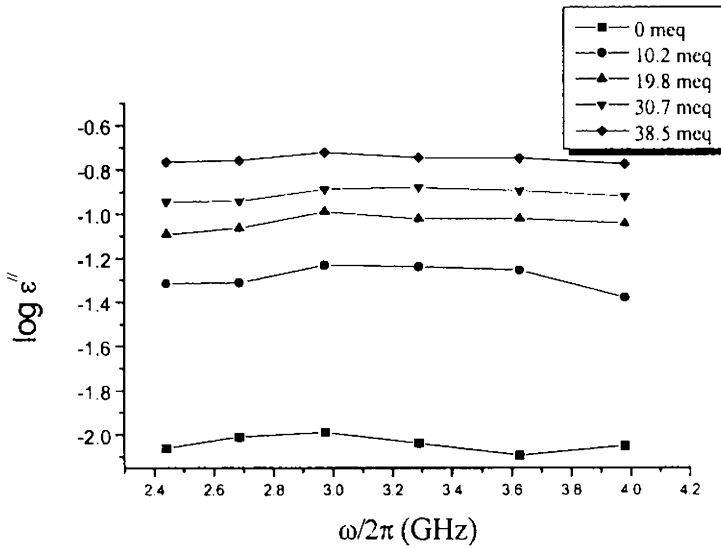
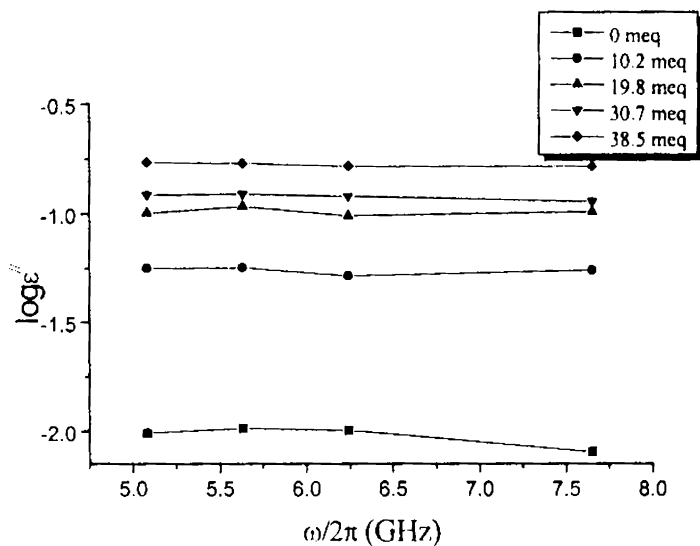
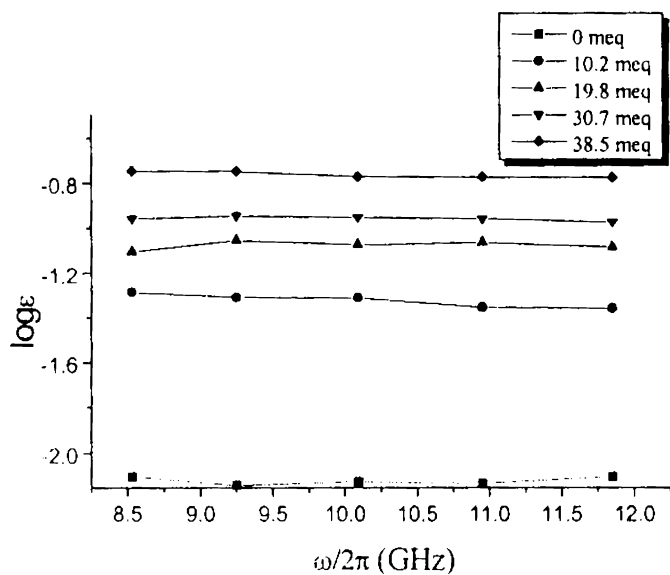


Figure 5.4 Plot of $\log \epsilon''$ with frequency for various ion content at the S band

Figure 5.5 Plot of $\log \epsilon''$ with frequency for various ion content at the C bandFigure 5.6 Plot of $\log \epsilon''$ with frequency for various ion content at the X band

At higher frequency, the rotatory motion of the molecules may be sufficiently rapid so that the equilibrium is not attained with the field. The polarization then acquires a component out of phase with the field, and the displacement current acquires a conductance component in phase with the field, resulting in thermal dissipation of energy. When this occurs, dielectric losses will be generated. At higher ionic content, the molecular interactions would lose the flexibility of the polymer chains.

5.3.2 Complex conductivity

5.3.2.1 Real part of the complex conductivity (σ')

The real part of the complex conductivity (σ') is generally considered as a.c. conductivity¹⁷ also σ' is often used to describe the frequency dependence of conductivity. In the present work, it was revealed that the ac conductivity of the ionomer has been affected by both frequency and ionic content. The figures 5.7 to 5.9 show the log plots of conductivity at various frequencies for the base material and its ionomers. Conductivity was found to increase with increasing ionic content. It was also found that at all bands, the ac conductivity increased with increasing frequency. The conductivity in polymers depends chiefly on the mobility of very small quantities of ions and electrons¹⁴. In metallically conducting polymers, it is related to the quantity of doping material used. So in the case ionomers conductivity strongly depends on the amount ionic content, the more charge carriers there likely to be and as a result, conductivity will increase. The conductivity of the ionomer under the microwave field may be attributed to the polarization caused by the alternating accumulation of ionic associations. Plots of σ' frequency ($\omega/2\pi$) of the microwave signal may be considered as supplementary evidence for the above observations. At microwave frequencies, the polarized matrix between conducting elements modeled as a capacitor network becomes dominant. The displacement current flowing through the capacitor network contributes to ac conductivity.

G8510

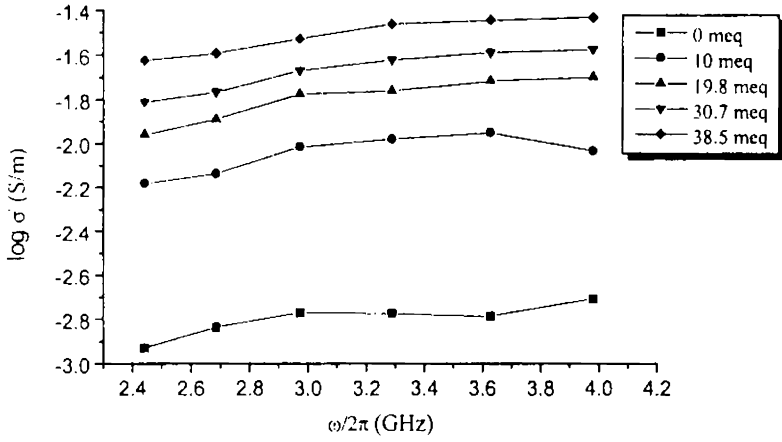


Figure 5.7 Plot of $\log \sigma'$ with frequency at the S band

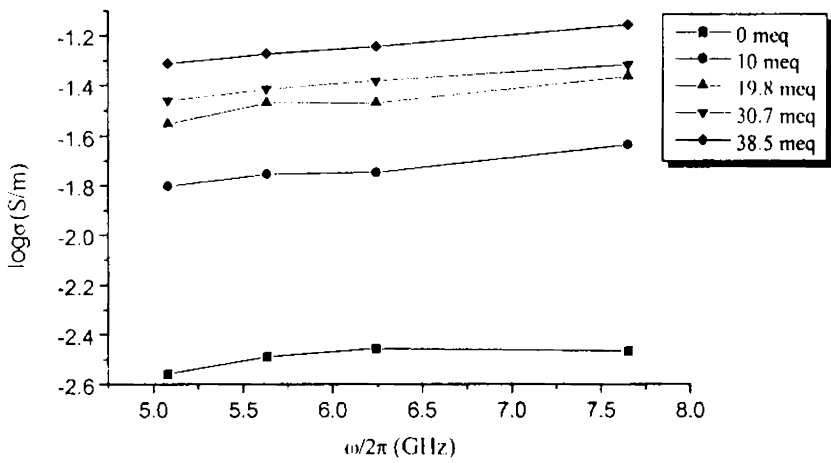


Figure 5.8 Plot of $\log \sigma'$ with frequency at the C band

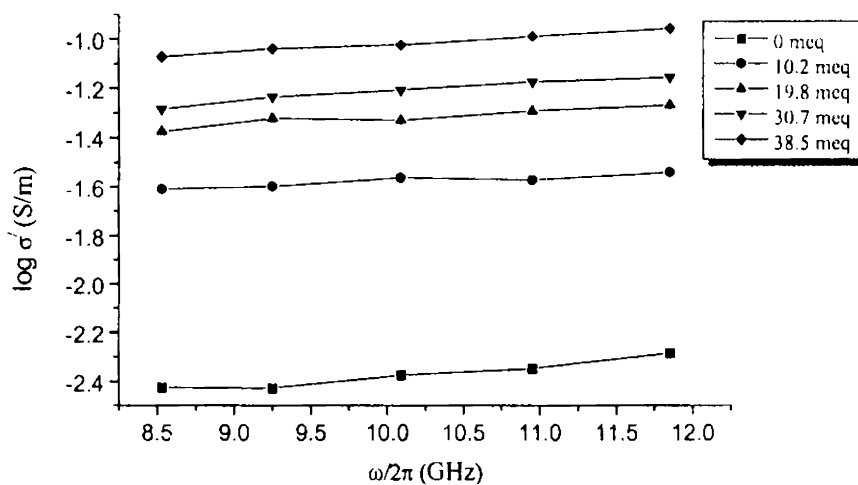
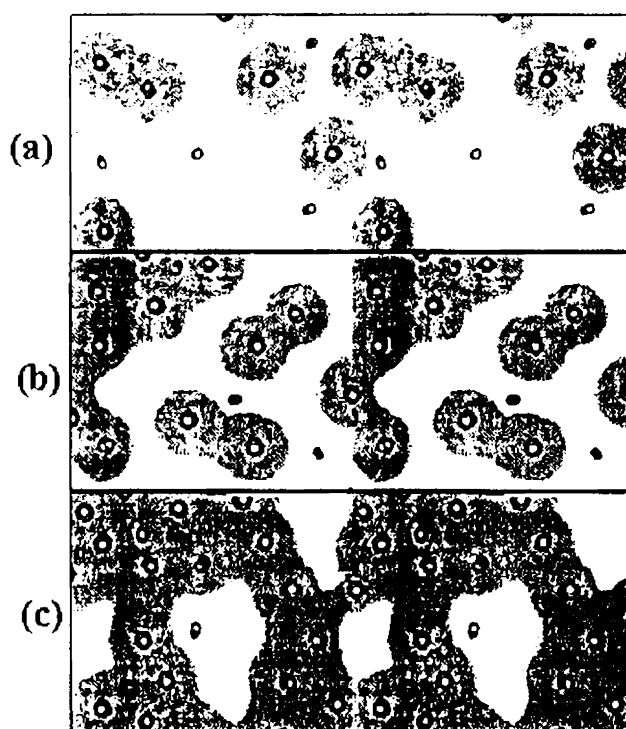


Figure 5.9 Plot of $\log \sigma'$ with frequency at the X band

The dipole attached to a flexible chain can re-orient more easily than the one attached to a stiff chain. Phase inversion and percolation threshold also would be occurring at higher ionic concentration⁵. At very high frequencies, the viscosity of the polymer hinders dipole movement and they cannot orient in the rapidly reversing field. Consequently, the dipoles do not influence the a.c. characteristics at very high frequencies. The many-fold initial increase in the conductivity of the base polymer upon incorporating zinc sulphonate groups may be attributed to the formation of the ionic nano clustering, which act as centers of conductance¹⁸. Because the hydrocarbon backbone cannot transport the charge carriers, the formation of the multiplets represented in scheme 5 may be creating a conducting path. This may be expected to be the main factor for the increase in the complex conductivity with the increase of the ion contents.



Scheme 5 Proposed representations of random ionomers at (a) low ion content, (b) intermediate ion content (c) high ion content. The shaded areas indicate regions of restricted mobility⁵ forming a conducting path.

At higher ionic content, the ion - dipole interaction within the clustering increases. The microscopic viscosity of the ion rich phase governs the conduction. In the case of the SBR ionomers, conduction is through the ion rich phase. In the ZnS - SBR ionomers, the zinc cations may be interacting with the sulphonic acid moieties during neutralization forming the higher multiplets.

5.3.2.2 Imaginary part of the complex conductivity (σ'')

Figures 5.10 to 5.12 shows the plot of imaginary part of the complex conductivity with respect to ionic content and frequencies. The imaginary part of the complex conductivity is linearly related to both ionic content and frequency. The results are

similar to that of the real part of the complex conductivity. This further clarifies that the complex conductivity of the base polymer improved up on its ionomer modification.

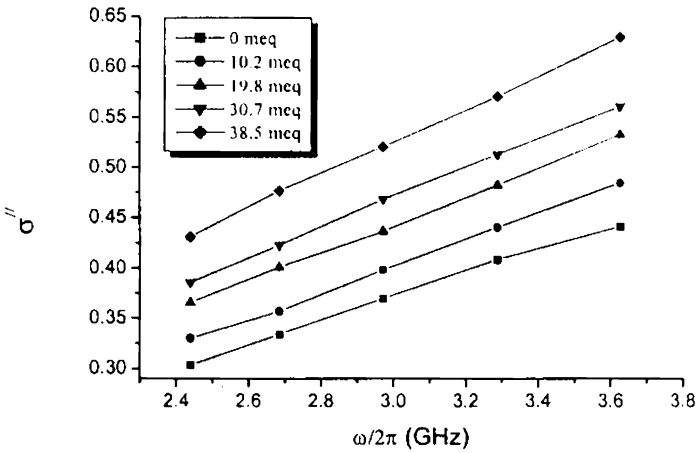


Figure 5.10 Plot of σ'' with frequency at the S band

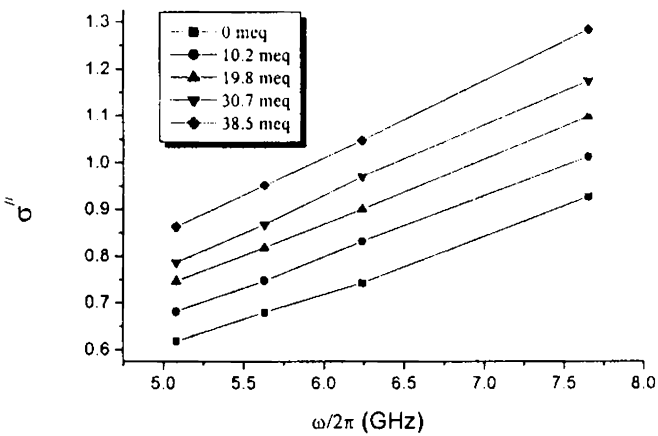


Figure 5.11 Plot of σ'' with frequency at C the band

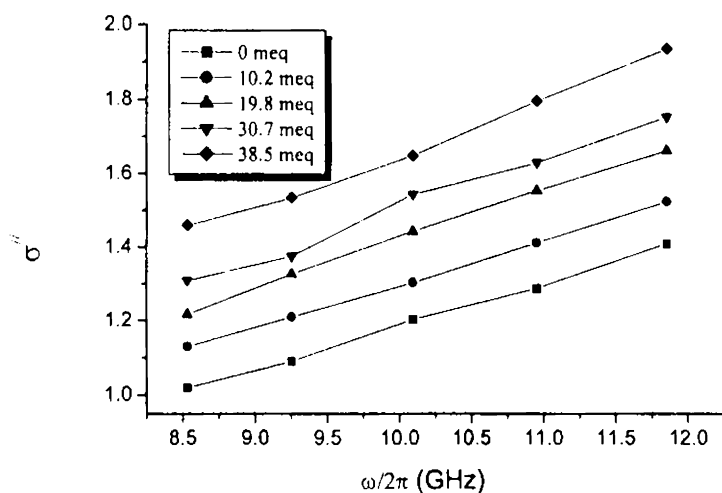


Figure 5.12 Plot of σ'' with frequency at X the band

5.3.3 Loss tangent

The ratio of the imaginary to real parts of the complex permittivity ($\epsilon_r'' / \epsilon_r'$) or tangent of the dielectric loss angle; is commonly employed as a direct measure of the dielectric loss. To evaluate the structure property relationship between the values of the tangent of dielectric loss angles of polymers and their chemical and morphological structures, we should examine the relationships among dielectric constant, dielectric loss, frequency, dipole moment, molecular size and viscosity of the polymer. The plots of loss tangent vs ionic content at various frequencies are given in figures 5.13 to 5.15. The loss tangents for these ionomers increase with ionic concentration. The loss tangent studies of the ionomers at microwave frequencies may be considered as one of the examples of analogy between the mechanical and electrical properties of the ionomers¹⁴.

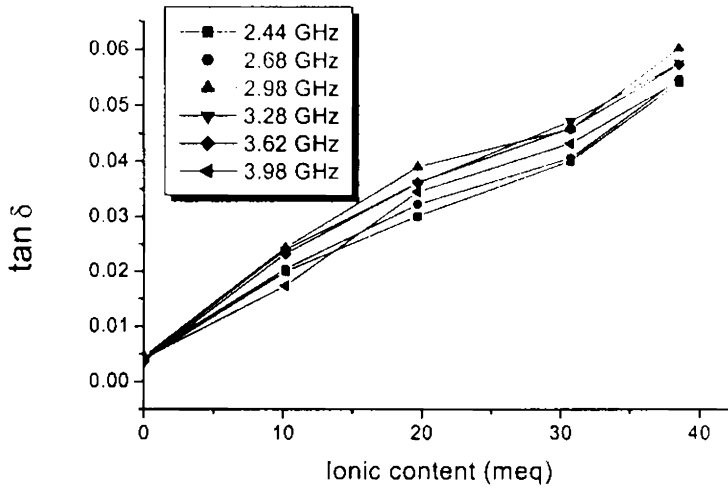


Figure 5.13 Variation of the loss tangent as a function of ionic content at the S band

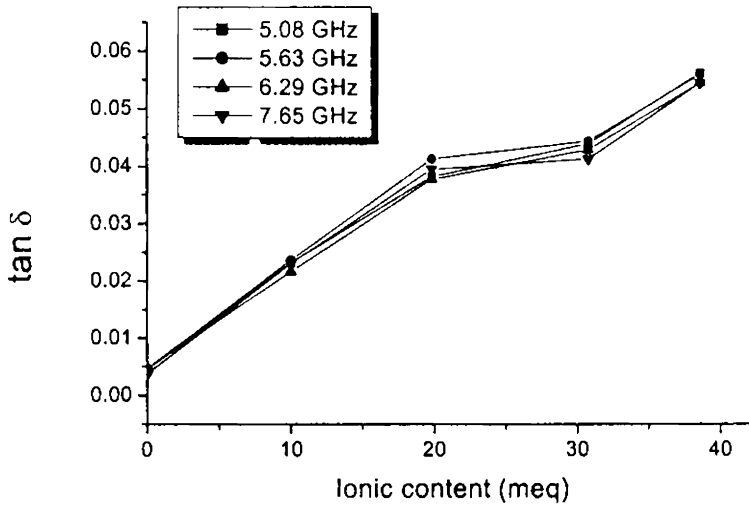


Figure 5.14 Variation of the loss tangent as a function of ionic content at the C band

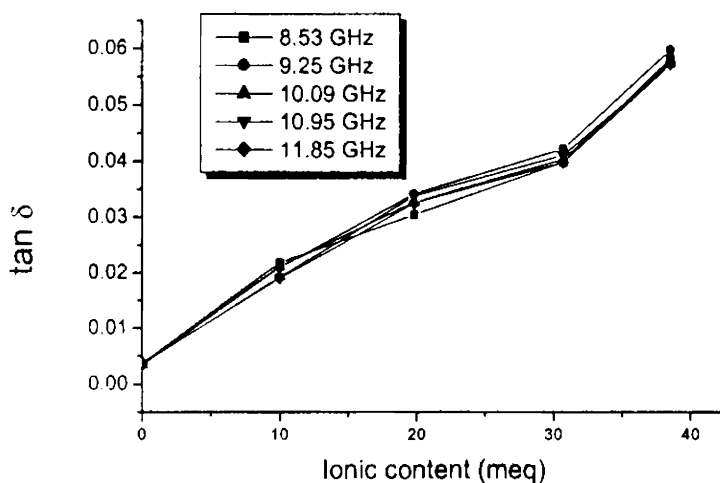


Figure 5.15 Variation of the loss tangent as a function of ionic content at the X band

5.3.4 Microwave heating coefficient (J)

Practically all applications of polymers in electrical and electronic engineering require materials with a low $\tan \delta$. However, one application that takes advantage of a high value of tangent loss is high frequency dielectric heating. In this application, the efficiency of heating is usually compared¹⁴ by means of a heating coefficient J. Figures 5.16 to 5.18 shows the variation of J with ionic content at different microwave frequencies. Smaller the J value, better the polymer for dielectric heating purposes.

Of course, the heat generated in the polymeric material comes from the loss tangent, but that loss may not come entirely from the relaxation loss. Rather, conductivity of the polymeric material may also contribute to the $\tan \delta$. This situation may be compared with ohmic heating of metals where the charge carriers are electrons. The polar centers are the charge carriers in dielectric polymeric materials. There has been considerable improvement in the microwave-heating coefficient of the polymers upon the ionomeric modifications.

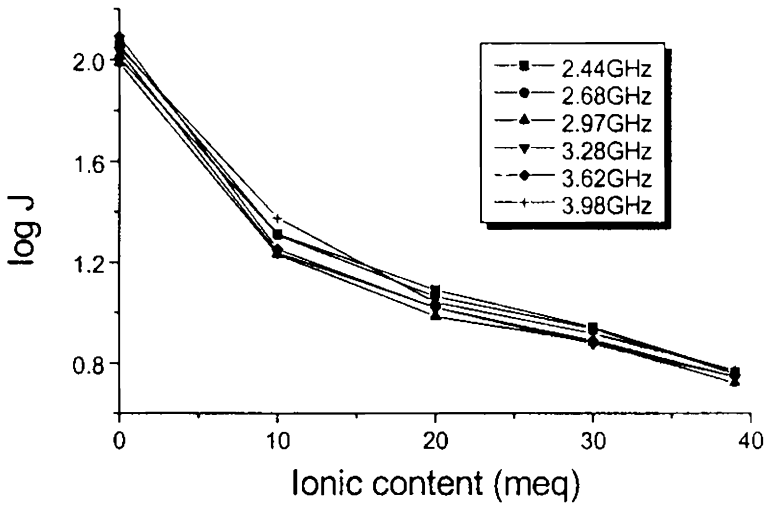


Figure 5.16 Variation of log J with ionic content at S band

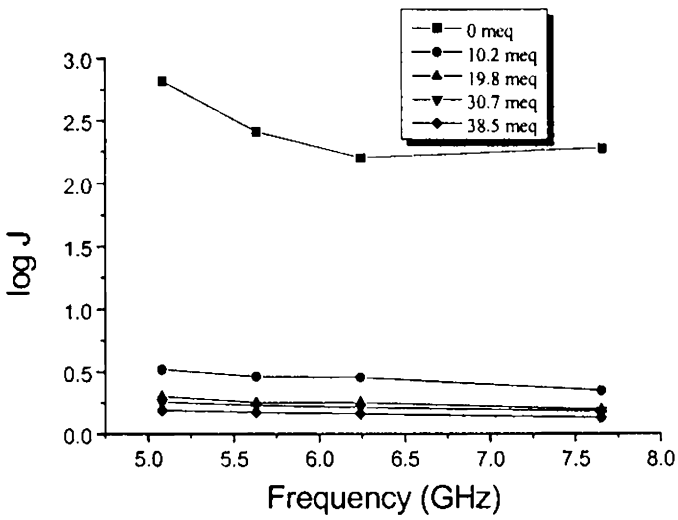


Figure 5.17 Variation of log J with frequency at the C band

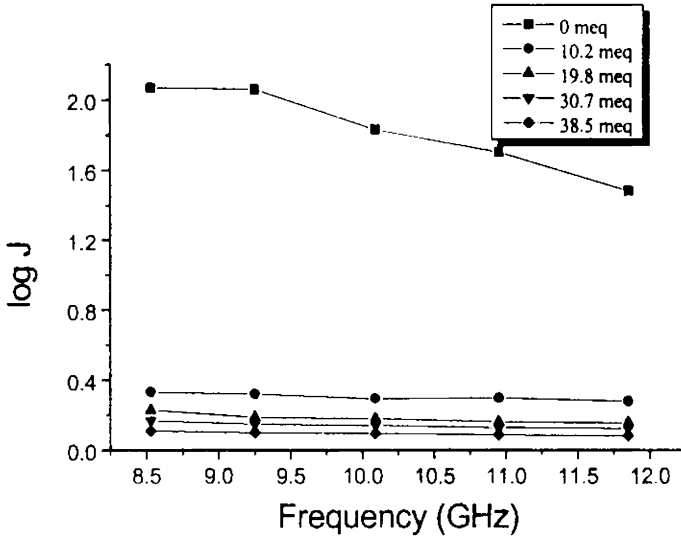


Figure 5.18 Variation of log J with frequency at the X band

5.3.5 Absorption coefficient

The properties of materials in microwave frequency region are usually described by their relative complex permittivity (frequency dependent parameter) and materials can be classified in terms of their transparency of waves passing through it¹⁹. One important parameter derived from the complex permittivity with respect to propagation and absorption of electromagnetic waves when it passes through the medium is the absorption coefficient (α_f). Plots of absorption coefficient vs. frequency are given in figures 5.19 to 5.21. The absorption coefficient increased with increase in frequency and ionic content, which reveals that the material could be very useful in microwave devices.

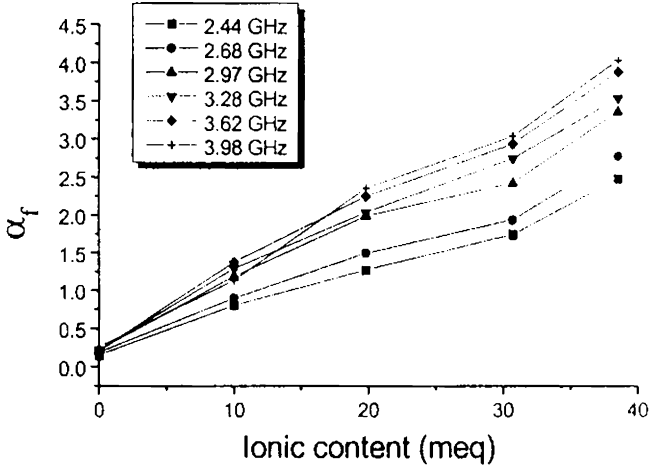


Figure 5.19 Plot of α_f with various ionic content at the S band

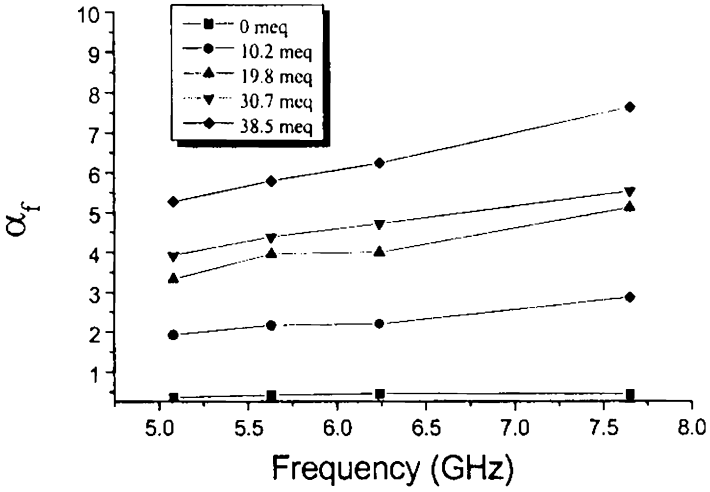


Figure 5.20 Plot of α_f with frequencies at the C band for various ion content

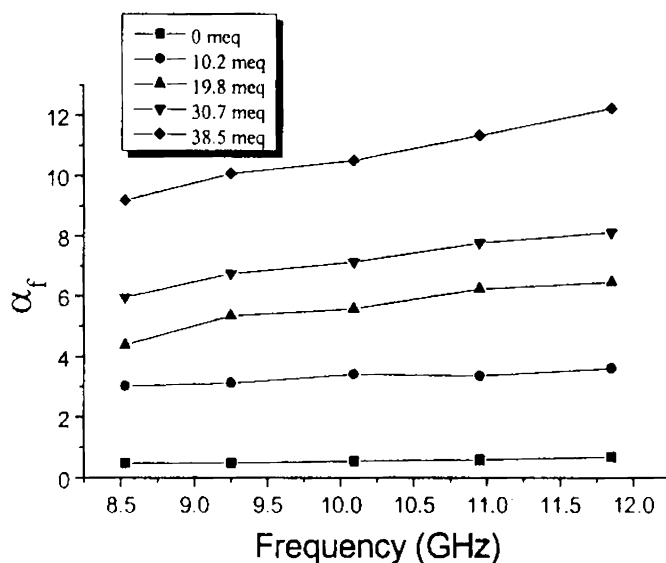


Figure 5.21 Plot of α_f with frequencies at the X band for various ion content

5.3.6 Penetration depth (skin depth)

Skin depth is basically the effective distance of penetration of an electromagnetic wave into the material²⁰. The concept can be applied to a conductor carrying high frequency signals; the self-inductance of the conductor effectively limits the conduction of the signal to its outer shell. The shell's thickness is given by skin depth. The skin depth is inversely related to the frequency and ionic content (figures 5.22 to 5.24). If the material is a perfect conductor, i.e., resistivity $\rho = 0$, meaning $\delta_f = 0$, the skin depth is zero. Incorporation of ionic groups reduces the skin depth.

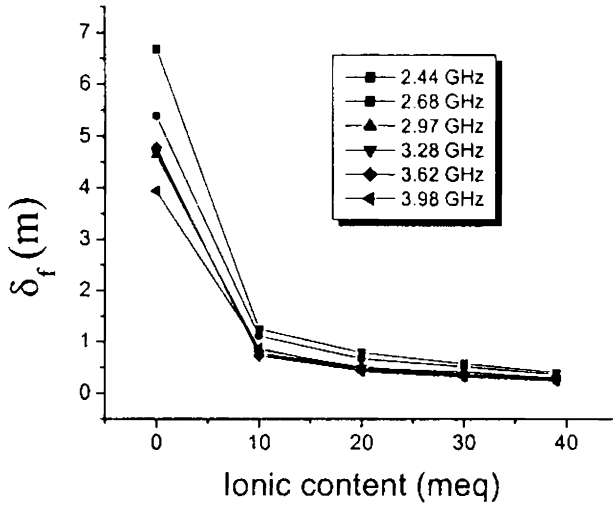


Figure 5.22 Plot of δ_f with ionic content at the S band

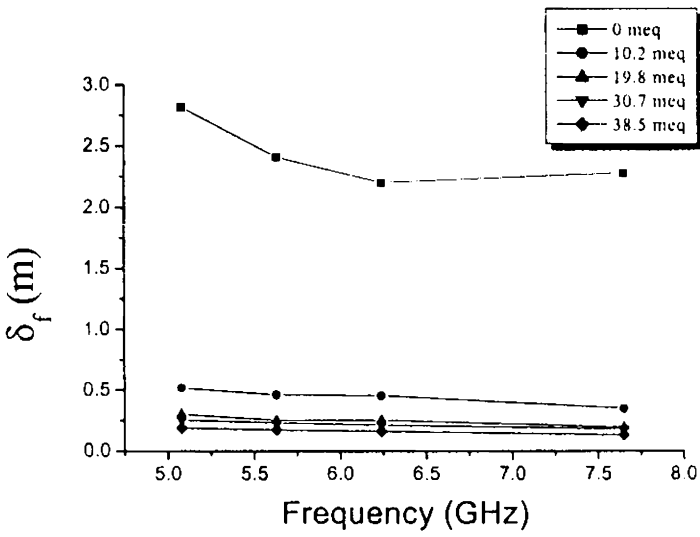


Figure 5.23 Plot of δ_f with frequency at the C band

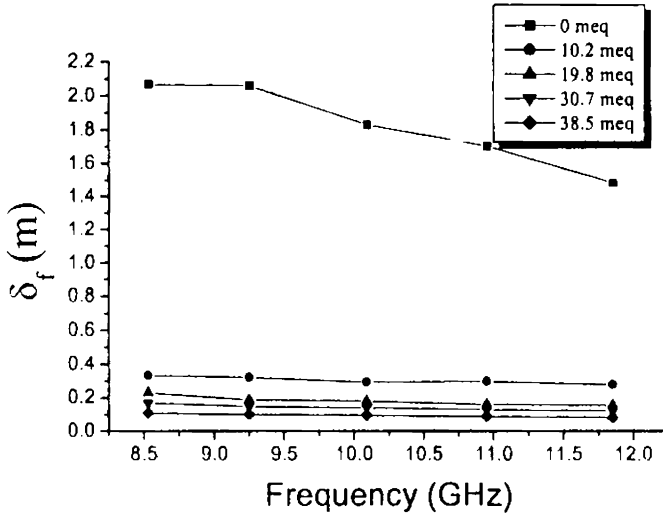


Figure 5.24 Plot of δ_f with frequency at the X band

5.4 Conclusion

The four key parameters –the real part of the complex permittivity (dielectric constant), imaginary part of the complex permittivity (dielectric loss), dielectric loss tangent, and conductivity of the ionomers measured at microwave frequencies have been discussed. The presence of ionic groups in the polymer, which are held through coulombic forces, are observed to affect the electrical properties. Incorporation of ionic groups leads to increase of dielectric constant and conductivity. The measurement at room temperature showed that the complex permittivity and the relative complex conductivity were increased with increase in the ionic concentration. The heating coefficient decreased with increasing ionic content. The absorption coefficient is linearly related to both frequency and ion content. The penetration depth was decreased with increasing ion content and frequency.

5.5 References

1. Eisenberg, A. and Kim, J. -S, *Polymeric Materials Encyclopedia*, , CRC Press, Vol.5, 1996.
2. Vanhoorne, P. and Register, R.A., *Macromolecules*, **29**, 598 (1996).
3. MacKnight, W.J. and Earnest T.R. Jr., *J. Polym. Sci., Macromol. Rev.*, **16**, 41 (1981)
4. Eisenberg, A. , Hird, B., and Moore, R.B., *Macromolecules*, **23**, 4098 (1990)
5. Eisenberg, A.; Kim, J. -S. in *Introduction to Ionomers*. Wiley Interscience Publication, New York, (1998).
6. Bur, A. J. *Polymer*, **26**, 963 (1985).
7. Joo, J; Epstein, A. J. *Plastics Portable Electronics*. Retec Proceedings, Las Vegas, 140 (1995).
8. Thuery, J. In: *Microwaves: "Industrial, Scientific, and Medical Applications"*. Grant, E.H. Ed., ARTEC HOUSE, INC, Norwood, 1992.
9. Read, B.E.; Carter, E.A.; Connor, T.M.; MacKnight, W.J. *Brit. Polym. J.*, **1**, 123 (1969).
10. Phillips, P.H.; MacKnight, W.J. *J. Polym Sci A-2*, **8**, 727 (1970).
11. Hodge, I.M.; Eisenberg, A. *J. Non-Crys. Solids*, **27**, 441 (1978).
12. Dabek, R. *Polym. Eng. Sci.*, **36**, 1065 (1996).
13. Mathew, K.T.Raveendranath,U.In:"*Sensors Update*"Baltes,H.;Gopel,W.;Hesse,J. Ed.WILEY-VCH (Germany), chapter 7, 185, 2000.
14. Chen. C. Ku; Raimond Liepins, "*Electrical Properties of Polymers: Chemical Principles*. Hanser Publishers: Munich, 1987.
15. Bozkurt, A., *J. of Physics and Chemistry of Solids* **63**, 685 (2002).
16. Kyristis, A., Pissis, P., Grammatikakis, *J. Polym. Sci. Part B: Polym. Phys.* **33**, 51 (1995).
17. Ngai, K.L.; Rendell, R.W. '*Dielectric and Conductivity Relaxations in Conducting Polymers*' In: *Hand Book of Conducting Polymers*, Skotheim, T.A. (Ed.), Marcel Decker, New York, 1986.
18. Ezquerro, T.A.; Kremer, F.; Wegner, G. "*AC Electrical Properties of Insulator Conductor Composites*" In "*Dielectric properties of Heterogeneous Materials*"(Progress in Electromagnetic Research 6) Priou, A. Ed., Elsevier, New York, 1992.
19. Bradford, I. S., Carpentier, M-H., "*The Microwave Engineering hand book*" Chapman and Hall, London, 1993.
20. Stephen, C. W., Frederic, H. L., "*Microwaves made simple: principles and applications*" United States Bookcrafters, Chelsea, 1985.

Chapter 6

Technological Compatibilisation of the SBR/NBR Blends

- 6.1. *Introduction*
 - 6.2. *Cure characteristics*
 - 6.3. *Differential scanning calorimetry*
 - 6.4. *Dynamic mechanical thermal analysis*
 - 6.5. *Physical properties*
 - 6.6. *Scanning electron microscopy*
 - 6.7. *Influence of carbon black*
 - 6.7.1 *Cure characteristics*
 - 6.7.2 *Physical properties*
 - 6.7.3 *Dynamic mechanical thermal analysis*
 - 6.7.4 *Morphological studies*
 - 6.8. *Mechanism of compatibilisation*
 - 6.9. *Conclusion*
 - 6.10. *References*
-

6.1 Introduction

There is an increased interest in the use of blends of dissimilar elastomers in various applications since single elastomers do not provide all the necessary properties^{1,2}. Polymer blends are considered as mixtures of macromolecular species. Properties of polymer blends are sensitive to variations in the amounts of the individual polymers and the compatibiliser used^{3,4}. The necessary condition is that the amount of minor component must exceed at least five percent by weight. Most of the polymer blends are found to be immiscible and incompatible. In the case of miscible blends, the overall physico-mechanical properties depend on two structural parameters: (a) proper interfacial tension which leads to a phase size small enough to allow the material to be considered as macroscopically homogenous, (b) an interphase adhesion strong enough to assimilate stresses and strains without disruption of the established morphology. For a very long time, attempts have been made to find compatible polymeric systems or to compatibilize various polymeric mixtures. Only a few systems are known in which two homopolymers are compatible over a very wide composition range. However, compatible blends are desirable because the properties of the mixture are intermediate between those of the homopolymers, rather than giving some type of the superposition of the homopolymer properties.

The compatibility of the blend components is enhanced by interactions such as ionic and H-bonds, as well as donor - acceptor interactions. Ionic groups in the polymers are capable of creating specific interactions between the component polymers in the blend. The compatibility in the case of blends of an ionomer with other polar polymers arises due to ion - ion or ion - dipole interactions. Mixing the polymers in the molten state has facilitated polymer blends preparation. This type of 'reactive blending' may lead to chemical reactions, depending upon the chemical structure of the polymer. This kind of reactive melt-processing technology has many advantages. It

is complementary to polymerization, has high flexibility and versatility, and makes less negative impact on the environment.

Nitrile rubber is a general purpose material resistant to a large variety of oils and greases. It is the workhorse of oil sealing owing to cost/performance compromise. Different nitrile rubber compounds are available for use in contact with fuels and for industrial fluids. Nitrile rubber is generally serviceable between -40°C and 105°C ; it can withstand 120°C intermittently. It is possible to use a blend of high acrylonitrile NBR with SBR to get a degree of oil resistance equal to that given by a low acrylonitrile NBR with an overall economy in cost. Products from high acrylonitrile NBR have a tendency to shrink in contact with hot lubricating oils. However replacing a part of NBR by SBR may overcome this defect. Along with oil resistance property, oil seals and gaskets some times require compression set resistance at higher temperatures. Compression set resistance can be improved by blending with SBR. SBR can also improve its processing properties. For a rubber product with the specifications of good chemical, oil and compression set resistance at high temperature, the NBR/SBR blend may be a good alternative. These blends are, however, found to be immiscible.

Various approaches have been taken to enhance the miscibility of immiscible polymer blends⁵⁻⁹. The SBR/NBR blends can possibly be made miscible by using compatibilisers that can have interactions with SBR and NBR. Compatibilization of SBR/NBR blends using various compatibilisers has been reported^{10,11}. An attractive alternative route for compatibilization is the use of ionomers¹². Studies on few blends have demonstrated that zinc sulphonated ionomers act as good compatibilisers in certain blends¹³. The storage modulus and loss tangent of blends were correlated with the structure parameters^{14,15}. The segments of the ionomers are chemically identical to SBR, and it is possible for the polar zinc sulphonate groups of the ionomer to have interaction with the acrylonitrile unit of NBR.

This chapter deals with the technological compatibilisation of the commercially important binary blend of SBR and NBR. The investigations were made with reference to their cure, thermal, dynamic mechanical, physical and morphological observations. In this study, the effect of zinc sulphonated styrene-butadiene rubber ionomer (ZnS-SBR) on the compatibility of SBR/ NBR blend was investigated. It has been observed that the compatibility of SBR and NBR could be enhanced, and the mechanical properties of the blend improved by the addition of the ionomer.

6.2 Cure characteristics

The 38.5 ZnS-SBR ionomer, used as the compatibiliser, was added to the preblended SBR/NBR at various concentrations in the range of 0-10 phr. The required quantity of curatives were then added and mixed properly with the preblended mixes as per the basic formulations given in the table 6.1. CBS (primary accelerator) and TMTD (secondary accelerator) have been used for making the vulcanisates. If the mixing of two rubbers is not proper, there will be insufficient cross-linking between the phases, which results in poor mechanical properties of the blends.

Table 6.1 Formulation of SBR/NBR blends

Ingredients	Blend -1(Phr)	Blend -2 (Phr)	Blend -3 (Phr)
SBR	70	50	30
NBR	30	50	70
38.5 ZnS-SBR	0, 2.5,5,10	0,2.5,5,10	0,2.5,5,10
Stearic acid	1.2	1	0.8
Zinc oxide	5	5	5
CBS	0.7	0.8	0.3
Sulphur	1.69	1.5	1.01
TDO	1	1	1

In the entire blend compositions, there is considerable enhancement in torque was observed on increasing the compatibiliser content. The torque increases progressively with ionic content (Table 6.2). The presence of 38.5 ZnS-SBR may be enhancing the effect of inter diffused chains leading to optimum vulcanization. This may be due to the effective cross-linking upon increasing molecular level homogeneity. The optimum cure time of the blends increased as the 38.5 ZnS-SBR content increased. This may be due to the large interfacial area formed by the uniformly distributed blend matrix. The influence of the ionomer compatibilizer on the scorch time of the 50/50 SBR/NBR blend is also shown in the table 6.2.

Table 6.2 Cure characteristics

Blend composition (Phr)	Amount of compatibiliser (Phr)	Scorch time (min)	Optimum cure time (min)	Maximum torque (Nm)
	0	2.4	5.24	0.387
SBR/NBR	2.5	2.65	5.08	0.3745
70/30	5	2.88	5.50	0.4013
(Blend-1)	10	2.96	6.12	0.4223
SBR/NBR	0	2.6	7.65	0.4013
50/50	2.5	3.2	7.8	0.4123
(Blend-2)	5	2.65	8.2	0.4180
	10	2.920	8.0	0.4236
SBR/NBR	0	3.2	8.50	0.4023
30/70	2.5	3.0	8.65	0.4204
(Blend-3)	5	2.820	8.65	0.4455
	10	2.920	8.50	0.4772

The optimum cure time was found in this case, as more time is needed for the formation of greater number of interface cross-links. These results predict the behaviour of 38.5 ZnS-SBR as a compatibiliser in SBR/NBR blend, which is further, confirmed by physical property measurement, differential scanning calorimetry, dynamic mechanical thermal analysis, and scanning electron microscopy

6.3 Differential scanning calorimetry

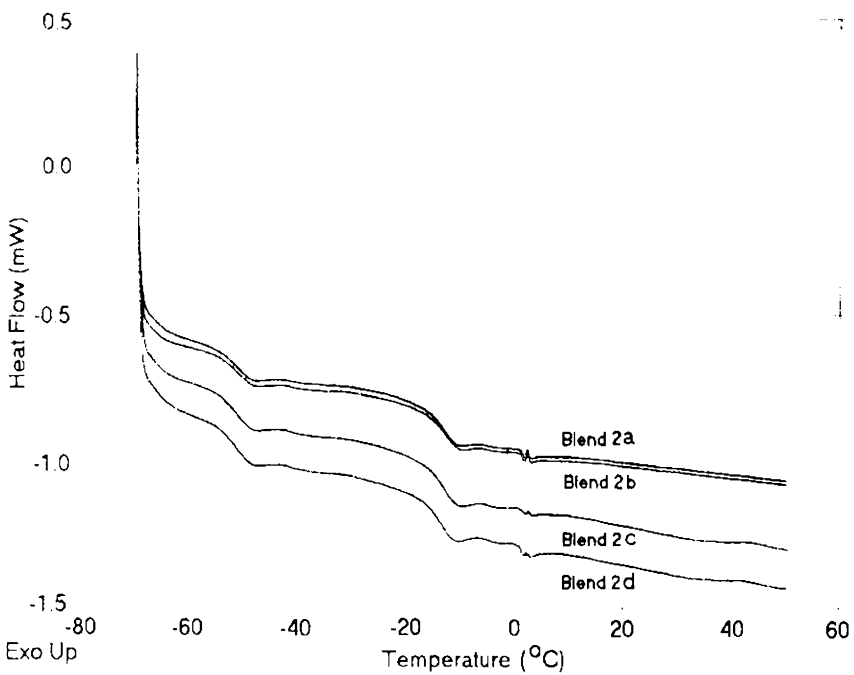


Figure 6.1 DSC thermal profiles of 50/50 SBR/NBR blends:
Blend-2a (0 compatibilizer); Blend-2b (2.5 phr compatibilizer);
Blend-2c (5 phr compatibiliser); Blend-2d (10 phr compatibiliser).

The DSC traces of pure 50/50 SBR/NBR blend with and without compatibiliser are shown in figure 6.1 and the results are summarized in table 6.3. The characteristic glass rubber transitions (T_g s) of SBR and NBR, for the uncompatibilized 50/50 SBR/NBR blend, appeared at -51.44 °C and -12.72 °C. The incorporation of ionomer in to the blends affected their T_g . This may be due to the interaction between the zinc sulphonate groups of ionomer and the nitrile groups (-CN) of the NBR resulting in reduction in the interfacial tension due to the interfacial activity¹³⁻¹⁵.

Table 6.3 DSC Results of cured SBR/NBR Blends

Samples	Thermal transitions	
	SBR (T_g^1) °C	NBR (T_g^2) °C
Blend-2a	-51.44	-12.72
Blend-2b	-51.44	-12.72
Blend-2c	-51.08	-13.07
Blend-2d	-50.96	-13.52

Blend-2a (0 compatibiliser); Blend-2b (2.5 phr compatibiliser);
Blend-2c (5 phr compatibiliser); Blend-2d (10 phr compatibiliser)

The glass rubber transition behaviour of solid polymer blends has long been used as a measure of component miscibility; as each glass transition observed in the blend reflects a distinct segmental relaxation. The interactions operating within the compatibilised SBR/NBR blend system may be sufficient enough to produce the technological compatibility in SBR/NBR system, as manifested by the significant achievement in the synergistic physical properties.

6.4 Dynamic mechanical thermal analysis

Dynamic mechanical thermal analysis is often more sensitive in detecting T_g in blends than DSC. $\tan\delta$ values obtained from compatibilized and uncompatibilized 50/50 SBR-NBR blends are shown in figure 6.2. The DMTA results are summarized in table 6.4. The low temperature $\tan\delta$ peak for the uncompatibilized blend in the range -40 to -20 °C arises from the glass transition of the SBR matrix, and another $\tan\delta$ peak in the temperature range -15 to $+15$ °C arises from the NBR phase. The DMTA results of cured 50/50 SBR/NBR blend shows two T_g 's (T_g^1 corresponds to SBR phase and T_g^2 corresponds to NBR phase) at -40.494 °C (T_g^1) and -0.404 °C (T_g^2) respectively, due to the presence of immiscible SBR and NBR phases respectively. But in the case of compatibilised blends there is a change in the individual glass rubber transitions.

The addition of ionomer reduced the difference between the two glass-rubber transition temperatures. The degree of compatibility may thus be enhanced by the addition of ionomer. The use of ionomer is particularly attractive in this respect since the ionic groups introduce the possibility of strong ion-ion, ionpair-ionpair or ion-dipole interactions with NBR. The interaction of the NBR with the compatibiliser may be reducing the interfacial tension between the SBR and NBR, which may result in the improvement in the miscibility of the components. The appearance of a single, reasonably sharp loss tangent peak at a glass transition temperature is indicative of molecular homogeneity, while the appearance of the multiple T_g 's reflects macro phase separation or partial miscibility of the blend's components¹⁶⁻¹⁸. The presence of two glass-rubber transition temperatures does not imply complete incompatibility of the two components; i.e., the two phases could be present with some degree of compatibility¹¹

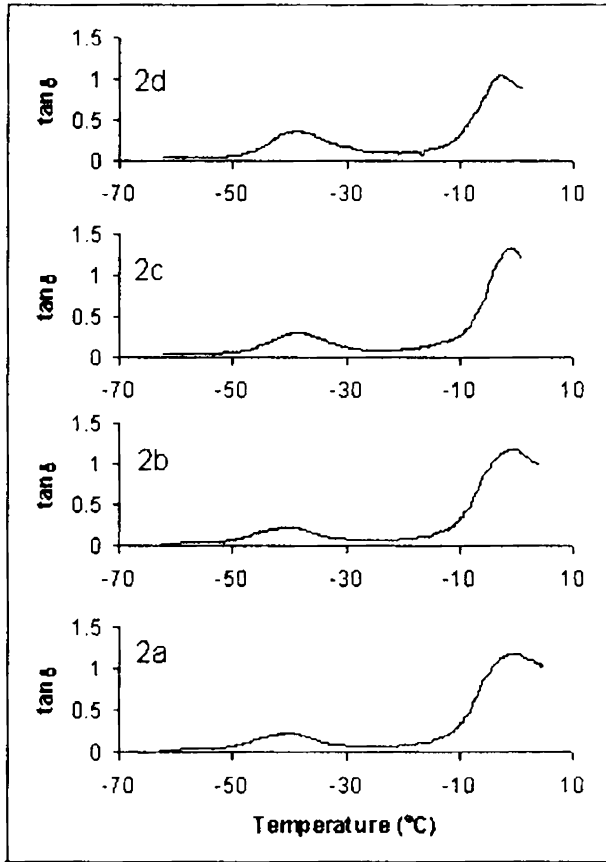


Figure 6.2 DMTA plots of the SBR/NBR blends:

Blend-2a (0 compatibiliser), Blend-2b (2.5 phr compatibiliser),
Blend-2c (5 phr compatibiliser), Blend-2d (10 phr compatibiliser).

Generally compatibilisers locate at the interface between the components of the blend with their segments completely penetrating the respective compatible phases. Alternatively, a compatibiliser interface may be formed between the blend phases^{21,22}. In fact, some of the SGNR copolymer units of the ionomer are believed to

penetrate in to the NBR phase to some degree and their polar zinc sulphonate moiety exhibits a greater affinity with the polar –CN group of NBR. The appearance of the variation in the loss tangent corresponding to the NBR shows that there has been enhanced interaction between NBR and the ionomer. This might be the reason for the miscibility of SBR-NBR system and has been further supported by their improved physical properties.

Table 6.4 DMTA Results of cured 50/50 SBR/NBR Blends

Samples	Thermal transitions corresponding to		Tan δ at		Log E' (Pa) at	
	SBR (Tg ¹)°C	NBR (Tg ²)°C	(Tg ¹)	(Tg ²)	(Tg ¹)	(Tg ²)
Blend-1b	-40.494	-0.404	0.27	0.98	8.57	6.80
Blend-2b	-40.370	-0.284	0.30	0.99	8.56	6.93
Blend-3b	-39.074	-1.324	0.29	1.10	8.51	7.03
Blend-4b	-38.354	-3.084	0.320	1.05	8.56	7.46

Blend-2a (0 compatibilizer); Blend-2b (2.5 phr compatibilizer);
Blend-2c (5 phr compatibilizer); Blend-2d (10 phr compatibilizer)

6.5 Physical properties

The physical properties of the compatibilised blend in comparison with uncompatibilised are given in tables 6.4 – 6.6. The mechanical properties of the blends normally improved with the addition of compatibilisers⁹⁻¹¹. The mechanical properties increases with increase in the amount of compatibiliser added. It is interesting to note that the compatibilized SBR/NBR system shows synergism in tensile strength, tear

strength and hardness, which may be ascribed to the formation of a technologically compatible polymer blend, wherein intermolecular ionic interactions assist in compatibilisation. The compatibilising action is believed to be due to the interaction of nitrile group of NBR and zinc sulphonate moieties of ZnS-SBR. The interfacial ionic cross-links improve the interfacial adhesion, thereby helping to transfer the stress from one phase to other phase. Compared to uncompatibilised blend the compatibilised blends show an increase in modulus and tensile strength; indicating that compatibilising action is efficient in all compositions. The stress strain properties are not governed by crosslinking alone, it depends on the distribution of crosslinks, and the domain size of the phases. The elongation at break also increases with increasing dosage of compatibiliser.

Table 6.5 Physical properties of compatibilised and uncompatibilised 70/30 SBR/NBR blends

Properties	Blend- 1a	Blend-1b	Blend-1c	Blend- 1d
Modulus (MPa) at 300% elongation	2.52	2.65	2.8	3.2
Tensile strength (MPa)	2.8	3.2	3.5	4.4
Elongation at break (%)	342	341	362	385
Tear strength (N/mm)	15.5	15.7	17.5	20.4
Hardness (Shore A)	40	40	42	43
Compression set (%)	17.25	17.4	16	15.5

Table 6.6 Physical properties of compatibilised and uncompatibilised
50/50 SBR/NBR blends

Properties	Blend- 2a	Blend-2b	Blend-2c	Blend- 2d
Modulus (MPa) at 300% elongation	2.40	2.62	2.89	3.10
Tensile strength (MPa)	3.60	3.86	4.9	5.6
Elongation at break (%)	345	385	465	442
Tear strength (N/mm)	15.9	16.9	23.0	24.8
Hardness (Shore A)	42	42	44	45
Compression set (%)	18.2	18	16.5	16.2

The tear strength improved with increasing the amount of compatibiliser. There is structural similarity between the segments of the compatibilizer and SBR. This also enhances compatibilising action of ZnS-SBR in the blends.

Table 6.7 Physical properties of compatibilised and uncompatibilised
50/50 SBR/NBR blends

Properties	Blend- 3a	Blend-3b	Blend-3c	Blend- 3d
Modulus at 300% elongation (MPa)	2.40	2.56	2.89	3.10
Tensile strength (MPa)	3.20	3.6	4.7	4.9
Elongation at break (%)	360	366	445	442
Tear strength (N/mm)	16.9	18.8	22.5	22
Hardness (Shore A)	42	42	44	46
Compression set (%)	18.5	17.6	17.4	16.8

The hardness which is a measure of modulus of elasticity at low strain, also improved in the case of compatibilised blends. This may be due to the higher crosslinking in

presence of compatibiliser. The compression set values are decreased with increase in ionomer content. Which is also support compatibilisation effected by ionomers. If the segments of the added copolymer are chemically identical with those of in the respective phases or adhered to one of the phases then they act as efficient compatibilizers¹⁹.

6.6 Scanning electron microscopy

Morphology of the blends, studied using Scanning electron microscope (SEM) are given in figures 6.3- 6.5. SEM photomicrographs of the SBR/NBR with 5 and 10phr ionomer were compared with the SBR/NBR without compatibiliser. These micrographs clearly indicate that clear morphology difference is generated by introducing compatibiliser. Generally compatibiliser reduces the domain size and increases the interconnection between the two phases of the blend²⁰.

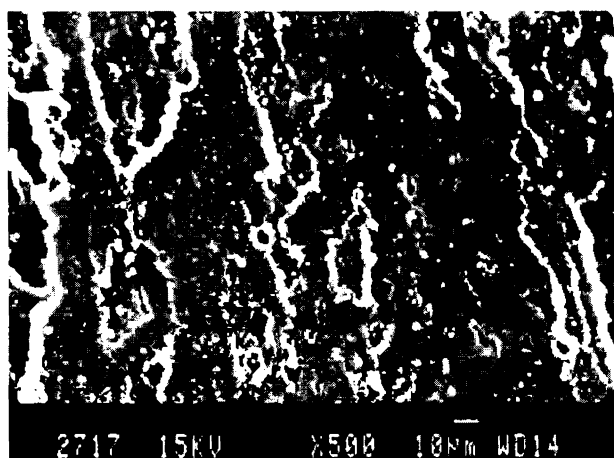


Figure. 6.3 SEM photomicrographs of the fractured surface of the cured uncompatibilized 50/50 blend of SBR/NBR

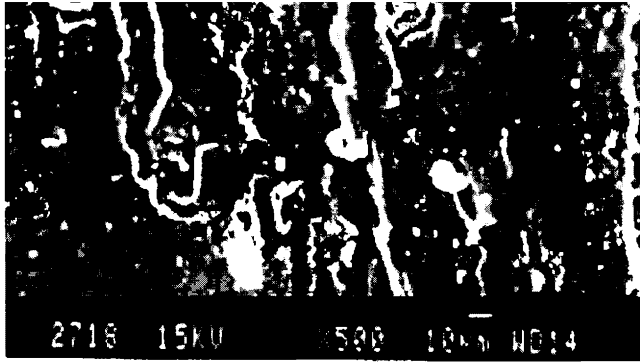


Figure 6.4 SEM photomicrographs of the fractured surface of the cured 50/50 blend of SBR/NBR with 5 phr ionomer

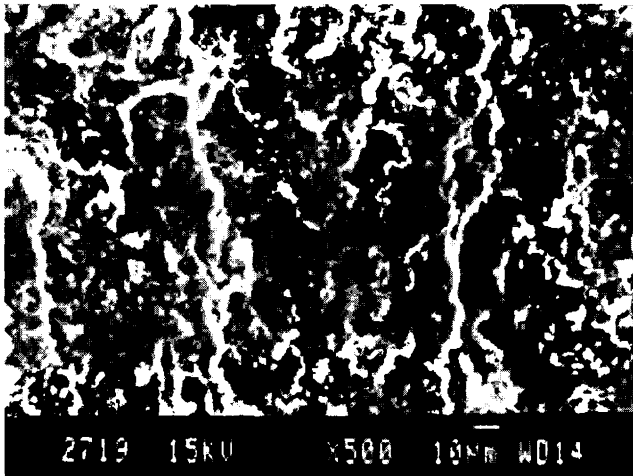


Figure 6.5 SEM photomicrographs of the fractured surface of the cured 50/50 blend of SBR/NBR with 10 phr ionomer

These observations with respect to the uncompatibilised blend are obviously due to the inhomogeneity in the blend. The poor adhesion between the phases in the uncompatibilised blend may be the reason for their low mechanical properties. The SEM photomicrographs on the tensile fractured surface of the cured 50/50 SBR/NBR blend compatibilized with 10-phr ionomer reveal that there is uniform curing within the phases and at the interface, which results in better adhesion between the phases. The modified systems having improved mechanical properties than the corresponding unmodified blend have a better co-continuous nature of the phases permitting direct load transfer of the components. The co-continuity of the matrix in the case of modified system is a result of improved adhesion.

6.7 Influence of HAF carbon black

The main use of fillers in rubber-rubber blend is to improve the mechanical properties. Fillers are considered to improve the phase morphology of the incompatible blends. It has been found that the thermodynamic compatibility of many binary blends is further improved by the addition of fillers. This ability of fillers comes from its tendency to reduce zone size of dispersed domains in polymer blends.

6.7.1 Cure characteristics

Formulations of carbon black filled 50/50 SBR/NBR blends with and without compatibilisers are given in table 6.8. The effect of addition of varying concentration of carbon black on the cure characteristics of the uncompatibilized and 10-phr compatibilized 50/50 SBR/NBR blends are shown in the table 6.9. The addition of small quantity of 38.5 ZnS-SBR causes a rise in the rheometric torque of the blend. The torque has been further enhanced on adding HAF carbon black as filler. Increase in viscosity of rubbers on incorporation of carbon black is well known.

Table 6.8 Formulation of carbon black filled 50/50 SBR/NBR blend

Ingredients	Uncompatibilized (Phr)	Compatibilised (Phr)
SBR/NBR blend	100	100
38.5 ZnS-SBR	0	10
Stearic acid	1.5	1.5
Zinc oxide	5	5
CBS	1	1
TMTD	0.5	0.5
HAF black (N330)	10-40	10-40
Aromatic oil	1-4	1-4
Sulphur	1.5	1.5
TDQ	1	1

The reinforcing effect of fillers is attributed to better polymer filler interaction. In SBR/NBR blends carbon black showed preferential migration to SBR phase compared to NBR phase²¹. The maximum torque depends on the cross-link density and chain entanglement, which result from higher interaction of SBR and NBR through ZnS-SBR unit. This may be due to an increased level of crosslinking. The scorch time and the optimum cure time of the 5-phr compatibilized blend decreased with carbon black content. It is assumed that ZnS-SBR reduces the interfacial tension giving increased interfacial cross-linking due to more homogeneous mixing of the two rubbers.

Table 6.9 Rheometric data of carbon filled compatibilized and uncompatibilized 50/50 SBR/NBR blends

Blend composition	Amount of compatibiliser (Phr)	Amount of HAF (Phr)	Scorch Time (min)	Optimum cure time (min)	Maximum torque (Nm)
SBR/NBR 50/50	0	0	2.6	7.65	0.4013
	0	10	3.2	6.16	0.415
	0	20	2.10	4.10	0.5663
	0	30	1.90	4.0	0.630
	0	40	1.60	3.20	0.7170
SBR/NBR 50/50	10	0	2.92	8.0	0.4236
	10	10	2.0	5.168	0.4775
	10	20	2.2	4.18	0.5615
	10	30	1.65	3.20	0.623
	10	40	1.52	2.8	0.7275

6.7.2 Physical properties

Physical properties of the filled systems are increased with increase in filler content and properties are superior over the uncompatibilized system. This may be due to the more interaction between compatibilizer and blend constituents. Due to the reduction of interfacial tension on these blend compositions there is also an improved polymer filled interaction and more uniform distribution of filler in the two rubbers.

Table 6.10 Physical properties of cured uncompatibilized 50/50 SBR/NBR blend filled with carbon black

Amount of HAF (Phr)	Tensile strength (MPa)	Elongation at break (%)	Tear strength (N/mm)	Hardness (Shore A)
10	9.25	332	28.8	51
20	14.4	304	36.8	55
30	18.20	285	38.2	60
40	20.06	272	42.5	65

Table 6.11 Physical properties of cured 50/50 SBR/NBR blend filled with carbon black containing 10 phr ionomer

Amount of HAF (Phr)	Tensile strength (MPa)	Elongation at break (%)	Tear strength (N/mm)	Hardness (Shore A)
10	10.45	322	29.8	51
20	16.94	314	38.8	57
30	20.20	295	40.2	62
40	22.26	270	41.6	65

6.7.3 Dynamic mechanical properties

DMTA results of the compatibilised and uncompatibilised cured 50/50 SBR/NBR Blends filled with 40 phr HAF are shown in figure 6.6 and the results are summarized in table 6.12. It was also observed multiple T_gs with significant changes upon compatibilisation.

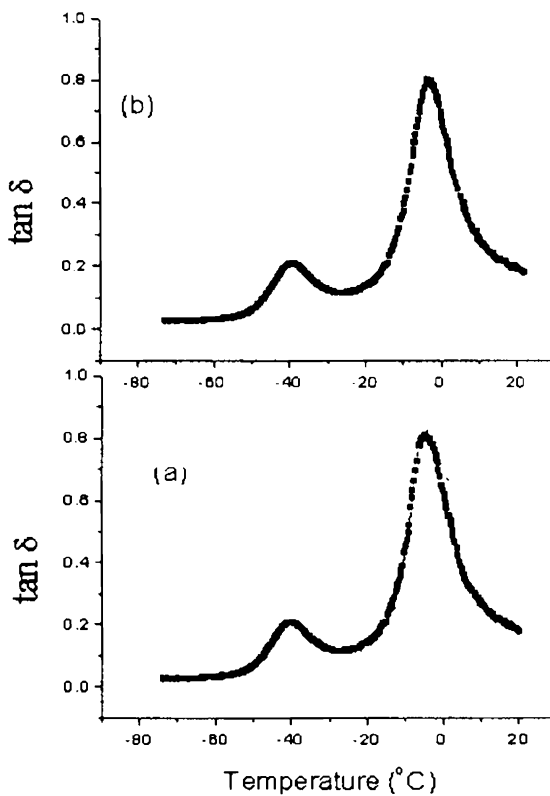


Figure 6.6 DMTA results of cured 50/50 SBR/NBR Blends

Blend-a (0 compatibilizer + 40 phr HAF); Blend-b (10 phr compatibilizer + 40 phr HAF)

Table 6.12 DMTA Results of cured 50/50 SBR/NBR Blends with 40 phr HAF

Samples	Thermal transitions corresponding to		Tan δ at		Log E' (Pa) at	
	SBR (T ¹ g) ^o C	NBR (T ² g) ^o C	T ¹ g	T ² g	T ¹ g	T ² g
Blend-a	-40.554	-4.840	0.270	0.80	8.8	7.8
Blend-b	-40.438	-5.296	0.267	0.84	8.8	6.9

Blend- a (0 phr compatibilizer + 40 phr HAF); Blend-b (10 phr compatibilizer + 40 phr HAF)

6.7.4 Morphological studies

The comparison of the SEM photomicrographs of the tensile fractured surfaces of the filled uncompatibilised and compatibilised blends show further evidence for the reinforcement by HAF carbon black. Figure 6.7 represents the filled uncompatibilised blend and figure 6.8 represents the filled compatibilised system. The distribution of fillers in an immiscible blend system is unequal. However, on compatibilization the matrix becomes uniform and hence the transfer of fillers at the interface may be high². This migration is due to a greater solvation between the filler and the compatibiliser. The ionomer at the interface of the SBR/NBR facilitates the better dispersion of HAF black as evident from the figure 6.8, which shows a smooth dispersion of filler particles in the compatibilised system.

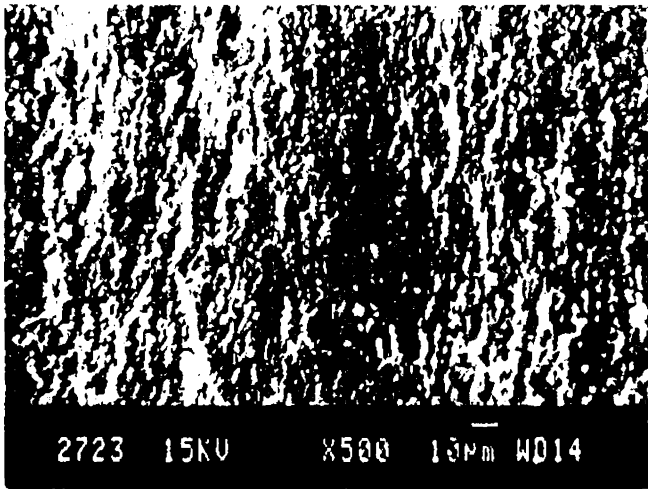


Figure 6.7 SEM photomicrograph of the tensile fractured surface of cured uncompatibilized 50/50 SBR/NBR blend filled with 40 phr carbon black

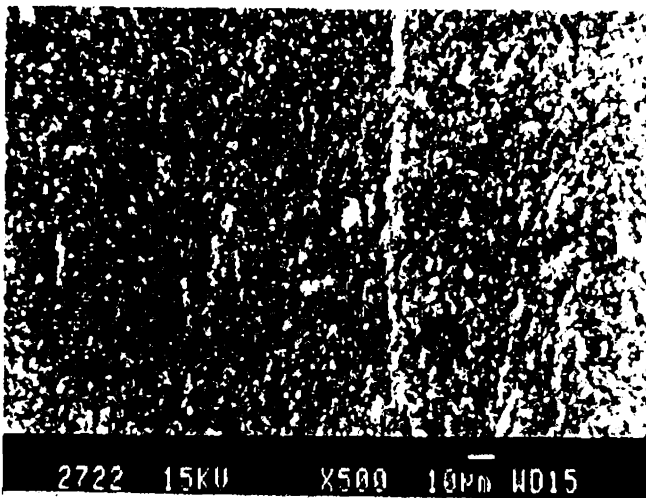
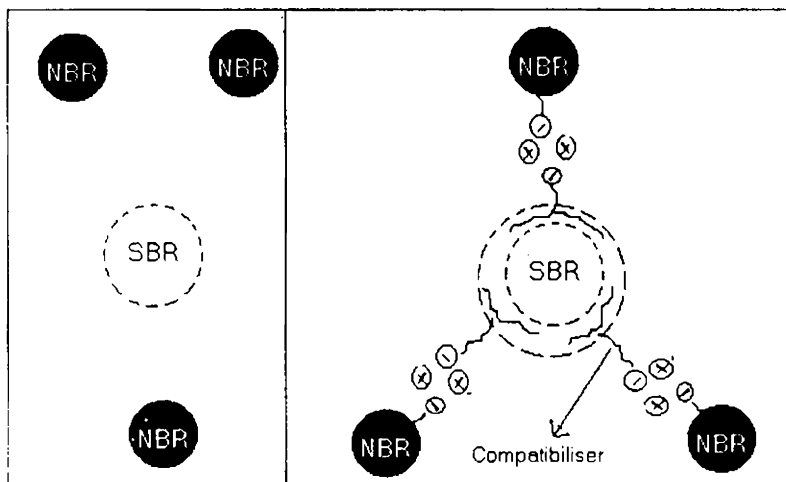


Figure 6.8 SEM photomicrograph of the tensile fractured surface of cured compatibilised (10 phr) 50/50 SBR/NBR blend filled with 40 phr carbon black

6.8 Mechanism of the compatibilisation

The DSC and DMTA results suggest that the compatibiliser exist in the interface of two polymers, and there may be stronger interaction of the -CN groups of the NBR with the ionic multiplet of the ionomer. The interaction of the NBR with the compatibiliser may be reducing the interfacial tension between the SBR and NBR, which might have resulted in the partial miscibility of the components.

The presence of the ionomer at the interface between the SBR and NBR was investigated morphologically. The SEM micrographs of the fractured surfaces of the compatibilised blend show that the compatibiliser reduces the domain size and increases the interconnection between the phases of the blend, which suggests that the compatibilizer is located preferentially at the interfaces. The possible models showing the interaction of the ionomer with the blend systems are shown in the scheme 6.1.



Scheme 6.1 Proposed model showing the uncompatibilized and compatibilised blend system

The present method of compatibilisation consists of the mixing of zinc-sulphonated styrene butadiene rubber with the SBR/ NBR system, which upon mixing may be 'anchored' at the interface of SBR/ NBR polymer system. The anchoring of the ionomer on the SBR interface may be facilitated by the similarity in the 'architecture' of their structural backbones, where as the anchoring of the ionomer on the NBR interface may be due to the interaction of the polar zinc sulphonated group on the ionomer with the polar -CN group on NBR. The anchoring of the ionomer at the SBR/ NBR interface increases the entropy of mixing, which therefore, reduces the surface tension or surface energy. This thermodynamic feasibility for mixing of the polymer components forces the chains of SBR and NBR to remain in close proximity. The technological compatibilisation of the SBR/NBR polymer blend system has been further established through the synergistic physical properties of the blend system.

The unfavourable interaction between molecular segments of the components leads to a large interfacial tension, which makes it difficult to disperse the components finely enough during mixing. This is responsible for the immiscibility of the polymer components. The poor interfacial adhesion in the solid state causes mechanical failure via these weak defects between phases. Solutions to these problems or compatibilisation can be effected by the addition of appropriate graft / block copolymers or ionomers that act as interfacial agents. For effective compatibilization, the molecular weight and architecture of the block copolymer need to be carefully optimized. Formation of the copolymer species at the interface reduces the interfacial tension, leading to the stabilization, which retards dispersed phase coalescence, strengthening the interface - in the solid state - between phases. A significant achievement in the physical properties of the blend may be considered as an evidence for the significant reduction in the dimensions of the phase domains. Compatibilisation shifts the balance between drop breakup and coalescence by lowering interfacial tension and introducing stabilization. These effects produce much smaller dispersed -

phase particles. Reactions at the interface are expected to lead to a reduction in the interfacial tension.

SBR and NBR are immiscible; miscibility enhancement can be achieved when an ionomer is used as a compatibilizer. The intermolecular polar – polar interactions between SBR/ZnS-SBR with NBR lower the heat of mixing so that the thermodynamics of blending can lead to miscibility enhancement of the blend components. The use of ZnS-SBR ionomer is particularly attractive in this respect since the ionic groups introduce the possibility of strong ion – ion, ion pair – ion pair or ion – dipole interactions with NBR.

6.9 Conclusion

Introduction of specific interaction into SBR/NBR blends improve the miscibility. Results of DSC studies of the blends showed multiple T_gs with changes upon compatibilization. The DMTA results support the DSC results and the possibility of existence of ionomer at the interface between the components of the blends. The significant changes in T_gs upon compatibilization may be ascribed to the preferential polar-polar interaction of the zinc sulphonate units and the -CN groups of the NBR, and similarity in the backbone of the ionomer and SBR. The dipole-ion interaction between NBR and 38.5 ZnS-SBR might have a significant role in improving the miscibility, resulting in changes in the glass-rubber transitions. The addition of zinc sulphonated styrene-butadiene rubber ionomer increased the physical properties of the blends. As expected for most immiscible polymer blends, the mechanical properties of binary blends of SBR and NBR were poor. However, addition of zinc sulphonated styrene butadiene rubber ionomers increased the stress-strain properties of the blends. The morphological studies gave support to the above arguments. In the HAF filled blend systems the effect of ionomer as a compatibiliser is evident. The novel

ionomer based on styrene-butadiene rubber may be used as a compatibilizer for obtaining technologically compatible blends from the immiscible SBR and NBR polymers.

6.10 References

1. Paul, D.R; Bucknall, C. B. *Polymer Blends vol 1* , Wiley Interscience Publication, New York 2000.
2. Paul, D.R; Bucknall, C. B. *Polymer Blends vol 2* , Wiley Interscience Publication, New York 2000.
3. Kim, Y., Won-Jei Cho, C-Sik Ha, *Polym. Eng. Sci.* **35**, 1592 (1995).
4. Subramanyam, P. M., *Polym. Eng. Sci.*, **27**, 1574 (1987).
5. Barensten, W.M., Heikens, D., Piet, P., *Polymer* **14**, 579 (1974).
6. Sundararaj, U., Macosko C.W., *Macromolecules*, **28**, 2647 (1995).
7. Del Giudice, L., Cohen, R.E., Attalla, G., Bertinotti, F., *J. Appl. Polym. Sci.* **30**, 4305 (1985)
8. Angola, J.C., Fujita, Y., Sakai, T., Inoue, T., *J. Polym. Sci., Part B. Polym. Phys.* **26**, 807 (1988).
9. Plochhocki, A.P., Dagli, S.S., Andrews, R.D., *Polym. Eng. Sci.* **30**, 741(1990).
10. Ramesan, M. T.; Rosamma, A., *J. Appl. Polym. Sci.* **68**,153 (1998).
11. Mansour, S.H, Tawfik, S.Y., Youssef, M.H., *J. Appl. Polym. Sci.* **83**, 2314–2321 (2002)
12. Halimatudahliana, H. Ismail , M. Nasir *Polymer Testing* **21**, 163-70 (2002)
13. Lu, X.; Weiss, R.A. *Mater. Res. Soc. Symp. Proc. 29 (Proceedings of the Fall Meeting of the Materials Research Society* 1990.
14. Coran, A.Y.; Patel, R. *Rubber Chem. Technol.* **54**, 892 (1981).
15. Vongpanish, P.; Bhowmick, A.K.; Inoue, T. *Plast. & Rubber Proc. & Applications* **19**, 117 (1993).
16. Olabisi, O.; Robeson, L.M.; Shaw, M.T. *Polymer-Polymer Miscibility*, Academic Press, New York 1979.
17. Macknight, W.J.; Karasz, F. E.; Fried, J.R. "Solid State Transition Behavior of Blends", in *Polymer Blends*, Paul, D.R.; Newman, S(eds.), Academic Press, New York 1978

-
18. Karasz, F. E. "Glass Transitions and Compatibility; Phase Behavior in Copolymer Containing Blends", in *Polymer Blends and Mixtures*, Walsh, D.J.; Higgins, J.S.; Maconnachie (eds.), Martinus Nijhoff Publishers, Boston 1985.
 19. Ouhadi, T., Fayt, R., Jerome, R., and Teyssie, J. *Appl. Polym. Sci.* **32**, 5647 (1986).
 20. Meier, D.J. *Hetero-Phase Polymer System*; American Chemical Society: Washington DC, 1990.
 21. Callan, J.E.; Hess, W.M.; Scott, C.E. *Rubber Chem. Technol.*, **44**, 814 (1971).

Chapter 7

Conclusion and future outlook

The synthesis, characterisation and investigation of the properties of novel class of ionomers based on styrene butadiene rubber and high styrene rubber are presented in this thesis. The effect of particulate fillers on the properties of the ionomer, the dielectric properties of the ionomer at 2-12 GHz frequencies and the efficiency of the ionomer as a compatibiliser in the binary blend of SBR/NBR system are also discussed.

Ionic elastomers with high elastomeric green strength are emerging as an important class of thermoplastic elastomers. A brief survey of the developments and recent studies on ionomers are presented in the first chapter. The specification of the materials and characterization techniques employed in this study are given in the second chapter.

The details of the synthesis of the ionomers based on SBR and HSR are outlined in the third chapter. The ionomers (ZnS-SBR and ZnS-HSR) could be prepared by sulphonation of the base unfunctionalised SBR and HSR using acetylsulphate followed by neutralization of the resultant sulphonic acids by using zinc acetate. The zinc sulphonated styrene-butadiene rubber was chosen as the model material for further studies. The microstructural changes occurring during ionic modification of both SBR and HSR have been studied by means of X-ray fluorescence (XRF),

infrared spectroscopy (FTIR) and NMR. DSC thermograms show that incorporation of the zinc sulfonate groups in to the styrene butadiene rubber and high styrene rubber significantly affect their T_g. Dynamic mechanical thermal analysis (DMTA) of the ionomers revealed that the thermo mechanical properties of the ionomers are superior to those of the vulcanized material. The glass transition temperature (T_g) of the ionomer increased with increase in the ionic concentration. DMTA measurements gave two separate mechanical loss tangent ($\tan\delta$) peaks. The value of the $\tan\delta$ at T_g ($\tan\delta_{\max}$) decreased with sulphonation, and a new relaxation occurred above the matrix glass transition temperature that corresponds to the cluster formation. Thermogravimetric analysis results showed improvement in the thermo-oxidative stability of the base polymer upon ionic modification. The increase in the concentration of ionic groups improved the physical properties presumably due to an increased number of ionic crosslinks. Reprocessability studies revealed the thermo-reversible character of the ionically modified rubbers.

Investigations on ionomers filled with particulate fillers such as carbon black (HAF), silica, and zinc stearate showed that the incorporation of fillers improved the physical, dynamic mechanical and thermal properties of the ionomer. Both DMTA and DSC supported the reinforcement of the ionomer with fillers. DMTA plots showed that both the low temperature and high temperature transitions were retained in all filled ionomers. The value of the thermal transitions suggests that both HAF black and silica reinforces the backbone chain, where as the zinc stearate play a dual role as a filler, and plasticiser. The thermoplastic elastomeric nature of the compounds was evident from the retention of the stress-strain properties even after three cycles of repeated mixing and moulding.

The four key parameters – the real part of the relative permittivity (dielectric constant), imaginary part of the relative permittivity (dielectric loss), dielectric loss angle, and conductivity of the ionomers could be measured at the microwave frequencies. The presence of ionic groups in the polymer, which are held through columbic forces, may affect the electrical properties. Incorporation of ionic groups leads to increase of dielectric constant and conductivity. These ionic associations act

as the centers of polarization at the microwave region. The measurements at room temperature showed that the complex permittivity and the relative complex conductivity increased with increase in the ionic concentration. The heating coefficient decreased with increasing ion content. The absorption coefficient is linearly related to both frequency and ion content. The penetration depth decreases with increasing ion content and frequency.

Introduction of specific interaction into SBR/NBR blend was successful in improving their miscibility. The 38.5 ZnS-SBR ionomer was useful as a compatibilizer for the immiscible SBR/NBR blend system. The incorporation of ionomer gave substantial improvement in the physical properties of the blends as well as the filled systems. DSC studies of the blends showed multiple T_gs which however, change on compatibilisation. The DMTA results also support the DSC and the possibility of existence of the ionomer at the interface between the components. The blends showed multiple T_gs with significant changes upon compatibilization. This may be ascribed to the preferential polar-polar interaction of the zinc sulphonate groups and the -CN groups of the NBR and the structural similarity of ZnS-SBR and NBR. That is, the dipole-ion interaction between NBR and ZnS-SBR play an important role in improving their miscibility, resulting in a change in the glass-rubber transitions. The addition of zinc sulphonated styrene-butadiene rubber ionomer increased the physical properties of the blends. The morphological studies support the above observations.

Suggestions for future work

The synthesis and characterization of novel ionomers based on conventional rubbers is an interesting area of further research. Some of the promising areas of research are,

1. Elastomer

The investigations on the use of elastomeric ionomers as a substitute for vulcanized rubber, and thermoplastic elastomer is an exciting area, which may lead to many novel applications.

2. Microwave devices

The microwave response of the ionomers at the S, C and X-band frequencies may be an area of useful study.

3. Compatibilizers

Ionomers, due to their unique properties and architecture, may be useful as a compatibilising agent for nonpolar- polar blend systems.

4. Ionomer-ionomer blends

Novel ionomer-ionomer blends of specific properties may be developed in specific applications.

5. Catalysts

The use of ionomers as catalysts in certain organic reactions may be another useful area of study.

List of Publications

International journals

1. Ionomers *Prog. Rub. Plast. Tech.* **16**, 1, (2000)
2. High Styrene Rubber Ionomers, an Alternative to Thermoplastic Elastomers *J. Appl. Polym. Sci.*, **85**, 2294, (2002).
3. Dielectric Properties of Ionomers at Microwave Frequencies, *Materials Letters*, **56** 248 – 251(2002)
4. Reprocessable Ionic Elastomers based on Styrene Butadiene Rubber; *Intern. J. Polymer. Mater.* (In Press)
5. Microwave Studies on ZnS-HSR Ionomers, *Materials Chemistry and Physics*, **9571**, -4, (2002)
6. Dynamic Mechanical and Dielectric Properties of Styrene Butadiene Rubber Ionomers, *J. of Materials Science* (communicated)
7. Compatibilization of SBR/NBR Blend by the Introduction of Styrene Butadiene Rubber Ionomers, *Polymer Testing* (communicated)

International seminars

1. Technological Compatibilization of SBR/NBR Blend by Introducing Specific Interaction, Proceedings of the *Asia RubTech Expo 2002*, International Conference on Rubber and Allied Materials, November 28-30, T2A-II, .2002.

2. Effect of Ionic Concentrations on the Dielectric Properties of Zinc Sulphonated Styrene Butadiene Rubber Ionomers, Proceedings of the *APT-O2*, International Seminar on *Advances in Polymer Technology*, December 13-14, 34, 2002.

National seminars

1. Influence of Compounding Ingredients on Ionomers; National Seminar on *Current Trends in Macromolecular Chemistry and Technology - MACROSEM 2000*, August, 23-25, 2000.
2. Novel Thermoplastic Ionomer based on Natural Rubber, Proceedings of the *Thirteenth Kerala Science Congress*, January 29-31, 2001.

Award

Presentation based on the work has been awarded **the Young Scientist Award for the year 2001** of the **State Committee on Science, Technology and Environment, Government of Kerala** for the best paper presented on Engineering and Technology at thirteenth Kerala Science Congress at Thrissur, Kerala, January 29-31, 2001.